Titre: Title:	The Role of Particles in the Processing of the Solid-Stabilized Emulsions
Auteur: Author:	Bing Wan
Date:	2018
Type:	Mémoire ou thèse / Dissertation or Thesis
Référence: Citation:	Wan, B. (2018). The Role of Particles in the Processing of the Solid-Stabilized Emulsions [Ph.D. thesis, École Polytechnique de Montréal]. PolyPublie. https://publications.polymtl.ca/3740/

UNIVERSITÉ DE MONTRÉAL

THE ROLE OF PARTICLES IN THE PROCESSING OF THE SOLID-STABILIZED EMULSIONS

BING WAN

DÉPARTEMENT DE GÉNIE CHIMIQUE

ÉCOLE POLYTECHNIQUE DE MONTRÉAL

THÈSE PRÉSENTÉE EN VUE DE L'OBTENTION

DU DIPLÔME DE PHILOSOPHIAE DOCTOR

(GÉNIE CHIMIQUE)

DÉCEMBRE 2018

UNIVERSITÉ DE MONTRÉAL

ÉCOLE POLYTECHNIQUE DE MONTRÉAL

Cette thèse intitulée :

THE ROLE OF PARTICLES IN THE PROCESSING OF THE SOLID-STABILIZED EMULSIONS

présentée par : WAN Bing

en vue de l'obtention du diplôme de : Philosophiae Doctor

a été dûment acceptée par le jury d'examen constitué de :

M. LEGROS Robert, Ph. D., président

M. FRADETTE Louis, Ph. D., membre et directeur de recherche

M. HENRY Oliver, Ph. D., membre

M. VERMETTE Patrick, Ph. D., membre externe

DEDICATION

To my mom and dad: you are the light of my life.

ACKNOWLEDGEMENTS

I want to express my sincere gratitude to my supervisor prof. Louis Fradette. I would not be able to go this far without his patience, support and guidance throughout these years. In the beginning of the Ph.D. path, I lost myself in the darkness and almost gave up. It is him, who always finds a way to lead me towards the brightness, where I could gain the confidence and motivation again. He has the magic to transform a “stone” into “gold”. Each time when I presented unexpected experiment results to him, he always imparting positive spirit to me and telling me how interesting they are. This encourages me to investigate further on the potential reasons behind, and sometimes it becomes a new discovery.I would like to thank all my jury memebers for taking your previous time to attend my defense. I would like to express my special appreciation to my close colleague Dr. Emir Tsabet, who contributes to my papers and translating the abstract. He always provides me with precious suggestions and ideas when I share results with him, and he will always encourage me saying “congrats Bing, you are closer to your defense”. His ideas are always inspiring to me and being essential to my work. I am very lucky to collaborate two papers of mine with him, his attitude towards the experiments always impress me. I would also like to thank my two other colleagues from Pickering group Rahi Avazpour and Alexandre Al-haiek. I enjoyed each group meeting we had together, from which, so many interesting ideas are fostered from the discussions for each one’s project. A thank you to Faezeh Sabri and Navid Elahipanah, who always being there for me when I am in the struggles of switching from doctoral to master. I could still remember they even made a list for me about the advantage and disadvantage of doing master and doing Ph.D. and told me not to make the rash decisions. Thank you for the support from my colleagues in URPEI group (David Vidal, Jean-michel Tucny, Shuli Shu, Bruno Blais, Charlotte Vanengeland, Bastien Delacroix, Igor Belot, MinhDung Nguyen), Office colleauges (Fatma Ben Dhieb, Adrian Carrillo, Charles Bruel, Mohaned Khalil, Yefeng Zhou) the technicians and the secretaries (Robert Dlisle, Dnaiel Pilon, Sylvie Taillon, Kalonji Mbelu, Monique Malouin, Yoan Ayassamipoulle) in the department. I appreciate the care and thoughtfulness from my friends (Chongyang Li, Zheni Ma, He Li, Hang Qu, Lili Wang, Lianfeng Zou, Qinghua Wu) and family, thank you for being loving, caring and kind to me.

Last but not least, a special thanks to the two most important people in the world, my parents, who raise me up with unconditional love and bring the sunshine into my life.

RESUME

L'utilisation de particules solides pour la stabilisation d'émulsions suscite de plus en plus l'intérêt des industriels en raison de leur capacité à générer des émulsions très stables en plus de leurs potentiels à produire des nouveaux matériaux. La présence de particules aux interfaces huile-eau peut cependant être à l'origine de problèmes de séparation au niveau industriel tel que c'est le cas dans le domaine pétrolier lors du traitement du pétrole brut ou de son dessalage. L'impact des propriétés des particules (mouillabilité, taille, forme, concentration, etc…) sur les émulsions produites a été largement étudié. Cependant, le manque d'information sur le comportement des particules durant le processing empêche l'optimisation des procédés d'émulsification et de déstabilisation. L'objectif de ce travail est donc de mettre la lumière sur le rôle exacte des particules durant les procédés d'émulsification, d'inversion de phase ou de déstabilisation d'émulsion. Ces trois opérations ont notamment été reproduites à l'échelle du laboratoire dans un dispositif standard de mélange en utilisant un système modèle avec des matériaux bien caractérisés incluant des huiles silicones, de l'eau déminéralisée et des microbilles de verre. L'évolution du type d'émulsion, de la taille de gouttes, et du taux de couverture des particules à l'interface huile-eau a été suivie en ligne en utilisant la sonde PVM® de Mettler-Toledo selon une nouvelle méthodologie qui a été validée en comparant les résultats aux distributions de taille obtenues avec le Mastersizer 3000 (Malvern Instruments).

Le premier article a été consacré à l'analyse de l'impact des particules sur les mécanismes de rupture et de coalescence des gouttes pendant la génération d'émulsions. Il a été observé que la rupture de gouttes était le mécanisme dominant dans la zone entourant l'agitateur, particulièrement durant les premières étapes de l'émulsification, alors que la coalescence dominait la région éloignée de l'agitateur équilibrant ainsi l'effet de la rupture après quelques minutes d'émulsification. Il a ainsi été possible de dissocier les processus de rupture et de coalescence et de les analyser séparément en introduisant la sonde dans la région concernée. Les résultats ont montré que la présence de particules réduisait l'efficacité de la rupture à travers l'altération des propriétés de la phase continue tandis qu'il a été révélé que la coalescence était affectée par le rapport entre le potentiel de couverture des particules et le potentiel de génération d'interface.

Le second article a été dédié à l'étude de l'impact des particules sur l'inversion de phase catastrophique des émulsions stabilisées par des solides. Similairement aux émulsions stabilisées par des tensio-actifs, l'addition progressive de l'huile a permis l'inversion de phase catastrophique des émulsions huile/eau à des émulsions eau/huile. La comparaison des points d'inversion de phase à différentes concentrations de particules a montré que la quantité d'huile

requise pour déclencher l'inversion de phase dépendait de la quantité de particules qui affecte notamment le taux de coalescence.

Le troisième article a été consacré à l'étude de l'impact des particules sur le processus de demulsification. Il a ainsi été possible de briser des émulsions stabilisées par des solides en ajoutant des particules de plus grosse taille que celles utilisées pour la stabilisation et ayant une plus grande affinité avec la phase dispersée. Les images de la sonde PVM® ont également révélé un processus d'attachement et de détachement des particules aux interfaces pendant le mélange. Le détachement des particules a été attribué au taux de cisaillement élevé dans la zone proche de l'agitateur. De plus, il a été observé que les particules ajoutées pendant le mélange remplaçaient les particules préalablement attachées aux interfaces. Ce comportement a été associé à la contamination des particules détachées par l'huile conduisant à une modification de leurs propriétés de surface. Ce phénomène a notamment été confirmé par des mesures de forces en utilisant la technique de la sonde colloïdale.

Globalement, en étudiant l'impact dynamique des particules pendant les procédés mettant en jeu des émulsions, ce travail a montré qu'il était possible de contrôler l'émulsification et l'inversion de phase par le biais de la concentration en particules tandis qu'il était possible de déstabiliser les émulsions par l'ajout de particules ayant certaines propriétés. Ces résultats proposent donc une approche plus écologique et moins coûteuse pour la séparation de l'huile et de l'eau en présence de particules.

ABSTRACT

The use of solid particles as an emulsion stabilizer is attracting an increasing interest of industry because of their ability to produce the well-stabilized emulsions (namely solid-stabilized emulsions or Pickering emulsions), together with their promising potential to create new materials. Nonetheless, the presence of particles at the oil-water interface generates separation problems in the industrial processes, such as in the case of crude oil dewatering, crude oil desalting.

The impact of particle properties (wettability, size, shape, concentration, etc.) on the resulting emulsions was extensively investigated by researchers. However, given the lack of consideration regarding the particle behaviour during the process, optimization of the emulsification and the demulsification of solid-stabilized emulsions appears to be a challenge. Thus, this work aims at exploring the role of particles during the dynamic processes involving emulsification, phase inversion and destabilization. These three processes were performed in a standard mixing configuration using a model system with well-characterized materials including silicone oil, demineralized water, and glass microbeads. The evolution of the droplet size, emulsion type and particle coverage at the oil-water interface was tracked using a probe-based microscope (PVM®, Mettler-Toledo), based on a new methodology validated through comparing the obtained particle size distribution with Mastersizer 3000 (Malvern Instrument).

The first paper was dedicated to analyzing the impact of particles on the droplet generation, fragmentation and coalescence during emulsification. Breakage is shown to be the predominant mechanism in the region surrounding the impeller, especially during the early stage of emulsification, while coalescence dominates in the region far from the impeller and balances breakage after a couple of minutes. These findings allow further analysis of breakage and coalescence process separately by confining the system to corresponding probing locations in the mixing tank. The results show that particles lower the breakage efficiency by altering the property of continuous phase whereas the coalescence reveals sensitivity to the ratio between particle coverage potential and interface generation potential.

The second paper was dedicated to investigating the impact of particles on catastrophic phase inversion of the solid-stabilized emulsion. Analogous to the surfactant-stabilized emulsion, gradual addition of the oil phase gives rise to the catastrophic phase inversion from O/W emulsion to W/O emulsion. Comparing the phase inversion points at various particle concentrations, we highlighted that the particle amount determines the required amount of oil to trigger the phase inversion, which is related to the variation in coalescence rate.

The third paper was dedicated to studying the impact of particles on the demulsification process. PVM® probe images revealed particles attachment/detachment process at generated interfaces during mixing. Particles detachment is attributed to the high shear level at the impeller zone. Additionally, we reported the replacement of freshly added particles with the particles that are already attached at droplet surfaces. Such behaviour is caused by the contamination of the detached particles with the oil phase which is evidenced by a colloidal probe technique, thus leading to the modification of surface properties. We further managed to break the solid-stabilized emulsion by adding larger particles possessing a high affinity with the dispersed phase.

Overall, through investigating the impact of particles in the dynamic processes, this work allowed better controlling the emulsification, phase inversion process by adjusting the particles concentration and achieving the destabilization by adding particles with given properties. The findings are anticipated to offer green, low-cost approaches to promoting the separation between oil and water in the presence of particles.

TABLE OF CONTENTS

LIST OF TABLES

LIST OF FIGURES

LIST OF SYMBOLS AND ABBREVIATIONS

Abbreviations

AFM	Atomic force microscopy
CMC	Critical micelle concentration
DSD	Droplet size distribution
DSD	Droplet size distribution
O/W	Oil-in-water
O/W/O	Oil-in-water-in-oil
PSD	Particle size distribution
PVM®	Particle vision microscope
RPM	Revolution per minute
SSE	Solid-stabilized emulsion
TPC	Three-phase contact
W/O	Water-in-oil
W/O/W	Water-in-oil-in-water

Roman letters

A_{cov}	Particle coverage potential
A_f	Area of the drainage film
A_{gen}	System generated interface
a_t	Acceleration in the flow field
Ca	Capillary number
D	Droplet diameter
D	Impeller diameter
d_{10}	10% population below this size
$d_{3,2}$	Surface mean diameter (Sauter mean diameter)
$d_{4,3}$	Volume mean diameter

d_{50}	50% population below this size
d_{90}	90% population below this size
d_{max}	Maximum droplet size
d_p	Particle diameter
E	Free energy
E_{coal}	Coalescence frequency
F_{att}	Attachment force of particles
F_{col}	Collision force
F_g	Particle weight
F_{hyro}	Hydrodynamic force
F_{lap}	Laplace force exerted on particles
g	Gravity force
h_{cr}	Critical thickness of the drainage film
h_i	Initial thickness of the drainage film
l_{cric}	Circulation between the droplet interface and the zero velocity into the droplets
L_m	Molecular characteristic length
m_p	Mass of particles
m_t	The total mass of water, oil and particles in the system
N	Impeller speed
n_p	Number of particles
N_p	Power number
P	Power consumption
P_c	Capillary pressure
R_{crTPC}	Critical Radius of the three-phase-contact line
R_d	Droplet radius
Re	Reynolds number
R_f	Radius of the drainage film

R_m	Macroscopic characteristic length
R_p	Particle radius
R_{TPC}	Radius of three-phase contact line
S	Available surface area
S_0	Surface area without particles in the system
S_f	Droplet surface covered by per unit mass of particles
T	Temperature
t_A	Particle adsorption time
t_c	Droplet contact time
t_d	Film drainage time
t_{def}	Droplet deformation time
u_t	Settling or creaming velocity
V_d	Volume of dispersed phase
vol%	Volume fraction
We	Weber number
wt%	Weight percentage
P_c	Capillary pressure

Greek letters

μ_d	Dynamic viscosity of the dispersed phase
ε	Energy dissipation rate
ε_{avr}	Average energy dissipation rate
θ_{ao}	Contact angle between air and oil phase
θ_{aw}	Contact angle between air and water phase
θ_{ow}	Contact angle between oil and water phase
λ	Kolmogorov length scale
ν	Kinetic viscosity
υ_{TPC}	Velocity of the expansion of three-phase contact line

π	Pi
ρ_c	Density of the continuous phase
ρ_d	Density of the dispersed phase
ρ_p	Particle density
σ	Interfacial tension
τ_c	Force acting on the droplet from the continuous phase
τ_d	Viscous stress within the droplets (if the dispersed phase is of high viscosity)
τ_s	Cohesive force acting on the droplet from the interfacial tension
Υ_{ow}	Interfacial tension between oil and water
Φ_d	Dispersed phase volume fraction
Γ_M	Particle flux towards the interface

CHAPTER 1 INTRODUCTION

1.1 Background

More than a century ago, the phenomenon of particles stabilization was introduced by Ramsden. A solid-stabilized emulsion (SSE), as known as Pickering emulsion, was named after Pickering, who published the first report on the paraffin oil in water emulsion stabilized by finely divided particles (Pickering, 1907). In this report, they provided evidence for the particle adsorption and the improved stability of SSEs (Pickering, 1907). Despite its well-explained advantages, the conventional emulsion stabilized by surfactant was still the preferred choice for industries due to its various application. It is not until a few decades ago did the SSEs attract attention from the scientific field worldwide.

SSEs are encountered in petroleum production and refining process. Water and brine are accompanied by crude oil during recovery from the reservoir. The water in crude oil emulsion stabilized by naturally existing fine particles is subsequently formed under the application of high shear stresses at the wellhead and choke valves (Sullivan et al., 2002). Additionally, the water in oil emulsion can also be found during the desalting of crude oil when more water is added (Yan et al., 1997). The content of sediment and water (BS&W) are limited below 1% (often 0.5%) before it is acceptable for future transportation. Crude oil, as a non-conducting electrolyte, will not prompt corrosion. However, in response to the flow conditions, the solid particles entrapped by a layer of water may sediment to the pipeline surface, and hence causing the internal corrosion of pipeline (Larsen, 2013). Moreover, an oxidation reaction may take place when the oxygen contained in the brine water is in contact with the metal. Therefore, it is of notable importance to remove the stabilized water droplets inside.

Considering the technological challenges appears in all phases of operations (including reservoir production, transportation, and refining), controlling and understanding the destabilization is crucial. Indeed, separation of water and oil phases by gravity is usually a slow process, especially in the case of viscous oil being the external phase. If aggregated and coalesced, the water droplets can be gravitationally separated from the oil phase. For this reason, the industries aim at inducing coalescence of the water droplets by the following approaches:

1) Addition of chemical demulsifier: the demulsifier displaces the natural surfactant at the interface and influences the droplet coalescence through enhanced film drainage. The

performance of the demulsifier can be improved by increasing pH which helps in destabilizing water-in-oil emulsions. (Bonakdar et al., 2001; Mercado et al., 2014)

2) Heating the emulsions: the high temperature reduces the oil viscosity to elevate the water droplets collision, coalescence, and settling rate (Martinez-Palou et al., 2013; Salager et al, 2001).

3) Application of electrostatic field: the electrostatic field promotes the movement of conductive droplets toward the electrodes, which facilitates droplet collision and hence coalescence (Xu, 2017; Yang et al., 2015).

4) Diluting the continuous oil phase with light oil: the lower the oil viscosity aids in accelerating water droplets settling rate (Feng et al., 2015; Slager et al, 2001).

5) Addition of mineral aggregate: the hetero flocculation is augmented to facilitate the droplet settling rate (Mercado et al., 2012).

The most common method of emulsion treatment is the combination of the above approaches: heating the emulsion coupled with adding appropriate chemical demulsifier to promote destabilization, followed by using electrostatic grids to improve the gravitational separation process. Nevertheless, such combination frequently leads to a relatively high operating cost, for this reason, the industries are seeking inexpensive and environmentally friendly alternatives for crude oil dewatering. It remains a challenge to enhance the coalescence of undesired emulsions with particles present, owing to the lack of understanding of the droplets behavior during the emulsification and demulsification process.

1.2 Structure of the thesis

This thesis is mainly composed of three articles which have been published in or submitted to scientific journals, and the detailed chapters are organized as follows:

- *Chapter 1* gives a brief overview about the background and problems.
- *Chapter 2* presents a literature review regarding this project.
- *Chapter 3* corresponds to the first article, which involves addressing the role of particles in the breakage and coalescence processes separately.
- *Chapter 4* refers to the second article, which discusses the impact of particles in the catastrophic phase inversion processes.
- *Chapter 5* regards the third article, which presents an approach of destabilizing solid-stabilized emulsion with the aid of particles.

- *Chapter 6* provides a general discussion over the work.
- *Chapter 7* provides a conclusion and recommendation for the future research.

CHAPTER 2 LITERATURE REVIEW

2.1 Features of solid-stabilized emulsions

Pickering emulsions offer advantages over the conventional emulsions (surfactant-stabilized emulsions) in various aspects. For example, they exhibit high resistance to droplet coalescence due to the irreversibly adsorbed particles (Binks & Whitby, 2005). In contrast, the stability of the conventional emulsions is extremely sensitive to the parameters such as system pH, salinity concentration, temperature, and oil nature (Chevalier et al., 2013). Besides, the SSEs is also known for its "surfactant-free" characteristic, allowing it to access to the potential applications such as food, pharmaceutical, cosmetic industry, where the surfactant often shows side effect.

2.1.1 Stabilization mechanism

The primary stabilization mechanism of the solid-stabilized emulsion is quite straightforward. The particles adsorb at the oil-water interface and form a densely packed particle layer, acting as a steric barrier around the droplets, which contributes to resisting coalescence (Binks et al., 2002). Apart from this, other mechanisms are proposed to explain the notable stability of solid-stabilized emulsion.

2.1.1.1 Adhesion energy and the thermal free energy

The energy ΔE required to remove a single spherical particle from the interface depends on the particle radius R_p, interfacial tension γ_{ow} and three-phase contact angle θ_{ow} (Levine et al., 1989)

$$\Delta E = \pi \gamma_{ow} R_p^2 (1 \pm cos\theta_{ow})^2 \quad \dots (2.1)$$

Inspection of the formula gives that the adsorption free energy is proportional to the square of the particle radius. Hence, ΔE elevates dramatically with a larger particle. The most stabilized emulsion is formed when the contact angle is equal to 90°, yet, on either side of the contact angle will lead to relatively smaller adsorption energy (Aveyard et al., 2003). Given that the desorption energy of one single nanoparticle (thousands of of K_BT) is far greater compared to the thermal energy (order of K_BT), the particle coating presents a high barrier against coalescence (Aveyard et al., 2003).

2.1.1.2 Rheological property of 3D network formation in the continuous phase

The deformation of liquid around the particles give rise to the lateral capillary interaction between the particles (in Figure 2.1) and hence causing the particle adsorption at the fluid

interface. The force required to lateral displace the particles along the interface is much smaller than to remove a single particle from the interface (Tambe et al., 1994). Thus, the particles are prone to aggregating together rather than being detached from the interface (Danov et al., 2010).

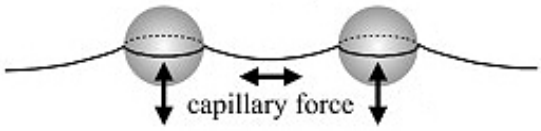

Figure 2.1 The capillary forces between two particles in the liquid-liquid interface.

The particle concentration at the interface is believed to enhance the viscoelasticity of the interface, and thus reducing the film drainage rate and promoting the emulsion stability (Tambe et al., 1994). Additionally, the aggregated particle attaches to the droplet interface and extends themselves into the continuous liquid phase, behaving as 3D particle network via particle-particle interaction as illustrated in Figure 2.2 (Abend et al., 1998).

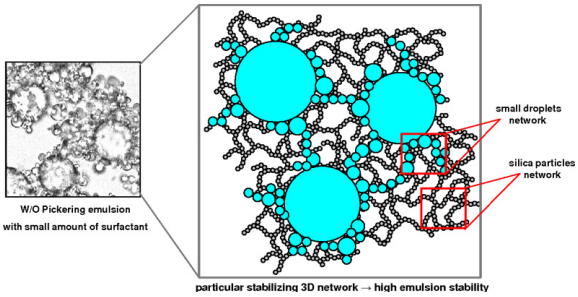

Figure 2.2 3D network formation in SSE (Nesterenko et al., 2014).

2.1.1.3 Particle bridging

Particle bridging is referred to the case when a single particle is absorbed into two droplets simultaneously. Horozov et al. (2006) and Horozov et al. (2005) attributed the generation of the bridge at the contact area to the long-range Coulomb repulsion between particles, induced by the very hydrophobic particles. Apart from the particle affinity, French et al. (2015) observed the particle bridge in the case, where there is insufficient particle to cover the generated interface (as displayed in Figure 2.3). One of the illustrations being an extremely stable emulsion obtained with particle coverage fraction as low as 5%, in the presence of the particle bridge at the contact region (Vignati et al., 2003). In fact, several researchers demonstrated the superior stability of the emulsion exerted by the bridged droplets. For instance, Walker et al. (2011) and Moghimi et al. (2014) proposed the inhibition of the coalescence under the aggregation of clustered droplets connected by the bridged particles. Similar behaviour was

found in the polymer blends (Nagarkar et al., 2012), where the solid-like rheology of the blends was discovered in the presence of the particle bridge.

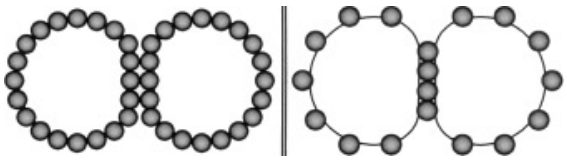

Figure 2.3 Schematic representation of closely packed monolayer (left) and dilute monolayer with bridge (right) (French et al., 2015).

2.1.2 Effective particle types

A wide range of organic and inorganic particles are proved to be able to fulfill the wetting conditions for various oil types, including calcium carbonate, clays, barium, sulphate, morillonite, laponite, carbon black, latex, magnetic particles, carbon nanotubes, and block copolymer micelles (Chevalier et al., 2013). Recent findings revealed several functional/ stimuli-response particles stabilizer, whose wettability could be modified corresponding to given external stimuli (pH-sensitive, thermal-sensitive, ionic-sensitive particles, etc.). In addition, some odd particles are known to be potential stabilizers, such as cationic nanocrystals, spores, and bacteria.

2.1.3 Emulsion types

As shown in Figure 2.4, oil-in-water emulsion (O/W) consists of oil droplet suspended in the continuous water phase whereas water-in-oil (W/O) emulsion is of the opposite. An emulsion in the emulsion is defined as a double emulsion or multiple emulsion, including water-in-oil-in-water emulsion (W/O/W) and oil-in-water-in-oil emulsion (O/W/O). Phase inversion is a process of switching the emulsion type from O/W to W/O or vice versa, which could be achieved either via transitional inversion or catastrophic inversion.

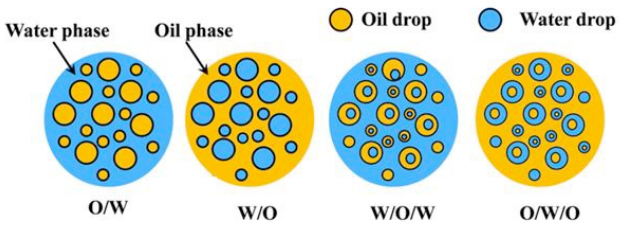

Figure 2.4 Schematic illustration of different emulsion types (He et al., 2015).

2.1.4 The relationship between particle contact angle and emulsion type

2.1.4.1 One type of particle present

If the oil and water phase are of equal volume fraction, the monolayer curvature of the particle coating, to some extent, determines the resulting emulsion type. Specifically, the particle monolayer tends to curve the way such that a greater fraction of particle surface remains on the external phase. In the case of the hydrophilic particle ($\theta_{ow} < 90^{\circ}$), the majority part of the particle resides in the aqueous phase, vice versa for ($\theta_{ow} > 90^{\circ}$) which is displayed in Figure 2.5. A comprehensive study of the particle wettability and corresponding emulsion type was summarized by Aveyard et al. (2003) as shown in Table 2.1. This table shows that the water-wet hydrophilic particles would stabilize O/W emulsion whereas the oil-wet hydrophobic particles favors forming W/O emulsion. Not fully agree with the above opinion, Kaptay (2006) proposed the dependence of emulsion type on the number of particle layers and revealed that the double particle layers with contact angle of $15^{\circ} < \theta_{ow} < 129^{\circ}$ could stabilize O/W emulsion while particles with contact angle of $51^{\circ} < \theta_{ow} < 165^{\circ}$ produces W/O emulsion.

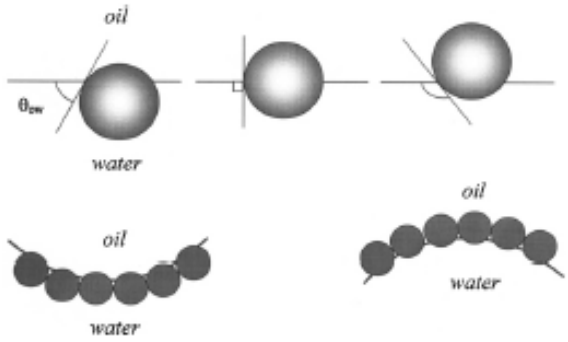

Figure 2.5 The particle position between oil and water phase and the corresponding resulting emulsion type (Aveyard et al., 2003).

Table 2.1 The link between particle contact angle and final emulsion type (Aveyard et al., 2003).

Solid	Oil	Θ_{ow}	Emulsion types
Hydrophilic silica	Dodecane	38	o/w
	Cyclohexane	37	o/w
	PDMS 50cS	81	o/w
	Isopropyl myristate	32	o/w

	Unedecanol	38	o/w
Partially hydrophobic silica	Dodecane	83	o/w
	Cyclohexane	87	o/w
	Isopropyl myristate	101	w/o
	Undecanol	110	w/o
Hydrophobic silica	Dodecane	135	w/o
	Cyclohexane	135	w/o
	PDMS 50cS	172	w/o
	Isopropyl myristate	175	w/o
	Undecanol	151	w/o

The particles are unable to stabilize an emulsion if the particles are either too hydrophilic or too hydrophobic. Instead, they remain dispersed in the water (oil) phase. In order to meet the partial wetting conditions, the surface modification is essential to make the particles more hydrophobic or more hydrophilic, either from 1) adsorption of different types of molecules or from 2) chemical grafting of organic molecules. The latter one is preferred as the organic molecules are more tightly attached through a chemical bond. The grafting degrees can be tuned to control the particle wettability characteristics and the resulting emulsion types (Chevalier et al., 2013).

2.1.4.2 Two types of particle present

Several researchers showed the incapacity of forming a stable particle coating in the presence of two types of particles. Briggs (1921) attempted to produce a stable emulsion with the mixture of silica particle, favouring forming O/W emulsion, and carbon black, favouring producing W/O emulsion. However, the author was unable to produce a stable emulsion using such particle mixture.

In a similar fashion, Whitby et al. (2010) failed to stabilize a W/O emulsion with the mixture of particles (containing extremely hydrophilic silica nanoparticles and hydrophobic titania particles) that can stabilize different types of emulsions on their own. The authors attributed the instability of the final emulsion to a growing proportion of the hydrophilic silica particles, which could barely stabilize W/O emulsion. In contrast, Tarimala et al. (2004) demonstrated the possibility of stabilizing emulsion in the presence of both hydrophobic (~117°) and hydrophilic (~59°) solid particles with a diameter of 1μm. These particles were observed to

simultaneously segregate to the same interface as reported in Figure 2.6, resulting from the amphiphilic nature of the oil-water interface.

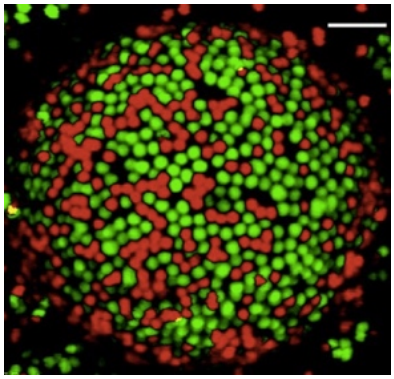

Figure 2.6 Droplet interface of simultaneously self-assembled mixing of green hydrophobic (~117°) and red hydrophilic (~59°) particles with diameters of 1 μm. The scale bar is 5 μm (Tarimala et al., 2004).

2.1.5 Factors affecting the stability of the emulsion

2.1.5.1 Particle concentration

In the conventional emulsion system, the droplet size falls with the surfactant concentration owing to the lowered interfacial tension, till reaching the critical micelle concentration (CMC). (Gelot et al. (1984) observed the same trend in the SSEs system. The authors pointed out the dependence of emulsion stability on the particle concentration, evidenced by the notably improved emulsion stability with an increasing amount of silica particles or carbon graphite. Later, Binks et al. (2004) established the same relationship between emulsion stability and particles concentration, in the emulsification of silicone oil and water with partially hydrophobic nanoparticles. Tcholakova et al. (2008) proposed two regimes of emulsification process based on the emulsifier concentration shown in Figure 2.12 (right). In the “insufficient emulsifier” zone, the droplet size falls dramatically with the particle concentration. As the available particles are unable to cover all the interface generated from breakage, the droplet size mainly depends on the coalescence process. In the “sufficient emulsifier” zone, however, the droplet size remains the same regardless of the emulsifier concentration. Indeed, Frelichowska et al. (2010) confirmed the presence of excess particles from the vial and the small peak in the droplet size distribution in the “sufficient particles regime” as shown in Figure 2.7. Thus, they further attribute the pronounced stability to the excess particles, which exhibits as a gel in the continuous phase.

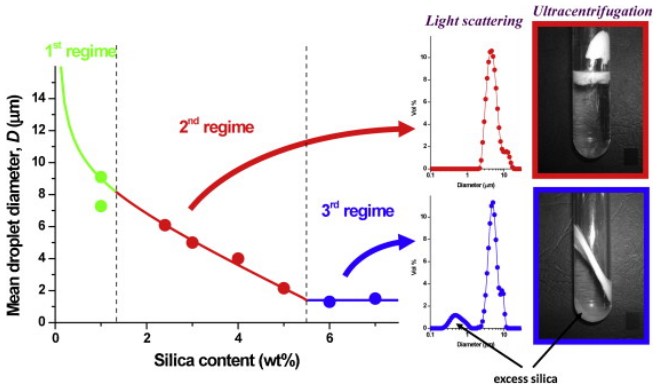

Figure 2.7 The effect of HDK® H30 hydrophobic silica concentration on the mean droplet diameter of o/w SSEs of 2-Ethylhexyl stearate oil (Frelichowska et al., 2010).

2.1.5.2 Oil-water ratio

Chen et al. (2005) achieved the maximum stability of O/W emulsion at an equal oil-water ratio. Binks et al., (2004) reported a dramatically elevated uniformity of oil droplet distribution and droplet size upon increasing of the oil-water ratio. Arditty et al. (2003) validated the limited coalescence phenomena under various mixing conditions and dispersed phase volume fraction, which allows for obtaining a narrow size distribution. Using a high volume fraction of the dispersed phase along with insufficient particles to cover the interface, they successfully produced a monodispersed emulsion. In fact, in given conditions, an elevated oil-water ratio could result in catastrophic phase inversion (explained in detail in the "catastrophic phase inversion" section) (Binks et al., 2004).

2.1.5.3 Emulsification time

Verbich et al. (1997) observed a reduction of droplet size with longer emulsification time. They attribute this observation to the enhanced effectiveness of emulsifier over time. However, Chen et al. (2005) argued that a longer duration is not necessary to result in a more stable emulsion. Instead, they claimed that 15mins of emulsification (in Figure 2.8) is optimal for excellent stability even after standing for 24 hours. Beyond 15mins, the stability weakened as a result of the migration of the emulsifier. Binks et al. (2004) proposed the dependence of emulsification time on the dispersed phase volume regime. At a lower volume fraction, i.e. Φ_d= 33 vol%, the decline of droplet size is observed, along with improved stability, over the emulsification time until insufficient energy is supplied for overcoming further deformation. However, the coalescence dominates at a higher volume fraction (i.e. 60 vol%) close to the phase inversion points, resulting in intensified collision and coalescence events. Thus, continuous agitation could yield phase inversion in this case (in Figure 2.9).

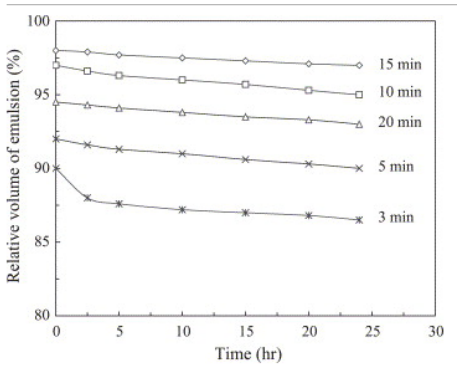

Figure 2.8 The effect of emulsification time on the stability of emulsion (Chen et al., 2005).

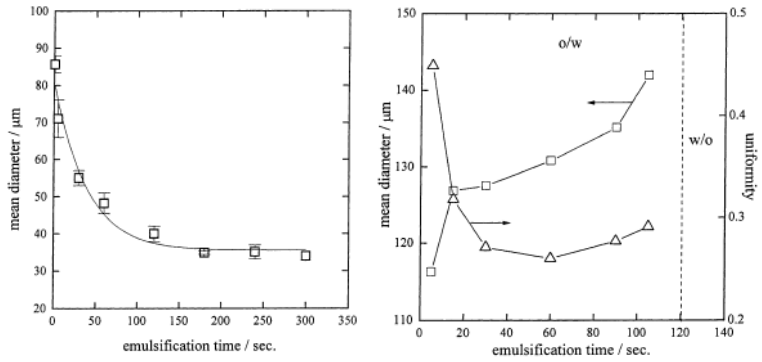

Figure 2.9 The effect of emulsification time on the mean diameter in different oil volume fraction at 350 cS PDMS in 10-2 M NaCl emulsion stabilized by 0.7 wt % hydrophobic silica in the aqueous phase : left: 33 vol %; the right one: 60 vol% (Binks et al., 2004).

2.1.5.4 Electrolyte concentration

Yang et al. (2006) attempted to produce a paraffin O/W emulsion with positively charged LDHs particles. A stable emulsion is obtained under salt condition, while they are unable to produce an emulsion with the removal of salt. Accordingly, the salt promotes the particle aggregation and network formation at the interface, which is confirmed by a declined zeta potential. This structure contributes to the particle adsorption into the interface, resulting in a stable emulsion. Binks et al. (1999) revealed the correspondence of the initiation of the improved emulsion stability to the point where the particles start to flocculate. In both cases, the salt enhances the emulsion stability by varying the particle flocculation conditions. In contrast with the above discussions, Lucassen-Reynders et al. (1963) argued that the particles are rendered more hydrophobic by the salt, altering the extent of particle immersion at the interface.

2.1.6 Novel applications

The unique features of the SSE that do not share with the surfactant-stabilized emulsion allow it to applies to various promising field. The replacement of surfactant with particles brings about

numerous advantages regarding its stability against storage, oxidational, temperature and digestion. Frelichowska et al. (2009) used SSE as an encapsulation for controlled drug release, wherein silica particles coating behaves as a barrier to prevent the transfer of materials. A three-fold higher penetration rate was observed in the SSEs, which is attributed in part to the higher adhesion forces between the particles and the skin. Recently, a wide array of novel stimuli-responsive Pickering capsules have been proposed in the literatures. Exploiting pH- sensitive chitosan coated particles stabilized emulsion as a template, Xu et al. (2005) prepared a colloidosome encapsulated with insulin, which can be released at a controlled rate via pH adjustment. Shah et al. (2010) adopted poly (N-isopropylacrylamide) (PNIPAm) nanoparticles as a thermos-sensitive capsule shell, where the drug is released from the capsule under the shrinkage of the particles at high temperature.

Apart from the drug delivery, SSE could also be encountered in the fabrication of novel materials. With SSEs templates, the researchers are able to prepare materials with desired porosity through polymerization, such as TiO_2-stabilized hybrid hollow spheres (Chen et al., 2007), highly porous nanocomposite polymer foams (Blaker et al., 2009) (in the Figure 2.10 right), macroporous polymers (Ikem et al., 2010; Menner et al., 2007; Zheng et al., 2013) and core-shell structured microsphere (Zhang et al., 2009). The structure of the resulting material was proved to possess high mechanical strength, interfacial area, and permeability (Xu et al., 2005). Generally, the polymerization process is followed to support the structure formed by the SSE. Given that the coating of solid particles resists the further deformation and remain the desired structure, the droplet is then emoved by evaporation, dissolution, drying or freezing. To illustrate, Figure 2.10 (left) gives an example of the 3-steps procedure to obtain a hierarchical porous TiO_2-based material using high internal dispersed phase Pickering emulsion as a template.

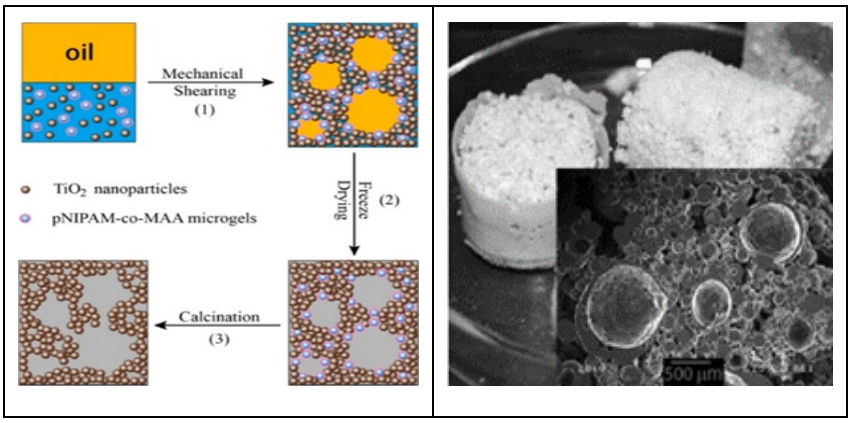

Figure 2.10 Left: 3 steps process for obtaining hierarchical porous TIO2-based materials using high internal dispersed phase SSE as a template (Li et al., 2014). Right: polymer foams, hollow spheres (Blaker et al., 2009).

2.2 Emulsification of solid-stabilized emulsions

Figure 2.11 illustrated the droplet passage during the emulsification process in the mixing tank (Tsabet et al., 2015b). Accordingly, the emulsification process starts by generating the oil/water interface in the high shear zone near the impeller, followed by the particle adsorption in the stabilization zone. If the droplets are not fully covered by the particles, they merge in the coalescence zone which is far from the impeller. Subsequently, they will go back to the impeller zone and completes one circulation (Tsabet et al., 2015b). Tcholakova et al. (2008) presented emulsification process as steps including the deformation, breakage, collision of the droplets and the occurrence of coalescence providing that the adsorption time is longer than the contact time and deformation time (in Figure 2.12).

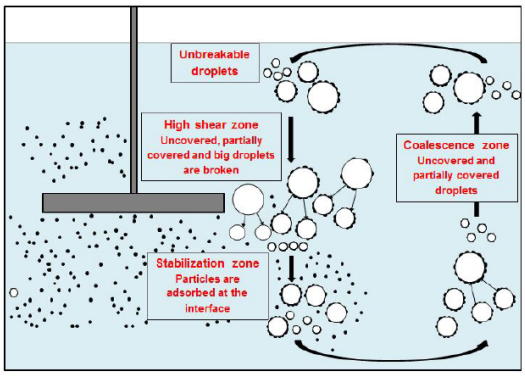

Figure 2.11 The schematic presentation of the emulsification process in the tank (Tsabet et al., 2015b).

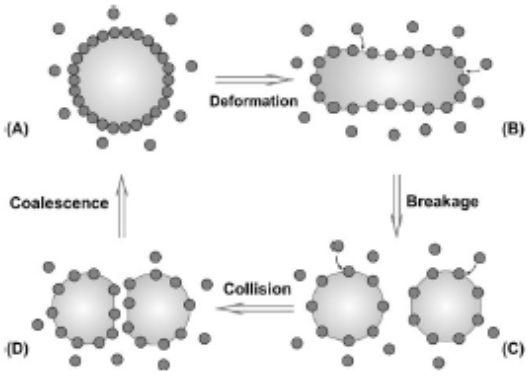

Figure 2.12 The schematic presentation of the emulsification process (A) to (B) deformation; (B) to (C) breakage; (C) to (D) collision; (D) to (A) coalescence (Tcholakova et al., 2008).

2.2.1 Characteristic time

Characteristic times are compared to estimate the probability of a given process during the emulsification. For example, Tcholakova et al. (2008) deduced the coalescence possibility by

comparing the particle adsorption time and droplet deformation time and contact time. Numerous researchers correlated the characteristic time scales (particle adsorption time, droplet deformation time, film drainage time, droplet contact time) involved in the emulsification.

In the turbulent regime, particle adsorption time t_A is identified as the mass of particles adsorption at the interface versus the particle flux towards the interface Γ_M in the following equation (Tcholakova et al., 2008):

$$t_A \approx \frac{\Gamma_M}{C_{pc}(\varepsilon d)^{\frac{1}{3}}} \ldots (2.2)$$

$$\Gamma_M \approx \frac{4C\rho_{pr_p}}{3} \ldots (2.3)$$

From these equations, we can find that the adsorption time extends linearly with the particle size r_p. Thus, one can expect that the particles with higher weight require longer time to adsorb at the interface. The droplet deformation is controlled by the synergic impact of droplet stretching in the flow, along with the droplet shape relaxation resulting from the interfacial tension (Cristini et al., 2003). The time for low viscous droplets in turbulent flow to deform is proposed by linking the sufficiently elongated droplet length over the stretching rate of the droplet in the turbulent flow (Cristini et al., 2003):

$$t_{def} \approx \frac{d^{\frac{2}{3}}}{\varepsilon^{\frac{1}{3}}} \ldots (2.4)$$

Where d is the droplet size and ε is the energy dissipation rate. Levich (1962) derived the contact time t_c between particle and droplet from a dimensional analysis in the turbulent system:

$$t_c \backsim \frac{(d_p+d)^{\frac{2}{3}}}{\varepsilon_{avr}^{\frac{1}{3}}} \ldots (2.5)$$

Where d_p is the particle size. Drainage time t_d is defined as the time duration required for the thin film between droplets to be ruptured. The deformability and mobility of the interfacial colloidal particles are believed to be the major driving forces for the drainage process. The relationship between film drainage time t_d and the film thickness is derived from the Reynolds equation:

$$t_d \backsim \frac{3}{16\pi}\frac{\eta_c {A_f}^2}{F_{col}}\left(\frac{1}{{h_{cr}}^2} - \frac{1}{{h_i}^2}\right) \ldots (2.6)$$

Where η_c is the dynamic viscosity of the continuous phase; $A_f = \pi R_f^2$ is the area of the film at t=0 when $h_{cr}=h_i$; R_f refers to the radius of the film; F_{col} is the collision force exerted on the droplets; h_{cr} is the critical film thickness and h_i is the initial film thickness. Jeelani et al. (1994) proposed the film drainage time t_d equation under the condition of immobilized film, where they assumed zero interfacial tangential velocity to the sphere surfaces at the particle boundary:

$$t_d = \frac{3\pi R_f^4 \eta_c}{4h_{cr}^2 F_{col}[1+(\frac{3\eta_c l_{cric}}{2h_i \eta_d})]} \ldots (2.7)$$

Here, η_d is the dynamic viscosity of the droplet, l_{cric} is the circulation distance between the droplet interface and the zero velocity into the droplets.

2.2.2 Interface generation

The droplet size, interfacial tension, viscosity of both phases and hold up fraction play essential roles in the deformation of droplets (Coulaloglou, 1977). Under the mechanic energy, the interfaces are deformed and generate some large droplets, which proceed to break into smaller ones. In general, the extent of fragmentation is determined by the amount of energy supply during the emulsification. An elevation of the local dissipation energy ε_{avr} was reported to be the most effective way of reducing droplet size (Graillat et al., 1990). The breakage ceases when the generated energy is insufficient for further droplet deformation (Whitesides et al., 1995). In turbulent flow, the force generated by the eddies containing in the turbulent flow is able to deform the droplets. However, if the eddy size is larger than the droplets, it will carry the droplets rather than breaking them.

Within the smallest scale of turbulent (Kolmogorov length), the viscosity is the dominant effect due to the conversion of the kinetic energy to the heat. In this case, the Capillary number Ca, defined as the interplay between viscous stresses to interfacial tension (capillary pressure) and controls the droplet deformation and shape, is used to determine the droplet breakage. Above the Kolmogorov scale λ, however, the droplet ruptures at high turbulent kinetics over the interfacial tension, depending on the Weber number We.

Weber number $$\mathrm{We} = \frac{\rho_c N^2 D^3}{\sigma} \ldots (2.8)$$

Reynolds Number $$\mathrm{Re} = \frac{\rho_c N D^2}{\eta} \ldots (2.9)$$

Capillary number $Ca = \frac{We}{Re}$ …(2.10)

Kolmogorov length scale $\lambda = (\frac{\nu^3}{\varepsilon_{avr}})^{\frac{1}{4}}$ … (2.11)

Power consumption $P = N_P \rho_c N^3 D^5$… (2.12)

Energy dissipation rate $\varepsilon_{avr} = \frac{P}{m_t}$ … (2.13)

Where ρ_c is the density of the continuous phase; N is the rotation speed; D is the diameter of the impeller; σ is the interfacial tension; ν is the kinetic viscosity; η is the dynamic viscosity; N_P is the power number and m_t is the total mass of the system.

In fact, two forces are acting on the droplet in the turbulent regime: one is a disruptive force τ_c derived from the turbulence velocity fluctuation in the hydrodynamic, while the other one is cohesive force τ_s, arising from the interfacial tension, which opposes the droplet deformation (Tsabet, 2014). Kolmogorov et al. presented the first successful theory in droplet breakage in turbulent flow. The authors correlated the maximum stable droplet size d_{max} in given turbulent flow by equating the disruptive with the cohesive forces. If the dispersed phase is of high viscosity, the viscous stress τ_d within the droplets must be taken into account to the cohesive forces.

$$\tau_c \approx \rho_c \varepsilon^{\frac{2}{3}} d^{\frac{2}{3}} \ldots (2.14)$$

$$\tau_s \approx \frac{\sigma}{d} \ldots (2.15)$$

$$d_{max} = C_1 (\frac{\sigma}{\rho_c})^{\frac{3}{5}} \varepsilon_{max}^{\frac{-2}{5}} \text{ (low viscous dispersed phase) } \ldots (2.16)$$

$$\tau_d \approx \mu_d \frac{(\tau_c/\rho_d)^{\frac{1}{2}}}{d} \ldots (2.17)$$

2.2.3 Particle adsorption at the interface

In the flotation process, the bubble-particle interaction was first divided into three main steps: 1) collision: contacting between the bubble and the particles 2) attachment: drainage and rupture of the continuous film and the contact line movement. 3) stability: the occurrence of detachment in the case of unstable bubble-particle aggregate (Derjaguin et al., 1993). In parallel to the flotation system, particle adsorption onto a liquid-liquid interface involves the collision between particles and the droplets, driven by the hydrodynamic force, the stabilization of particles at the interface, and the detachment of the adsorbed particles by shear (Tsabet, 2014).

The particles will only be stabilized at the interface under these two conditions: 1) the film between the particle and interface has to be ruptured; 2) the formation of the three-phase contact line. The particle adsorption possibility at the interface is estimated from a comparison between the contact time versus the film drainage time, which is similar to the widely-studied coalescence efficiency E_{coal} between two droplets.

$$E_{coal} \approx \exp(-\frac{t_d}{t_c})\ldots(2.18)$$

The adsorption takes place if the drainage time is shorter than the contact time, which signifies that the film could be drained during the contact. The formation of a three-phase-contact line (TPC line) is also responsible for the stable meniscus around the particles after the collision. Minimum TPC line radius has to be achieved during the collision of particle and droplet, to obtain the TPC line expansion. The expansion of TPC line is very rapid for only a few milliseconds, Vachova et al. (2013) recorded the whole process with the high-speed digital camera, as shown in Figure 2.13 and estimated the expansion velocity of the TPC line υ_{TPC} by:

$$\upsilon_{TPC} = \frac{dR_{TPC}}{dt} = \frac{\gamma_{ow}}{9\ln(R_m/L_m)\eta}(\theta_e^3 - \theta^3(t))\ldots(2.19)$$

Where R_m refers to the macroscopic characteristic length (particle radius R_p); L_m is the molecular characteristic length; θ_e is the equilibrium contact angle; R_{TPC} is the radius of the TPC line; The theoretical critical TPC line thickness R_{crTPC} is assessed based on the thermodynamic balance of the free energy of the film before rupture and after the formation of TPC line:

$$\frac{2h_{crTPC}}{R_{crTPC}sin\theta_e} = 1 + (\frac{1-cos\theta_e}{sin\theta_e})^2 \exp(\frac{-2h_{crTPC}}{R_{crTPC}sin\theta_e})\ldots(2.20)$$

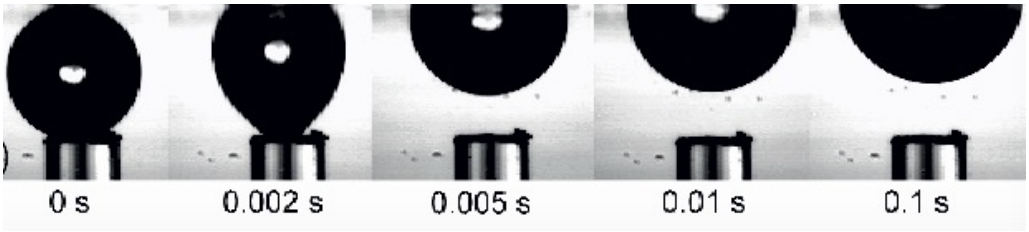

Figure 2.13 Sequence of photos showing the bubble adhesion on a horizontal plane: the evolution of TPC line as a function of time (Vachova et al., 2013).

There is a high chance that the particle could be sheared off from the interface in the high shear zone, where it has the highest energy dissipation rate (40-120 times of the average). To determine if the particles could be detached, the force balance must be taken into consideration

within the circulation time. Attachment force of the spherical particles in the liquid interface is defined as (Scheludko et al., 1976):

$$F_{att} = 2\pi\gamma_{ow}R_p(\cos\left(\frac{\theta_{ow}}{2}\right))^2 \ldots(2.21)$$

γ_{ow} and θ_{ow} are the interfacial tension and contact angle between oil and water respectively; R_p is the particle radius. On the other hand, the detachment force of a spherical particle at the interface is mainly stem from the sum force of hydrodynamic, *Laplace* pressure and particle self-weight. The *Laplace* pressure force F_{lap} exerted on each particle would be (Tsabet et al., 2015b):

$$F_{lap} = (\pi R_p^2 sin^2\theta_{ow})\frac{2\gamma_{ow}}{R_d} \ldots(2.22)$$

moreover, the particle weight F_g is presented as:

$$F_g = \frac{4}{3}\pi R_p^3\rho_p g \ldots(2.23)$$

Scheulze et al. (1993) proposed the hydrodynamic force F_{hyd} exerting on the particle at the oil-water interface:

$$F_{hyd} = \frac{4}{3}\pi R_p^3\rho_p a_t \ldots(2.24)$$

Where the acceleration a_t in the flow field is given as (Scheulze et al., 1993):

$$a_t = \frac{1.9\varepsilon_{avr}^{\frac{2}{3}}}{(R_d+R_p)^{\frac{1}{3}}} \ldots(2.25)$$

Here, R_d is the droplet radius. This collision of the large particle contributes to the detachment, which should be taken into account as part of detachment force.

2.2.4 Limited coalescence

The coalescence involves two steps, collision of the partially covered droplets and a subsequent film drainage process. The coalescence will take place if the film drainage time is shorter than the drop contact time. Otherwise, the two droplets would repulse from each other. For the conventional emulsion, the surfactant plays a pronounced role in lowering the interfacial tension and suppressing the coalescence. Jeffreys et al. (1971) explained that the enhanced droplet deformation is arising from the diminished interfacial tension and results in a larger drainage area and longer drainage time. Alternatively, Hodgson et al. (1969) attributed the inhibited coalescence to the reduced interfacial mobility.

Pickering (1907) first found that the aggregation of fine surface-active particles hinders the coalescence process. Ata (2008) visualized and recorded the coalescence dynamics between air bubbles covered with particles (displayed in Figure 2.14) and highlighted the impact of particles in coalescence. The notable difference in the coalescence dynamic between the uncoated-uncoated bubbles and between the particle-coated bubbles again confirms the resistance of coalescence exerted by the particle coating. Whitesides et al. (1995) claimed the coalescence starts after the droplet fragmentation until the particle coverage at the drop interfaces is sufficient to prevent further coalescence. Following the pioneering work, Arditty et al. (2003) termed such unique behaviour as *limited coalescence* and established a linear relationship between average droplet size and the mass of particles m_p at a given degree of particle coverage.

$$\frac{1}{d} = s_f \frac{m_p}{6V_d} \ldots (2.\ 26)$$

Here, s_f is the droplet surface area covered by per unit mass of particles, V_d is the volume of the dispersed phase, d is the droplet diameter. In the absence of particles, the interfacial area is reducing gradually to seek for the lower thermal condition. As indicated in the correlation, the final droplet size falls with particle concentration, while particle density at the interface remains constant (Arditty et al., 2003). In line with this theory, Tsabet et al. (2015a) reported a sharp reduction in droplet size with particle until reaching the plateau, beyond which the drop size is governed by the system breakage capacity. Exploiting the limited coalescence model, Pauchard et al. (2014) successfully predict the size of W/O emulsion stabilized with asphaltenes. Likewise, Daware et al. (2015) validated the model in predicting the droplet size of an emulsion stabilized by micron sized silica rods. In contrast, Gautier et al. (2007) argued that the coalescence cease further before the closely-packed particle interface in the presence of particle bridges, for this reason, they insisted that inter particle attractive interaction could also prevent the droplet against further coalescence.

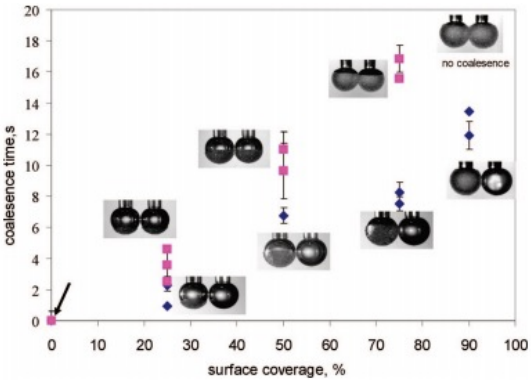

Figure 2.14 Coalescence time as a function of the surface coverage area by the particles. Square indicates the bubbles are both coated by particles whereas the diamond-shaped indicates only one bubble covered by particles (Ata, 2008).

Apart from the dependence on the particles, the coalescence rate is also sensitive to the parameters which could influence collision and drainage process. In detail, coalescence process is affected by the droplet size during the film drainage process. After establishing the drainage film, a larger droplet possessing a larger drainage area requires more time to drain the film, and hence leading to a longer coalescence time. Moreover, Kamp et al. (2017) and Binks et al. (2004) claimed that a higher dispersed phase volume fraction elevates the collision frequency between the droplets, resulting in an enhanced coalescence probability. The viscosity ratio affects the coalescence through the drainage process, whereas the impeller speed varies the coalescence frequency during the collision process.

2.2.4.1 Techniques for investigating coalescence frequency/ breakage frequency

Howarth (1967) made the first attempt to control the droplet size by a coalescence process alone, where a sudden reduction of rotation speed induced the variation of the fluid hydrodynamic condition. This technique was then used to determine the coalescence frequency quantitatively through the droplet population balance (Tobin et al., 1990). Later, Taisns et al. (1996) deduced the extent of droplet coalescence from the variation emulsion refractive index, by mixing a natural and a brominated emulsion. Inspired by the previous techniques, Danner et al. (2001) studied the coalescence process by colouring the dispersed droplets with two dyes. The colour change (a third colour) resulting from coalescence is then quantified by *Monte Carlo simulation* (Danner et al., 2001).

Based on the fact that the fragmentation dominates the droplet size in the impeller region, Konno et al. (1982) visualized the breakage process using a high-speed camera. The camera was set to the location near the impeller region. The recording was initiated once the dispersed phase was added to the continuous phase. Nienow (1994) performed a investigation of the

breakage process alone by introducing surfactant to the system, in order to avoid the coalescence. Norton et al. (2009) studied the breakage process by reducing the impeller speed from 250 RPM to 500 RPM, whereas the coalescence process is followed by a step-down of impeller speed from 1000 RPM to 500 RPM.

2.3 Coalescence and demulsification of solid-stabilized emulsions

After homogenization, the oil and water phases tend to separate, seeking lower thermal energy in the system by reducing the interfacial area. Five emulsion stability types are commonly encountered, including well-dispersed good emulsion, coalescence, flocculation, creaming, and breaking of the emulsion (displayed in Figure 2.15). Within a given distance, the droplets tend to flocculate under the attractive interaction energy. Subsequently, the creaming/ settlement, flocculation, coalescence, and even separation process will take place. For the coalescence to occur, the thin film between the droplets must be ruptured (Whitby et al., 2016).

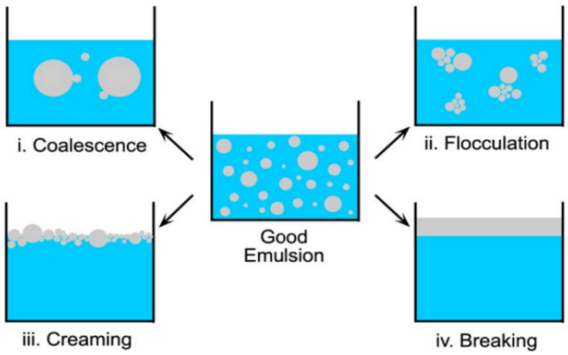

Figure 2.15 Emulsion destabilization types (Marko et al., 2013)

Besides coalescence, droplets coarse through the Ostwald ripening based on the solubility of the organic phase in the aqueous phase. Ashby et al. (2000) reported the continuous droplet swelling process in the O/W emulsion stabilized by laponite clay nanoparticles. According to the authors, the process did not halt until the particles formed an insoluble barrier around the droplets. Ostwald ripening in the flocculated toluene droplets-in-water emulsion was observed by Juarez et al. (2012). Their work revealed the continuous transfer of the toluene from the smaller droplet to larger ones (as shown in Figure 2.16) until there are insufficient particles to attach at the interface. Likewise, the swelling of droplets arrests when there are insufficient particles to cover the droplets or when the particle adsorption is faster than the Ostwald ripening (Ettelaie et al., 2014).

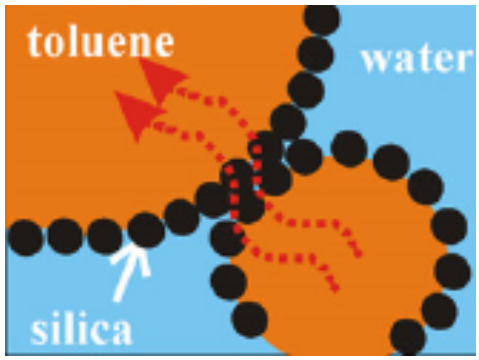

Figure 2.16 Schematic presentation of the Ostwald ripening between two flocculated droplets stabilized by silica (Juarez et al., 2012).

2.3.1 Destabilization caused by the addition of a second emulsifier

Some researchers observed the particle detachment and even emulsion destabilization when adding surfactant to the SSE. On the one hand, some insisted that surfactant replace the particles and cause destabilization. As an example, exposing the glyceride crystals to the surfactant, Lucassen-Reynder et al. (1963) attributed the particle detachment to the lower particle interaction caused by the added surfactant, which is evidenced from the reduced interaction energy between glyceride crystals and an unchanged contact angle. Reynaert et al. (2006) supported that the surfactant adsorption could interfere with particle interaction forces by showing a looser latex particle network in the presence of the SDS solution. The particles could even be displaced entirely with a surfactant if the interfacial tension is sufficiently reduced by adding it.

On the other hand, Whitby et al. (2009) argued that the surfactant modifies the wettability of the particles and leads to the particle desorption. Namely, the adsorption of surfactant alters the extent of particle immersion in the liquid as well as the particle interaction forces (Alargova et al., 2004; Reynaert et al., 2006; Subramaniam et al., 2006). Katepalli et al. (2013) showed the destabilization in an opposite case by adding hydrophobic particles to the non-ionic surfactant-stabilized emulsion. The authors attributed it to the adsorption of the particles on the surfactant. Thus, the strong hydrophobic interactions between the particles result in the depletion of the surfactant from the interface. Similarly, Legrand et al. (2005) added hydrophilic silica particles to a cationic surfactant-stabilized bitumen-in-water emulsion, observing the partial coalescence under application of shear. In fact, Binks et al. (2007) concluded that the coalescence undergo in both preparation protocols: 1) addition of nanoparticles to the ionic surfactant-stabilized emulsion 2) inverse case, which, according to their study, is linked to the competitive effect between particle wettability and interfacial tension on the magnitude of adsorption energy.

2.3.2 Catastrophic phase inversion

Catastrophic phase inversion is triggered upon increasing the dispersed phase volume fraction or altering systems conditions, such as phase viscosity and stirring protocols (Rondon-Gonzalez et al., 2007). In detail, it takes place under the collapse of the dynamic balance between coalescence and breakup. For example, Binks et al. (2000a) conducted the catastrophic phase inversion from W/O to O/W emulsion at 70 vol% of water fraction, using nanometer-sized hydrophobic silica alone. Further, Binks et al. (2003) performed a systematic investigation of the inversion of triglyceride O/W emulsion, where they highlighted the role of the initial location of particles (Figure 2.17). For the particles initially dispersed in the water phase, the emulsion inverts from W/O to O/W at a low water fraction around 20 vol%, whereas, the emulsion inverts approximately 60 vol% when dispersing particles in the oil phase. The remarkable difference in the inversion points reportedly regards the hysteresis in contact angle at the three-phase line.

2.3.2.1 Mechanism of catastrophic phase inversion

Vaessen et al. (1996) argued that phase inversion occurred under the condition where the coalescence event overwhelmed the breakup event at sufficiently high dispersed phase volume. Indeed, the breakage frequency is proportional to the number of droplets per volume unit, whereas the coalescence frequency is proportional to the number of droplets per volume squared. Brooks et al. (1991); Sajjadi et al. (2000) considered the multiple emulsion as a precursor to phase inversion, which facilitates the process. The balance is set up between the inclusion and escape of droplets concerning the multiple emulsion. Groeneweg et al. (1998) and Jahanzad et al. (2009) attributed the phase inversion to the effective volume fraction induced by the inclusion mechanism, where the higher dispersed phase is achieved by enclosing the continuous phase into the dispersed phase under agitation. At a given dispersed phase volume fraction (e.g.75 vol%) near the phase inversion point, the inclusion could be accomplished merely by increasing the mixing time (Binks et al., 2003), the process of which is depicted in Figure 2.18. For the first time, the authors observed the multiple emulsion (Figure 2.18) in the SSE stabilized by a single particle type.

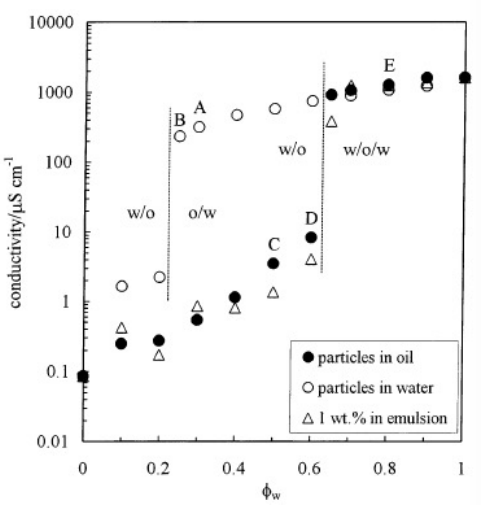

Figure 2.17 The effect of initial particle location on the emulsion type of water-tricaprylin batch emulsions stabilized by hydrophobic silica particles (Binks et al., 2003).

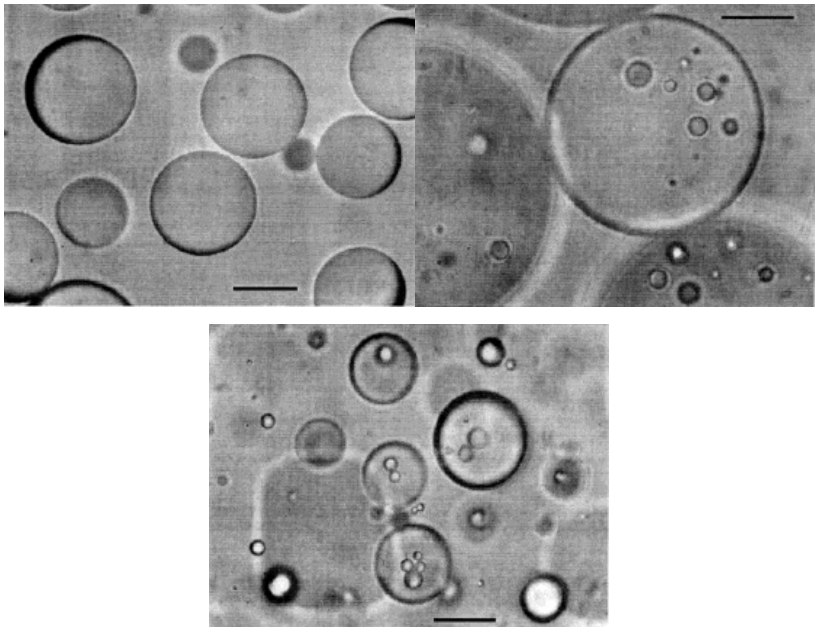

Figure 2.18 The effect of mixing time on the 75 vol% O/W emulsion prepared from 2 wt % particles in water from left to right are original o/w after 2 min, multiple w/o/w after a further 10 min and mixture of multiple o/w/o and simple w/o after a 13mins' mixing (Binks et al., 2003).

For the system containing surfactant, the phase inversion could be achieved merely by submitting an abnormal emulsion (the external phase is not predicted from Bancroft's rule) under agitation, without adding more dispersed phase volume fraction or emulsifier (Mira et al., 2003; Rondon-Gonzalez et al., 2009; Rondon-Gonzalez et al., 2008). Various factors including the initial water to oil ratio (Rondon-Gonzalez et al., 2006), phase viscosity (Rondon-

Gonzalez et al., 2007), stirring intensity (Mira et al., 2003) and the initial surfactant concentration (Rondon-Gonzalez et al., 2006) are reported to influence the phase inversion points under agitation alone.

Phase inversion is known to occur under the collapse of balance between droplet inclusion and escape. In a comparison between the phase inversion points in two cases, toluene-in-water emulsion inverts at 50~60 vol%, while triglyceride oil-in-water emulsion inverts at nearly 90 vol%. Groeneweg et al. (1998) attributed the droplet inclusion to coalescence frequency, since the higher coalescence frequency arising from, the less viscous toluene leads to a lower inversion point. Knowing that the emulsifier suppresses the coalescence frequency, Groeneweg et al. (1998) also compared the phase inversion points of the water-in-triglyceride-oil emulsion in the case containing and without surface-active impurities, where higher phase inversion point was observed with the surfactant present. Nevertheless, Ohtake et al. (1988) believed that the inclusion results from the droplet deformation (Figure 2.19(a)), driven by the pressure fluctuation and the natural tendency of the emulsifier. Followed by which, a thread of oil forms and ruptures into numerous small droplets as depicted in Figure 2.19 (b).

Regarding the escape mechanism, Groeneweg et al. (1998) observed the rupture of the film during the approach of the inner droplets to the boundary wall, with the escape of droplet as a result. Later, Klahn et al. (2002) highlighted the significant role that the drainage rate of the film is playing in the process of escape.

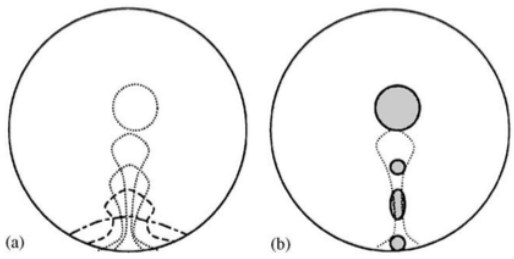

Figure 2.19 Schematic presentation of droplet formation by droplet deformation (Ohtake et al., 1988).

2.3.2.2 Emulsion destabilization by phase inversion

Phase inversion from W/O to O/W emulsion provides an avenue for facilitating the separation process. According to the Stokes' law:

$$u_t = \frac{(\rho_p - \rho) g d_p^2}{18\mu} \quad \ldots(2.27)$$

Where u_t is settling or creaming velocity, ρ_p is droplet density, d_p is droplet diameter and μ is fluid viscosity. From the inspection of the above equation, one can find that placing the less viscous phase (i.e. water) as the continuous phase imparts a more rapid creaming velocity of dispersed droplets (i.e. oil), resulting in a promoted coalescence.

2.3.3 Transitional phase inversion

Unlike the catastrophic phase inversion, transitional phase inversion is triggered by the variation of the particle wettability. The use of coloured hydrophilic and hydrophobic particles allows (Binks et al., 2017) to demonstrate the occurrence of the phase inversion at the interface.

At an equal volume fraction of oil and water, a variation of the mass ratio at constant total particle concentration can result in transitional phase inversion (Binks & Lumsdon, 2000b). Preuss et al. (1998) showed a linear reduction of the contact angle of the particle mixture with the increased portion of hydrophilic particles, which explained the above behavior. Furthermore, Binks et al. (2000b) concluded that the phase inversion takes place upon adding particles favouring the dispersed phase (such as, adding hydrophilic particles to W/O emulsion or adding hydrophobic particles to the O/W emulsion). Philip et al. (2005) performed the transitional phase inversion by elevating the concentration of a single type of particle (silica particles) alone. In fact, the gel formation via silanol-silanol hydrogen bond at higher silica particle concentration alters the particle wettability due to the reduction in the effective silanol content at the surface. Additionally, the wettability of particles could be modified by adding surfactant (see detail in section 2.3.1), which may result in transitional phase inversion.

2.3.4 Utilization of a stimuli-responsive particle stabilizer

Recently, considerable attempts have been made to stabilize the emulsion with stimuli-responsive particles (including pH, temperature, CO_2, light intensity, ionic strength, and magnetic field sensitive particles), which possess the capacity of responding to external triggers. Some non-modified nanoparticles, such as graphene oxide and biodegradable chitosan, are reported to be tuned by pH. Otherwise, surface-functionalization is required to render the particles a surface property that sensitive to the pH change. Haase et al. (2010) performed the emulsification with silica nanoparticle coated by 8-hydroxyquinoline (8-HQ). A stable emulsion was obtained between a narrow pH range (4.5~5.5), lower than which, the bi-layer formation of 8-HQ desorbs from the interface, higher than which, the presence of insufficient 8-HQ causes coalescence (Figure 2.20). Indeed, acidity plays a role in imparting the hydrophobic character, which is evidenced by the contact angle measurement. Fujii et al. (2006)

revealed the detachment of poly-silica nanocomposite particles under acidic conditions. Brugger et al. (2008) and Ngai et al. (2006) reported a similar behaviour in the emulsion covered with micro-gel. Tang et al. (2015) explained that tuning the pH of the aqueous phase leads to the propagation of the pH-sensitive functional group. More recently, CO_2 responsive particles have been proposed as an indirect approach of adjusting the pH of the system (Liang et al., 2014; Morse et al., 2013). The protonation conditions varies in the presence of CO_2, thus allowing the transformation from particles into micro-gels (Qian et al., 2014). Ultimately, the expelling of micro-gel will result in destabilization. Considering that adjustment of the pH is not suitable in some cases, thermal responsive grafted particles are used alternatively. The thermal-sensitive particles can increase the hydrophobicity of the particle under higher temperature. As an illustration, with a thermal responsive brushes poly (2-(dimethylamino)ethyl methacrylate) brushes (PDMAEMA) grafted on the silica nanoparticles, Saigal et al. (2010) achieved the separation of emulsion above the critical flocculation temperature. Later, a similar manner was observed when using poly(NIPAM) brushes (poly(NIPAM)-g-CNCs) as a thermal-responsive polymer (Zoppe et al., 2012). Nevertheless, limitations still exist in the application at a larger scale, where a significant amount of energy is required for heating or cooling.

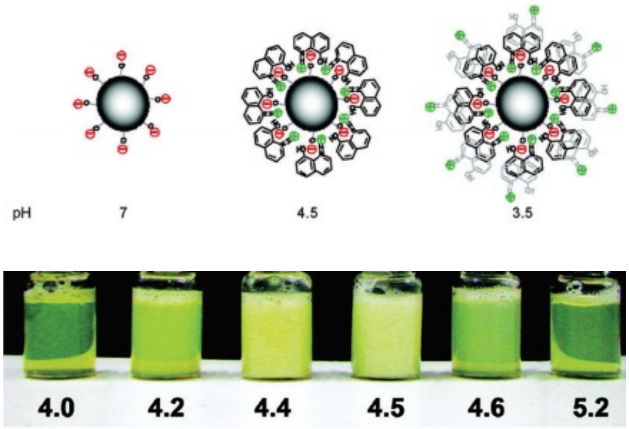

Figure 2.20 Upper illustrates the reaction between pH-responsive nanoparticles and 8-HQ. Lower demonstrate the emulsion stability at different pH using 8-HQ coated nanoparticles (Haase et al., 2010).

2.4 Summary of the literature review

As reviewed above, the stabilization mechanism of the solid-stabilized emulsion is well-addressed. Most works regarding the SSE focus on exploring the impact of external or internal factors on the characterization of the final emulsion while the dynamic studies in the emulsification process are relatively rare. Despite extensive studies on the coalescence and

breakage process involved in the liquid-liquid system, the knowledge regarding the impact of particles in the dynamic emulsification process is quite limited.

For the conventional emulsion stabilized with surfactant, the general mechanism of catastrophic phase has been partially elucidated through the inclusion and escape theory. However, for the SSEs system, the factors that can trigger phase inversion have yet to be determined. Therefore, a fundamental understanding of the mechanisms driving phase inversion is necessary.

Various structure of the particles at the interface (including bridged particles, 3D network formation, double layer, etc.), along with their effects on the emulsion stability has been proposed in the literature. A number of researchers attempted to destroy the particle structure at the interface (for instance, the addition of the surfactant, salt, applying shear, etc.) in order to break the emulsion. Nevertheless, the studies on the dynamic particle behaviour at the interface is still lacking.

CHAPTER 3 OBJECTIVES

This work aims at examining the role of particles in the emulsification process in order to explore a green, cost-effective approach to destabilize the solid-stabilized emulsion. The three specific objectives are listed as follows:

- Validation of PVM® for a real-time droplet size measurement in the 2nd article.
- Determine the impact of particles on each mechanism (droplet breakage, and coalescence) in the emulsification process. Accomplish of this objective has been presented in the 1st article.
- Determine the triggering parameter as well as the mechanism of in the catastrophic phase inversion of the solid-stabilized emulsion. Accomplish of this objective has been presented in the 2nd article.
- Determine the dynamic particle behaviour at the interface in response to fluid dynamics. Accomplish of this objective has been presented in the 3rd article

CHAPTER 4 ARTICLE 1: THE IMPACT OF PARTICLES ON BREAKAGE AND COALESCENCE PROCESSES DURING THE PREPARATION OF SOLID-STABILIZED EMULSIONS

Article history: Submitted to *Industrial & Engineering Chemistry Research* on November 27, 2018.

Authors: Bing Wan, Emir Tsabet, Louis Fradette

4.1 Summary

The dynamics of droplet breakage and coalescence is crucial for Pickering emulsion-based processes. We tracked the evolution of droplet size in real time using a probe-based microscope (PVM®; Mettler-Toledo, USA). Our results showed that placing the PVM® probe at any given location in the tank can provide information on the transient droplet size for a given process. We also studied the impact of particles during different stages of silicone oil-in-water emulsions stabilized with soda lime glass microspheres under controlled operating conditions. The particles lowered breakage efficiency by modifying the properties of the continuous phase in the early stage of emulsification (within 10 mins) where droplet breakage predominates. We also studied the effect of the interface–coverage potential ratio on the coalescence process. The dynamic balance of breakage and coalescence was disrupted when emulsification was controlled by the coverage potential. We obtained a bimodal size distribution of droplets using a formulation containing insufficient particles and a narrow unimodal size distribution with a formulation that provided sufficient particles to cover the system-generated interface. These two outcomes likely resulted from different breakage mechanisms.

Keywords: solid-stabilized emulsion (Pickering emulsion), breakage, coalescence, solid particles, emulsification process, droplet size evolution

4.2 Introduction

Solid-stabilized emulsions, also known as Pickering emulsions, are encountered in a variety of industrial processes, including crude oil dewatering, mining processes, and paint production. Until now, most research has focused on studying the impact of the various phases (particles, oil, and water) on the properties of the final emulsion, including emulsion type, size, rheology, and stability. However, the behavior of emulsions during the emulsification process is not well understood. The parameters that have received the most attention are particle type (Binks & Whitby, 2005; Sullivan et al., 2002), wettability (Binks et al., 2000c), size (Tsabet et al., 2015a),

and concentration (Frelichowska et al., 2010); oil type (Binks et al., 2000b), viscosity (Fournier et al., 2009), (Tsabet et al., 2015a), and polarity (Tsabet et al., 2015a); the pH of the aqueous phase (Binks & Whitby, 2005; Yan et al., 1996); and ionic strength (Horozov et al., 2007; Tsabet et al., 2015a). It is now well established that particle affinity with both phases is the key parameter controlling the type, size, and stability of emulsions (Aveyard et al., 2003; Binks et al., 2000c, 2000d) while their rheology is affected by particle interactions and the rheological behavior of the liquid phases (Aveyard et al., 2003; Binks et al., 2000b, 2000c; Binks et al., 2003; Horozov et al., 2007).

Tsabet (2015a and b) recently described the dynamic aspects of emulsions. They proposed that the generation of a solid-stabilized emulsion in an agitated tank follows a cycle from drop breakage-particle attachment to coalescence before it reaches an equilibrium (Emir Tsabet, 2014; Tsabet et al., 2015b). They reported that the impeller zone is dominated by interface generation and breakage, whereas particle attachment and coalescence take place outside this highly turbulent region. By analyzing the role of particles at each step, Tsabet (2015b) assumed that stabilization cannot be achieved unless the droplets are fully covered by particles (Tsabet et al., 2015b). They reported that the final emulsion size is controlled by the interface generation capacity of the system when there are enough particles to cover the interface, and that it is controlled by the particle coverage potential when there are not enough particles to cover the system-generated interface which they referred to as the limited coalescence mechanism (Gautier et al., 2007; Arditty et al., 2003; Whitesides et al., 1995). However, they showed that coalescence can stop before a closely packed particle network is formed around the droplets when bridges are formed between particles adsorbed to different droplets (Gautier et al., 2007).

The stabilization process involving particles was described by Tsabet (2015b) as a competitive effect between coalescence and particle attachment at the interface, which relied on collision efficiency, three-phase contact line efficiency, and coverage efficiency (Tsabet et al., 2015b). The stabilization mechanism was also studied by Tcholakova et al. (2008), who reported that the ability of particles to form a strong barrier around droplets depends on high desorption energy and strong capillary forces between particles trapped in liquid films (Tcholakova et al., 2008). They also defined a coalescence condition based on a comparison of particle adsorption time and droplet contact time (Tcholakova et al., 2008). Adsorbed particles not only form a steric barrier around droplets that hinders coalescence, they also make the interface more elastic, which can inhibit breakage (Arditty et al., 2005). Mei et al. (2016) reported that nanoparticles attached to the interface increase the critical capillary number at which breakup takes place.

Particles can affect both breakage and coalescence because of the properties of the continuous phase (Emir Tsabet, 2014). Given that breakage results from the competitive effect of forces that facilitate interface generation and those that hinder surface creation (Chen et al., 1967; Coulaloglou, 1977; Calabrese et al., 1986; Doulah, 1975), which is represented by the Weber number, the presence of particles enhances inertial effects. On the other hand, particles play a role in preventing coalescence by reducing the droplet–droplet collision frequency (Wright et al., 1994) and delaying film drainage between droplets during collisions (Chesters, 1991).

Very little work has been devoted to identifying the mechanisms involved in the emulsification process using solid particles and to determine the role of particles in each step in the process leading to the generation of an emulsion. These investigations were limited by the fact that the contribution of each mechanism was estimated by characterizing emulsions at the end of the process. We overcame this limitation by using a microscopic probe to track in-line droplet size during the emulsification process using the procedure developed Wan et al. (2017). The present study investigated the impact of particles in the breakage and coalescence involved in the emulsion generation process.

4.3 Materials and Methods

We performed a systematic investigation of the effect of particles on the evolution of droplet size under various conditions during the emulsification process, including the probe location, the preparation procedure, the particle concentration, and changes in impeller speed. We began by determining the importance of the real-time probe location in the emulsification tank. The impeller and coalescence zones were then used to investigate the breakage and coalescence processes, respectively. Particles were added at different time points during the emulsification process, including the early stage and the equilibrium state, to examine the effect of the disruption caused by the particles on the balance between breakage and coalescence. The coalescence mechanism was also studied by varying the impeller speed. The impact of particle concentration on the results was studied using concentrations ranging from no particles to sufficient particles (Table 4.2).

4.3.1 Materials

Pure silicone oil with a viscosity of 50cSt at 25°C (Clearco Products Co. Inc., USA) was used as the dispersed phase, and distilled water was used as the continuous phase. Soda lime glass microspheres with a Sauter mean diameter of d_{32}=3 μm and a measured contact angle at the oil/water interface of 90° (Cospheric, USA) were used in all the experiments.

4.3.2 Experimental Methods

4.3.2.1 Emulsification setup

Emulsifications were performed using a pitched 3-blade turbine impeller in a non-baffled flat bottom tank. The impeller was off-centered to avoid the formation of a vortex (see Figure 4.1). The specific geometrical characteristics of the emulsification system are given in

Table 4.1.

Table 4.1 Tank configuration and impeller parameters

Tank diameter	T	0.1630 m
Impeller diameter	D=1/3T	0.0543 m
Power number	N_p	1.2
Clearance	C=1/2T	0.0815 m
Liquid height	H=T	0.1630 m

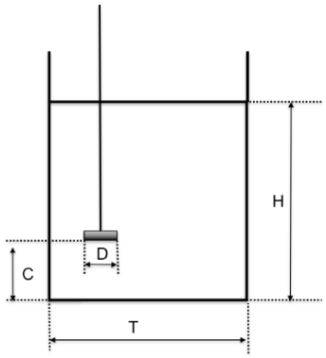

Figure 4.1 Emulsification setup

4.3.2.2 Emulsion characterization

Droplet sizes were measured using the technique proposed by Wan et al. (2017), which is based on the analysis of in-line images obtained from a PVM® V819 probe (Mettler Toledo, USA) at a rate of 10 frames/s. Assuming that the highest turbulence is generated around the impeller and that the lowest energy level occurs outside this zone, Zeitlin and Tavlarides (1972) divided the stirred vessel into a breakage-dominated zone close to the impeller (impeller zone) and a coalescence-dominated zone far from the impeller (coalescence zone). The PVM® probe was placed in one of the two zones (Figure 4.2), and images were recorded during emulsification. Droplet size distributions and Sauter mean diameters (d_{32}) were deduced and were further

analyzed. Preliminary tests were performed to ensure that the emulsification process was not affected by the insertion of the PVM® probe into the mixing tank.

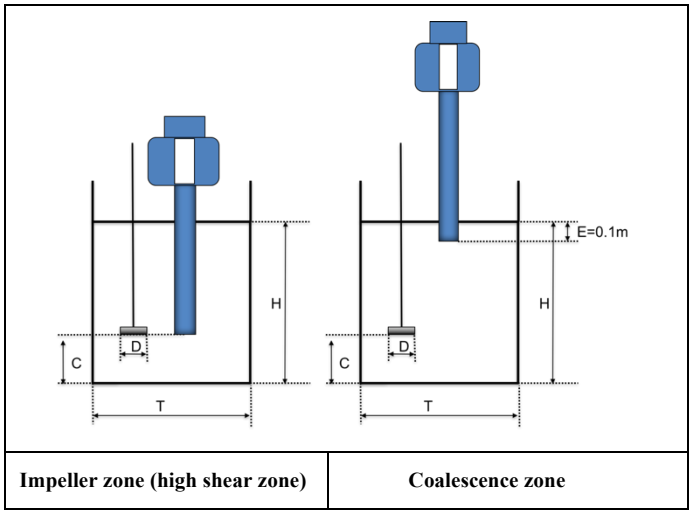

Figure 4.2 Location of the PVM® probe in the mixing tank

4.3.2.3 Emulsification process

Table 4.2 gives the oil, water, and particle formulations used in the present study. Three particle regimes (insufficient, sufficient, and intermediate) were determined from the droplet size–particle concentration curves. The insufficient particles regime refers to the region where the droplet size falls dramatically in parallel with the particle concentration. The sufficient particles regime refers to the region where the droplet size remains constant regardless of the particle concentration. The intermediate particles regime refers to the transition region between the sufficient and insufficient particles regimes. The particle formulations in the corresponding regimes were determined based on the work of Al-Haiek et al. (2018), who used the particle fraction Φ_p (mass of oil–mass of particles ratio) to represent the particles regimes: (1) the insufficient particles regime, where Φ_p=30, (2) the sufficient particles regime, where Φ_p=2, and (3) the intermediate particles regime, which is located between the sufficient and insufficient particles regimes, where Φ_p=12. The standard procedure for producing an oil-in-water (O/W) emulsion is to disperse the particles in distilled water and then to add the oil phase at a constant agitation rate of 700 RPM. The impact of altering some parameters on the evolution of the droplet size is described below.

Table 4.2 Oil, water, and particle formulations

Φ_{oil}	m_{water} (g)	m_{oil} (g)	$m_{insufficient}$ (g)	$m_{intermediate}$ (g)	$m_{sufficient}$ (g)
0.5 vol%	3383.05	16.32	0.54	1.38	7.10

5 vol%	3231.38	163.26	5.44	13.83	59.23
10 vol%	3064.43	323.55	10.96	27.41	142.29

4.3.2.3.1 PVM® location

The effect of the location of the PVM® probe on droplet size was tested using the 5 vol% O/W formulation with no particles at an agitation rate of 700 RPM. The PVM® probe was inserted into either the breakage or the coalescence zone to monitor the evolution of droplet size over a 12-h emulsification period.

4.3.2.3.2 Impact of the presence of particles in the early stage of emulsification

Assuming that emulsification is dominated by breakage immediately after adding the dispersed phase, the PVM® probe was inserted into the breakage zone. Breakage was studied for the first 180 min using the 5 vol% O/W formulation with an agitation rate of 700 RPM and a standard emulsification procedure with no particles, with sufficient particles, with sufficient unattachable particles, with insufficient particles, or with intermediate particles.

4.3.2.3.3 Impact of adding particles during the early stage of emulsification.

The impact of adding particles after the generation of the interface was also studied. Sufficient pre-wet particles were added to a 5 vol% liquid-liquid dispersion after 1 min of mixing at an agitation rate of 700 RPM.

4.3.2.3.4 Impact of adding particles after emulsification equilibrium is reached

The impact of the collapse of the balance between breakage and coalescence was investigated using an emulsion prepared using a 5 vol% oil fraction with insufficient particles (see Table 2, m particle = 5.44 g). Once equilibrium was reached (after 12 h), the amount of particles required to meet the intermediate particles case was added (m particle = 13.83 g). Once a new equilibrium was reached, more particles were added to meet with the sufficient particles case (m particle = 59.23 g). Lastly, 45.4 g of particles were added to the previous system to have many more particles than required to stabilize the system-generated interface.

4.3.2.3.5 Impact of the presence of particles on droplet coalescence

We devised an impeller speed strategy based on variations of N over time. By significantly reducing the impeller speed after a given time at a higher impeller speed, we can observe and

quantify the impact on droplet size in real time. Reducing the impeller speed dramatically reduced the breakage frequency and allowed coalescence to become the predominant mechanism in the tank. From the PVM® measurements, we can determine the evolution of the drop size, which is directly related to the change in the equilibrium between breakage and coalescence. We used a 5 vol% or 10 vol% oil fraction with the different particle loads indicated in Table 4.2 and an agitation rate of 700 RPM to reach the equilibrium size. The impeller speed was then stepwisely reduced to 350 RPM. The PVM® probe was inserted into the coalescence zone to quantify the evolution of droplet size during the transition imposed by the change in impeller speed. PVM® images were collected after a 12 h emulsification period at an agitation rate of 700 RPM, then after 30 min, 60 min, and 12 h at an agitation rate of 350 RPM.

4.3.2.3.6 Impact of the dispersed phase volume fraction and particles on the equilibrium droplet size distribution

In order to determine the impact of the dispersed phase volume fraction on the equilibrium droplet size distribution, the droplet size distribution was obtained from PVM® images of 0.5 vol%, 5 vol%, and 10 vol% O/W emulsions at various particle regimes (no particles, insufficient particles, and sufficient particles) after 12 h of mixing at an agitation rate of 700 RPM in the breakage zone.

4.4 Results and Discussion

4.4.1 Impact of the location of the PVM® probe in the mixing tank

The evolution of droplet size in the breakage and coalescence zones is illustrated in Figure 4.3. The procedure is explained in detail in section PVM® location. Two regimes can be seen in the two curves in Figure 4.3. In regime (1), a sharp decrease droplet size occurs while, in regime (2), a plateau is reached. Regime (1) corresponds to a breakage-dominated zone since the droplet size decreases rapidly, whereas regime (2) corresponds to a zone where coalescence counterbalances breakage in a dynamic equilibrium state. During the early stage of emulsification, larger droplets were observed in the coalescence zone, while the same droplet sizes were obtained in the two zones after 1 h of emulsification. This confirmed that breakage predominates in the breakage zone while more time is required to obtain the same droplet size in the coalescence zone. However, once the capacity of the system to generate an interface was reached, there was no significant difference in droplet size distributions in the breakage and coalescence zones, as can be seen in Figure 4.4, where the two size distributions overlap almost perfectly, a clear indication that droplet size and droplet size distribution no longer evolve.

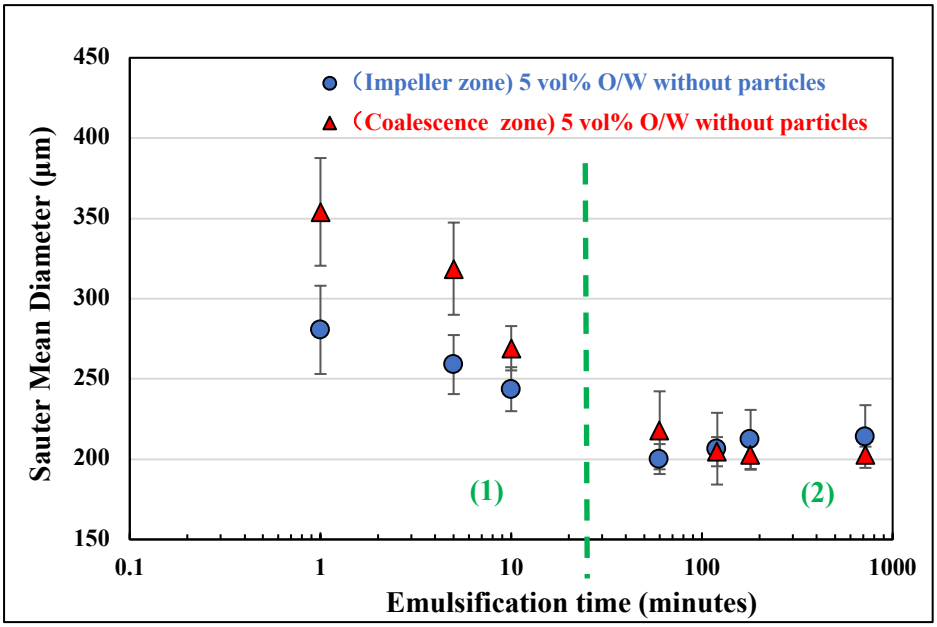

Figure 4.3 Evolution of droplet size in the breakage and coalescence zones during emulsification

(5 vol% O/W mixture without particles at an agitation rate of 700 RPM)

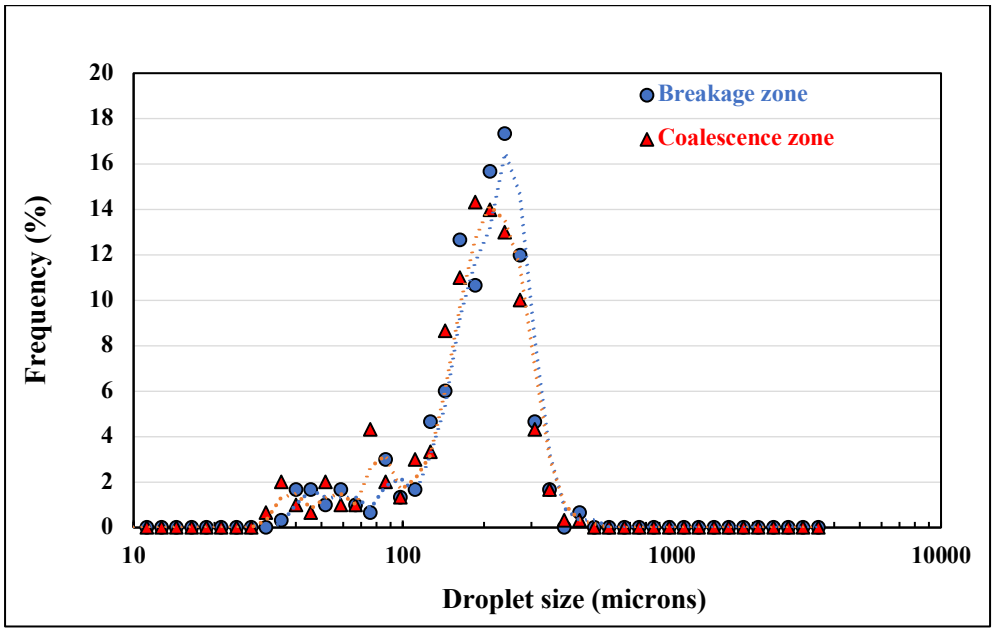

Figure 4.4 Droplet size distributions in the breakage and coalescence zones after 12 h of emulsification (5 vol% O/W mixture without particles at an agitation rate of 700 RPM)

4.4.2 Impact of the presence of particles in the early stage of emulsification

The impact of the presence of particles on the evolution of droplet size was investigated by comparing a 5 vol% pure liquid-liquid dispersion (without particles) with a 5 vol% O/W dispersion stabilized with sufficient particles at an agitation rate of 700 RPM using the

methodology given in section Impact of the presence of particles in the early stage of emulsification. Figure 4.5 shows the evolution of the Sauter mean diameter in the breakage zone. The droplet size decreased over time due to breakage in all cases. However, in the absence of particles, the plateau was reached after only 10 min while, in the presence of regular particles, the plateau was reached after 120 min. The rapid equilibrium effect is likely due to the fact that breakage predominated during the first 10 min, after which it was counterbalanced by coalescence, resulting in an equilibrium droplet size under mixing. However, a stabilization process is involved in the system containing regular particles, which led to a delay in reaching an equilibrium. Relatively large droplets with regular particles were generated during the first 20 min compared to the droplets generated in the absence of particles. Starting with a droplet size ratio of 1.3 in the first minute, the droplet sizes in the two systems (with and without particles) converged after 10 min of mixing due to less effective breakage.

In the absence of particles, the mixing energy dissipates as the droplets break up. On the other hand, in the presence of particles, part of the mixing energy dissipates when suspending the particles rather than breaking up the droplets. Since less energy is dissipated breaking up droplets in the system containing particles, the breakage zone is presumably smaller than in the liquid-liquid dispersion. Consequently, more droplet passages are required to reach a droplet size equivalent to that obtained in a liquid-liquid dispersion. The decrease in breakage efficiency may also be related to the adsorption of particles at interfaces that can make breakage even more difficult. Walstra (1953) compared the characteristic time with the eddy lifetime to determine the possibility of droplet breakage in liquid-liquid dispersions (Pieter Walstra, 1993). Based on a comparison of the eddy lifetime and the particle adsorption time using the correlations given below, we can assume that a significantly longer particle adsorption time (of the order of 10 s) may make droplet rupture more unlikely within a limited eddy lifetime (of the order of 0.01 s). Eddy lifetime is defined as the Kolmogorov scale–turbulent velocity ratio (P. Walstra, 1993).

$$\text{Eddy lifetime } t_{eddy} = \eta_k^{\frac{2}{3}} \varepsilon^{\frac{-1}{3}} \rho^{\frac{1}{3}} \quad \ldots (4.1)$$

$$\text{Particle adsorption time (Tcholakova et al., 2008) } t_A \approx \frac{\Gamma_M}{C_p (\varepsilon d)^{\frac{1}{3}}} \ldots (4.2)$$

$$\text{Mass of adsorbed particles per unit area (Tcholakova et al., 2008) } \Gamma_M \approx 4 R_p \frac{\rho_p \varphi_{cp}}{3} \quad \ldots (4.3)$$

$$\text{Energy dissipation rate } \varepsilon = \frac{P}{m_{oil} + m_{water} + m_P} \quad \ldots (4.4)$$

$$\text{Power consumption } P = N_p \rho_c N_I^3 D_i^5 \quad \ldots (4.5)$$

We also compared the results of a 5 vol% liquid-liquid dispersion containing particles that cannot attach to the interface (Figure 4.5) such that the presence of this type of particle affects energy dissipation but not particle attachment. The comparison of the initial droplet size in the three conditions clearly showed that the size of droplets with unattachable particles is situated between the droplet sizes in the other two conditions. As such, the relatively large droplet size obtained with regular particles is caused by the combined impact of particle attachment and energy dissipation, which together reduce breakage efficiency.

The system with regular particles was able to produce smaller droplets after more than 20 min, which is presumably due to the fact that the stabilization mechanism predominates and hinders further coalescence of the droplets. Based on these observations, it can be assumed that the equilibrium size for the liquid-liquid dispersion depends on the competition between breakage and coalescence events. On the other hand, when particles are involved, the droplet size is determined by the equilibrium among breakage, coalescence, and stabilization events.

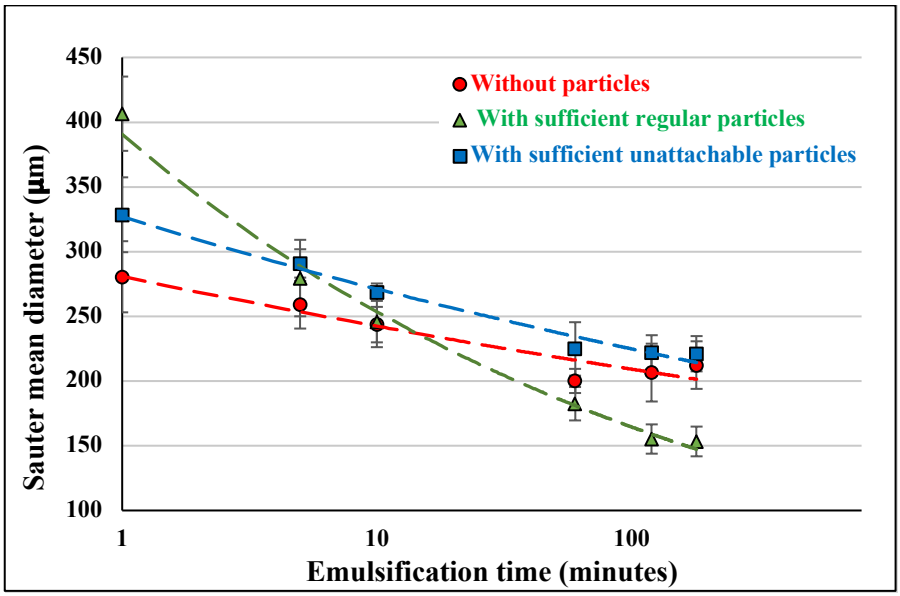

Figure 4.5 Evolution of droplet size during the emulsification of a 5 vol% O/W mixture at an agitation rate of 700 RPM

(Circles: Pure liquid-liquid dispersion; Triangles: Emulsification with sufficient regular particles;

Squares: Emulsification with sufficient unattachable particles)

To better understand the impact of the amount of particles on the evolution of droplet size during emulsification, 5 vol% O/W emulsions were prepared with different amounts of particles at an agitation rate of 700 RPM. Figure 4.6 shows the evolution of droplet size with insufficient particles, intermediate particles, and sufficient particles as mentioned in the Table 2. It can be

seen that reducing the number of particles results in larger droplets during all the emulsification processes, indicating that particles not only affect the breakage process during the early stage of emulsification but also affect coalescence. When a small number of particles were added (insufficient particles), larger droplets were observed than those obtained with the liquid-liquid dispersion (Figure 4.5), confirming that breakage is less efficient in the presence of particles. Nonetheless, when more particles were added to meet the intermediate particles case and the sufficient particles case (Figure 4.6), there was a decrease in droplet size, indicating that coalescence is also affected since the addition of particles is supposed to reduce breakage efficiency and increase droplet size. Adding more particles resulted in a more pronounced decrease in coalescence efficiency than in breakage efficiency. We can thus assume that coalescence efficiency is decreased because the particles stabilize droplets produced during the early stage of emulsification.

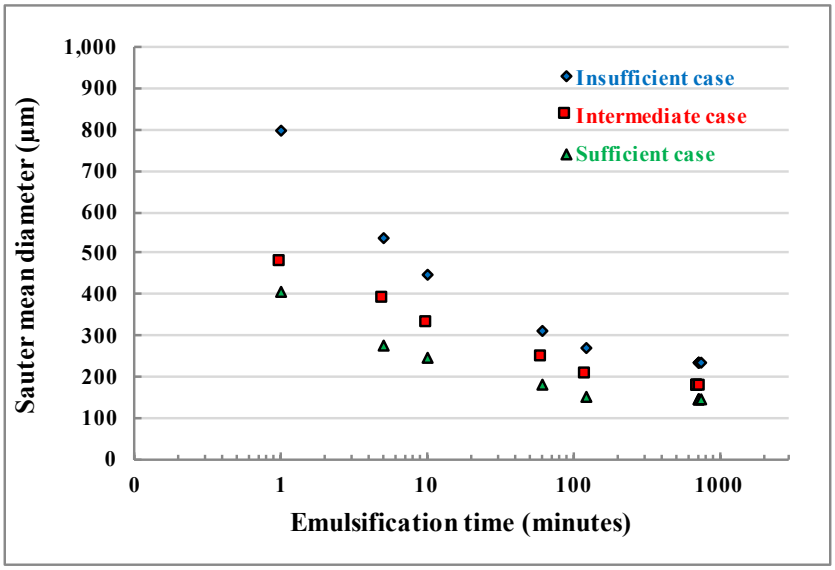

Figure 4.6 Impact of the amount of particles on the evolution of droplet size during the emulsification of a 5 vol% O/W mixture at an agitation rate of 700 RPM

To verify our assumption, emulsion samples were taken at different times during the first 10 min. Figure 4.7 shows that stable droplets are formed after only 1 min of emulsification in all the cases, indicating that particle coverage and emulsion stabilization occur as soon as mixing begins.

1 min	5 min	10 min	1 min	5 min	10 min	1 min	5 min	10 min

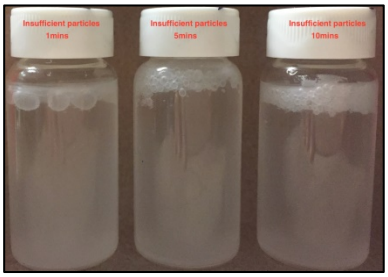

(a) Insufficient particles

(b) Intermediate particles

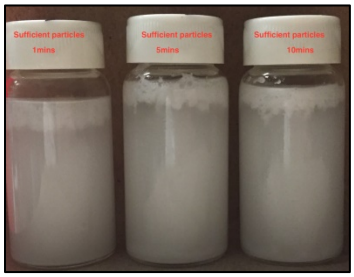

(c) Sufficient particles

Figure 4.7 Emulsion samples prepared using a 5 vol% oil fraction and different amounts of particles mixed at an agitation rate of 700 RPM and collected after 1, 5, and 10 min of emulsification

4.4.3 Impact of adding particles during the early stage of emulsification

Given that the system with particles produces larger droplets during the early stage of emulsification and smaller droplets after stabilization, particles were added after the generation of the interface (see detailed methdology in section Impact of adding particles during the early stage of emulsification.). Figure 4.8 shows the evolution of droplet size when the particles are added after mixing the liquid-liquid dispersion for 1 min (test emulsion), while the other two cases (liquid-liquid dispersion, standard emulsification procedure with particles) are reference emulsions. In general, the droplet size of the test emulsion followed a similar but delayed behavior as the two reference emulsions. After mixing for 1 min, the addition of the particles resulted in an immediate increase in droplet size equivalent to the size observed in the emulsion containing sufficient particles (blue circles). The fluctuation in droplet size again confirmed that adding particles decreases both breakage efficiency and coalescence, with a more pronounced impact on coalescence. The droplet size in the test emulsion decreased until it reached the droplet size in the liquid-liquid dispersion 30 min later. Beyond 180 minutes, the size of the droplets was equivalent to the size of the droplets obtained from a standard emulsification process with particles.

These findings indicate that adding particles disturbs the equilibrium between breakage and coalescence during the early stage of emulsification and results in a delayed equilibrium and that, during the first 10 min, breakage is the predominant mechanism, as indicated by the marked decrease in droplet size, even after adding particles. In fact, if particles are involved, larger droplets are observed due to the decrease in breakage efficiency caused by the addition of the particles. After 20 min, coalescence increased and counterbalanced breakage, resulting in an equilibrium droplet size. These results, which are in agreement with the previous

observation, again suggest that particles affect the breakage process by influencing the properties of the continuous phase.

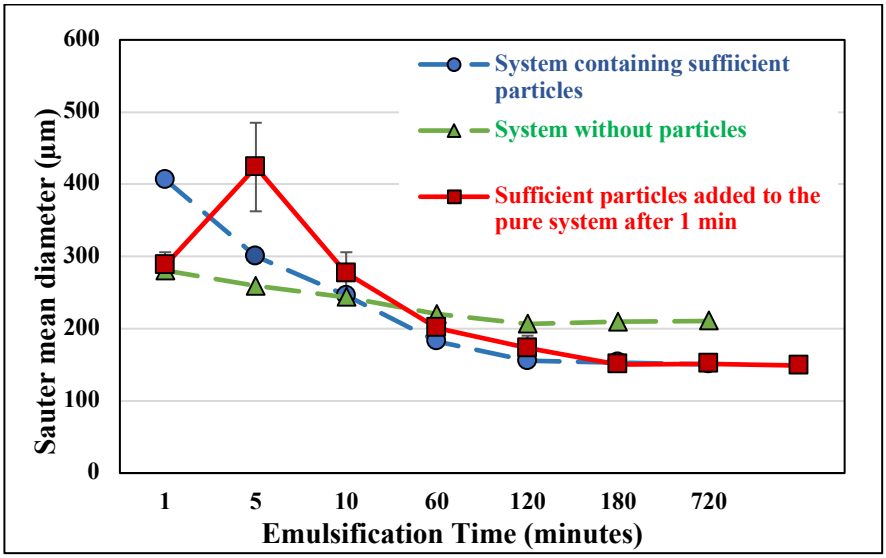

Figure 4.8 Impact of adding particles to a liquid-liquid dispersion (5 vol% oil fraction and sufficient particles mixed at an agitation rate of 700 RPM)

4.4.4 Impact of adding particles after emulsification equilibrium is reached

After investigating the impact of adding particles to a liquid-liquid dispersion during the early stage of emulsification, additional particles were added to systems already containing particles and after they had reached equilibrium size (see section Impact of adding particles after emulsification equilibrium is reached). Figure 4.9 presents the variations in droplet size when particles are added during emulsification (dashed line). The detailed procedure is described in the methodology. Particles were added at points ①, ③, and ⑤, as shown in Figure 4.9. The addition of particles to a system containing insufficient particles caused an increase in droplet size from ① to ② (from 238 to 537 µm or a 2.3-fold increase) within 1 min, followed by a decrease to ③ (178 µm) after mixing for 12 h. The same albeit less marked effect was observed when more particles were added to the system containing an intermediate amount of particles, as shown from ③ to ④ (from 178 to 263 µm or a 1.5-fold increase) in Figure 4.9. The droplet size decreased from ④ to ⑤ (from 263 to 148 µm) to the level of a system containing sufficient particles, suggesting that the system was still able to generate more interfaces and was only limited by the coverage potential of the particles. After this perturbation, when more particles are added to the system containing sufficient particles (⑤ indicated in Figure 4.9), the droplet size remained at 148 µm, which is the equilibrium size of sufficient particles. This indicated that the interface generation limit of the system had been reached, which is in line

with the results shown in Figure 4.8, where the droplet size increased dramatically when the particles were added to a liquid-liquid dispersion. Both cases showed that the addition of particles to an emulsion with a low coverage potential can disturb the breakage–coalescence balance. For the low coverage potential, the equilibrium droplet size is only considered as a dynamic balance between breakage and coalescence, and the addition of particles leads to a rapidly reduced impact on breakage. On the other hand, if there are enough particles to cover the system-generated interface (high coverage potential), the droplet size in the steady state can be considered as a stable equilibrium as it is not disturbed by the operating conditions.

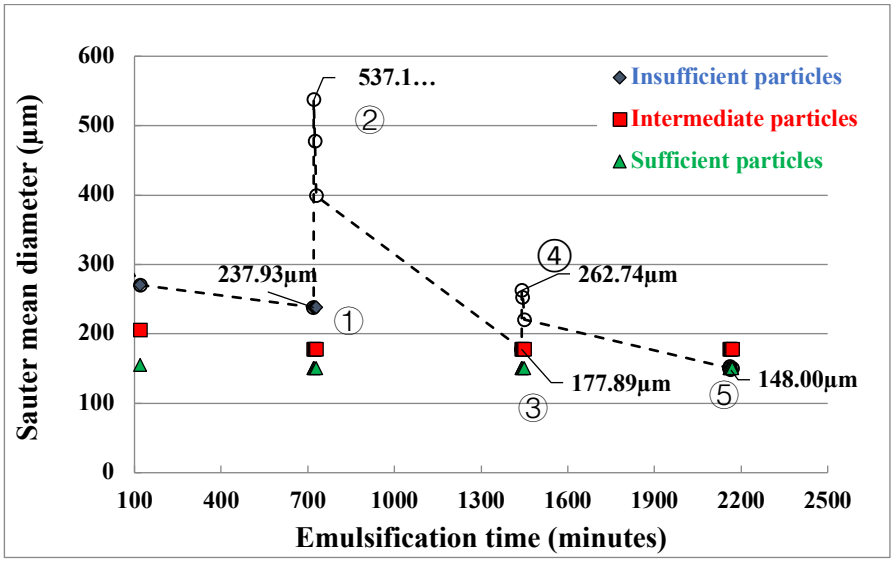

Figure 4.9 Impact of particle addition to Pickering emulsions during the emulsification of a 5 vol% O/W mixture at an agitation rate of 700 RPM

(① equilibrium state of the system containing insufficient particles; ② 1 min after adding particles at ①; ③ equilibrium state of the system containing intermediate particles; ④ 1 min after adding the particles at ③; ⑤ equilibrium state of the system containing sufficient particles)

4.4.5 Impact of particles on coalescence efficiency

In order to evaluate the impact of particles on coalescence, experiments were performed as described in section Impact of the presence of particles on droplet coalescence. Figure 4.10 and Figure 4.11show the evolution of the Sauter mean diameter when the impeller speed is reduced for the two cases studied here, i.e., 5 vol% oil fraction and 10 vol% oil fraction. Generally speaking, at an agitation rate of 700 RPM and after the emulsion has reached equilibrium, the droplet size always decreased in parallel with the amount of particles in the emulsion under all conditions and for the two oil fractions (as can also be seen in Figure 4.5 and Figure 4.8).

However, in the case without particles, emulsification produced smaller droplets than those observed when insufficient particles were used in either case, i.e., 5 vol% O/W or 10 vol% O/W. This result was similar to that observed in the early stage of emulsification when sufficient particles produced larger droplets in the first 10 min (Figure 4.5). It can thus be deduced that insufficient particles reduce breakage efficiency but that this reduction is not enough to decrease coalescence efficiency to the point where smaller droplets are produced than in the case without particles.

We should note here that reducing the impeller speed from 700 to 350 RPM results in an 8-fold reduction in power input since power is proportional to the cube of the rotation speed. Figure 4.10 and Figure 4.11 also show that the droplet size increased when the impeller speed was reduced from 700 RPM to 350 RPM for all the particle loads for both oil fractions, except when sufficient particles were used and where a plateau was observed, indicating that coalescence is prevented due to the full coverage of the droplets by particles. When no particles or insufficient particles were considered, there was a more significant increase in droplet size when the impeller speed was reduced due to the increase in the coalescence rate. The increase in droplet size was faster when a 10 vol% O/W mixture was used than when a 5 vol% O/W mixture was used, most likely due to the higher collision frequency in the 10 vol% O/W mixture.

Figure 4.12 shows the $\varphi_{cov/gen}$ ratio, which represents the coverage potential versus the calculated system-generated interface and which is calculated using the equations given in Tsabet and Fradette (2015) (Tsabet et al., 2015b). A $\varphi_{cov/gen}$ ratio value larger than 1 was obtained when sufficient particles were used in the four operating conditions (5 vol% O/W mixture at 700 RPM, 10 vol% O/W mixture at 700 RPM, 5 vol% O/W mixture at 350 RPM, 10 vol% O/W mixture at 350 RPM), which is in line with the stable equilibrium observed in Figure 4.10 and Figure 4.11. Nevertheless, the cases for which the agitation rate was 700 RPM and for which a ratio lower than 1 was calculated indicated that the system-generated interface could not be sufficiently covered by the potential coverage. The results also suggest that there is a dynamic equilibrium between breakage and coalescence, which is supported by the fact that the droplets grew in size when the impeller speed was changed (as can be seen in Figure 4.10 and Figure 4.11). For example, at 700 RPM, droplets in the 5 vol% O/W mixture with intermediate particles grew in size from 700 RPM_eq to 350 RPM_30 min (as can be seen in Figure 4.10), which could be explained by the $\varphi_{cov/gen}$ ratio (0.65), which is lower than 1 (Figure 4.12). On the other hand, at 700 RPM, the 5 vol% O/W mixture with insufficient particles had a lower $\varphi_{cov/gen}$ ratio (0.25) and led to a more significant increase in droplet size when the impeller speed changed. The behavior of emulsions characterized by the $\varphi_{cov/gen}$ ratio is thus linked to

the increase in droplet size caused by the change in impeller speed. Specifically, a lower $\varphi_{cov/gen}$ ratio results in a larger fluctuation in droplet size when operating conditions change.

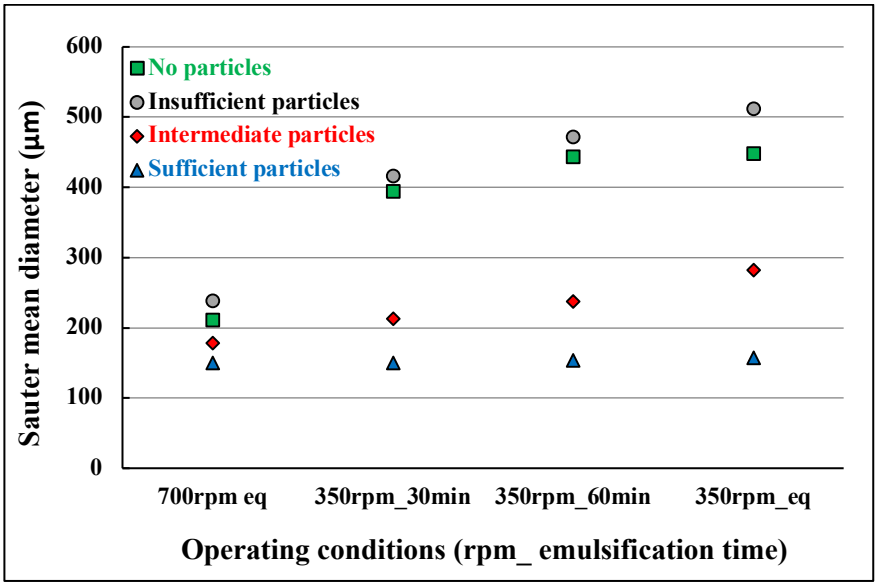

Figure 4.10 Impact on droplet size of reducing the impeller speed from 700 to 350 RPM (5 vol% O/W mixture, four particle loads)

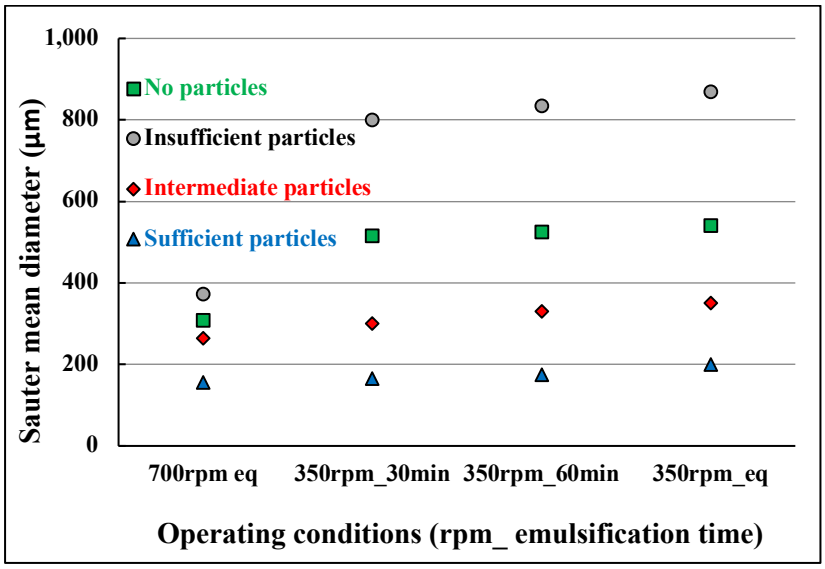

Figure 4.11 Impact on droplet size of reducing the impeller speed from 700 to 350 RPM (10 vol% O/W mixture, four particle loads)

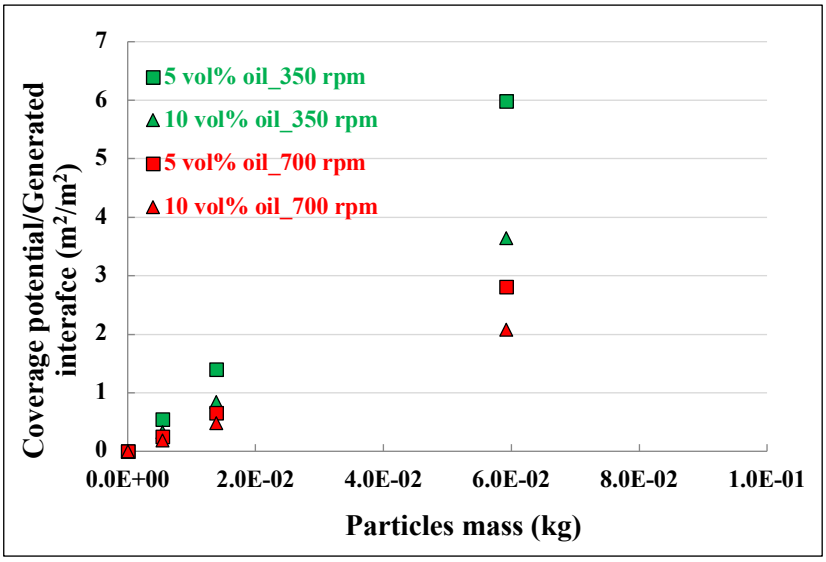

Figure 4.12 Impact of particle load on the ratio between the coverage potential and the system-generated interface without particles (the particle conditions from left to right of the particle mass are the cases of no particles, insufficient particles, intermediate particles, and sufficient particles)

4.4.6 Impact of the dispersed phase volume fraction and particles on droplet size distribution after equilibrium

Given that the coalescence rate depends on the droplet-droplet collision frequency, emulsions were prepared using different phase fractions (0.5, 5, and 10 vol% O/W) to control this parameter (see details in section Impact of the dispersed phase volume fraction and particles on the equilibrium droplet size distribution). In fact, the impact of droplet breakage can be isolated from coalescence in a diluted system with a dispersed phase as low as 0.5 vol% (Rueger et al., 2013). Figure 4.13 shows the droplet size distributions resulting from 0.5, 5, and 10 vol% O/W emulsions covered with sufficient particles. As the oil volume fraction increases, the distribution shifts to the right, indicating that larger droplets form due to the higher coalescence rate. This behavior was also seen in the systems with insufficient particles and without particles (see Figure 4.14 and Figure 4.15). However, a comparison of Figure 4.13, Figure 4.14, and Figure 4.15 clearly shows that decreasing the particle load leads to a broader droplet size distribution, coupled with a change in shape from a bimodal distribution to a unimodal distribution. The bimodal distribution is more pronounced with the lowest oil fraction (0.5 vol%), as can be seen in Figure 4.14 and Figure 4.15. This is because when the coalescence process predominates in a higher volume fraction (5 vol% and 10 vol%), it may mask the effect of breakage. Since breakage is the sole mechanism at play in the 0.5 vol% O/W mixture, the

bimodal distribution results from the breakage process in the case of insufficient particles or in the absence of particles.

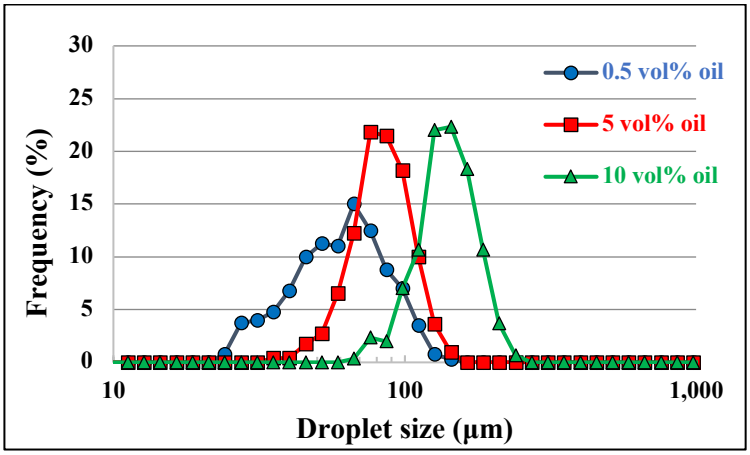

Figure 4.13 Impact of the oil fraction on droplet size distribution after equilibrium (sufficient particles at an agitation rate of 700 RPM)

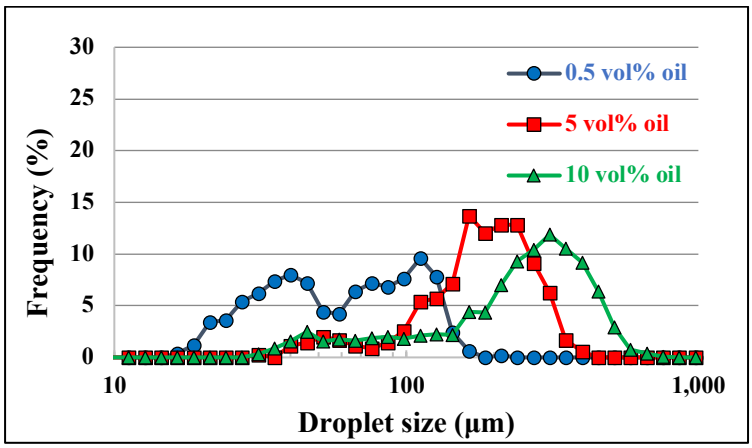

Figure 4.14 Impact of the oil fraction on droplet size distribution after equilibrium (insufficient particles at an agitation rate of 700 RPM)

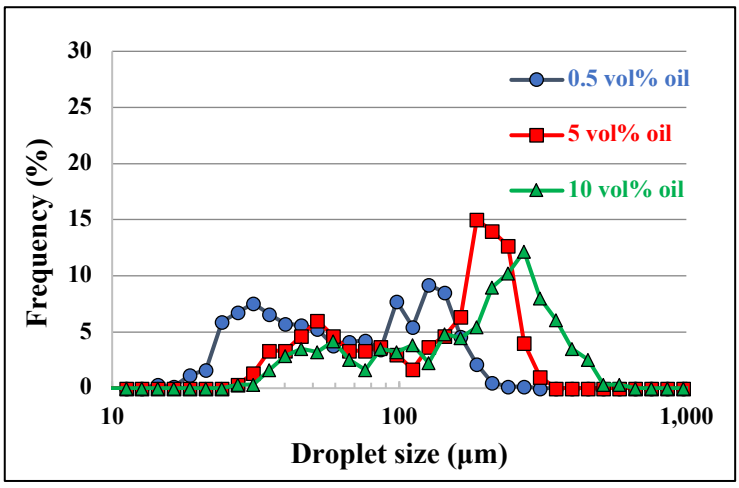

Figure 4.15 Impact of the oil fraction on droplet size distribution after equilibrium (no particles at an agitation rate of 700 RPM)

Much research has been devoted to predicting the droplet/bubble size distribution arising from the breakage process under a turbulent regime. Approaches based on statistical considerations or phenomenological analyses have been summarized by Liao Y. et al. (2009). Unlike the normal distribution proposed by Valentas K.J. et al. (1966) and Coulalogou et al. (1977), Hsia et al. (1983) and Lee C.H. et al. (1987) assumed binary distributions based on a beta function. Phenomenological models also considered statistical functions to deduce distributions of daughter droplets/bubbles but associated them with phenomena controlling droplet breakage. For instance, daughter bubble size distributions such as bell-shape distributions (Martinez-Bazan et al., 1999), U-shape distributions (Tsouris et al., 1994), and M-shape distributions (Lehr et al., 2002) have been proposed. Other researchers have developed empirical models to obtain daughter droplet size distributions. Tcholakova et al. (2007) investigated the effect of oil viscosity, interfacial tension, and the turbulent energy dissipation rate on the daughter droplet size distribution (Tcholakova et al., 2007). They reported that the distribution of the resulting daughter droplets depends on oil viscosity. They observed smaller satellite droplets with low viscous oils and more homogeneous breakage with viscous oils. They proposed two breakage mechanisms. On the one hand, they attributed the breakage behavior of viscous oil droplets to the capillary instability of long oil threads that are caused by viscous deformation under turbulent flow (at the bottom left of Figure 4.16). On the other, they proposed that collisions of small turbulent eddies with the mother droplet cause the breakage of less viscous droplets (bottom right of Figure 4.16) (Tcholakova et al., 2007). It can be assumed that stable droplets tend to result in more homogeneous breakage, as illustrated by the smooth distribution at the bottom left of Figure 4.16. It is also reasonable to obtain unimodal distributions with fully covered droplets as seen in Figure 4.13. This also provides a possible explanation for the wider and bimodal or multimodal distribution behavior seen with less stable droplets (Figure 4.14 and Figure 4.15), such as in systems containing insufficient or no particles (at the bottom right of Figure 4.16).

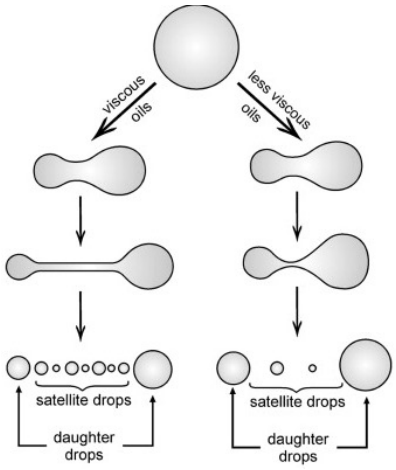

Figure 4.16 Impact of oil viscosity on the breakage process and droplet size distribution (Taken from Tcholakova S. et al. (2007))

4.5 Conclusion

The emulsification process was qualitatively analyzed using a PVM® probe under corresponding operating conditions. The following conclusions can be drawn with respect to O/W emulsions stabilized by micron-sized glass beads:

- Droplet size is markedly affected by the location of the PVM® probe in the tank until the droplets reached a steady state between breakage and coalescence.
- The presence of particles decreases breakage efficiency in the early state of emulsification due to the combined effect of particle attachment and enhanced energy dissipation in the continuous phase.
- Despite breakage being the predominant mechanism in the early stage of emulsification, droplet stabilization occurs as soon as emulsification starts.
- Fully covered droplets correspond to a stable equilibrium, while dynamic equilibrium is considered when there are insufficient particles to cover the system-generated interface (when $\frac{A_{cov}}{A_{gen}}$ is lower than 1). The coalescence frequency is associated with this ratio.
- As long as the emulsification is controlled by the coverage potential (i.e., an emulsion stabilized with insufficient particles or intermediate particles), the addition of particles to such a system will disrupt the balance between breakage and coalescence in the early stage and in the equilibrium state of emulsification.
- The breakage process is very sensitive to particle attachment at the interface as well as to the dispersed phase volume fraction, which might result in different droplet size distribution shapes.

The role of particles in the emulsification process is qualitatively understood, but few quantitative results are available. The development of simulation models for the breakage and coalescence processes would be very valuable for conducting further studies.

4.6 Reference

Arditty, S., Schmitt, V., Lequeux, F., & Leal-Calderon, F. (2005). Interfacial properties in solid-stabilized emulsions. *European Physical Journal B, 44*(3), 381-393. doi:10.1140/epjb/e2005-00137-0

Arditty, S., Whitby, C. P., Binks, B. P., Schmitt, V., & Leal-Calderon, F. (2003). Some general features of limited coalescence in solid-stabilized emulsions. *European Physical Journal E, 11*(3), 273-281. doi:10.1140/epje/i2003-10018-6

Aveyard, R., Binks, B. P., & Clint, J. H. (2003). Emulsions stabilised solely by colloidal particles. *Adv Colloid Interface Sci, 100*, 503-546. doi:10.1016/s0001-8686(02)00069-6

Binks, B. P., & Lumsdon, S. O. (2000a). Effects of oil type and aqueous phase composition on oil-water mixtures containing particles of intermediate hydrophobicity. *Physical Chemistry Chemical Physics, 2*(13), 2959-2967. doi:10.1039/b002582h

Binks, B. P., & Lumsdon, S. O. (2000b). Influence of particle wettability on the type and stability of surfactant-free emulsions. *Langmuir, 16*(23), 8622-8631. doi:10.1021/la000189s

Binks, B. P., & Lumsdon, S. O. (2000c). Transitional phase inversion of solid-stabilized emulsions using particle mixtures. *Langmuir, 16*(8), 3748-3756. doi:10.1021/la991427q

Binks, B. P., & Rodrigues, J. A. (2003). Types of phase inversion of silica particle stabilized emulsions containing triglyceride oil. *Langmuir, 19*(12), 4905-4912. doi:10.1021/la020960u

Binks, B. P., & Whitby, C. P. (2005). Nanoparticle silica-stabilised oil-in-water emulsions: improving emulsion stability. *Colloids and Surfaces a-Physicochemical and Engineering Aspects, 253*(1-3), 105-115. doi:10.1016/j.colsurfa.2004.10.116

Calabrese, R. V., Wang, C. Y., & Bryner, N. P. (1986). Drop breakup in turbulent stirred-tank contactors. *American Institute of Chemical Engineers, 32*(4), 4.

Chen, H. T., & Middleman, S. (1967). Drop size distribution in agitated liquid-liquid systems. *AIChE Journal, 13*(5), 989-995.

Chesters, A. K. (1991). THE MODELING OF COALESCENCE PROCESSES IN FLUID LIQUID DISPERSIONS - A REVIEW OF CURRENT UNDERSTANDING. *Chemical Engineering Research & Design, 69*(4), 259-270.

Coulaloglou, L. L. T. (1977). Description of interaction processes in agitated liquid-liquid dispersions. *Chemical Engineering Science, 32*(11), 9.

Doulah, M. S. (1975). An effect of hold-up on droplet sizes on liquid-liquid disperseion. *Industrial chemical engineering fundamentals, 14*(2), 2.

Fournier, C. O., Fradette, L., & Tanguy, P. A. (2009). Effect of dispersed phase viscosity on solid-stabilized emulsions. *Chemical Engineering Research & Design, 87*(4A), 499-506. doi:10.1016/j.cherd.2008.11.008

Frelichowska, J., Bolzinger, M. A., & Chevalier, Y. (2010). Effects of solid particle content on properties of o/w Pickering emulsions. *J Colloid Interface Sci, 351*(2), 348-356. doi:10.1016/j.jcis.2010.08.019

Gautier, F., Destribats, M., Perrier-Cornet, R., Dechezelles, J. F., Giermanska, J., Heroguez, V., . . . Schmitt, V. (2007). Pickering emulsions with stimulable particles: from highly- to weakly-covered interfaces. *Physical Chemistry Chemical Physics, 9*(48), 6455-6462. doi:10.1039/b710226g

Horozov, T. S., Binks, B. P., & Gottschalk-Gaudig, T. (2007). Effect of electrolyte in silicone oil-in-water emulsions stabilised by fumed silica particles. *Physical Chemistry Chemical Physics, 9*(48), 6398-6404. doi:10.1039/b709807n

Hsia, M. A., & Tavlarides, L. L. (1983). Simulation analysis of drop breakage, coalescence and micromixing in liquid-liquid stirred tanks. *The Chemical Engineering Journal, 26*(3), 189-199.

Lee, C.-H., Erickson, L., & Glasgow, L. (1987). Bubble breakup and coalescence in turbulent gas-liquid dispersions. *Chemical Engineering Communications, 59*(1-6), 65-84.

Lehr, F., Millies, M., & Mewes, D. (2002). Bubble-size distributions and flow fields in bubble columns. *AIChE Journal, 48*(11), 2426-2443. doi:10.1002/aic.690481103

Liao, Y. X., & Lucas, D. (2009). A literature review of theoretical models for drop and bubble breakup in turbulent dispersions. *Chemical Engineering Science, 64*(15), 3389-3406. doi:10.1016/j.ces.2009.04.026

Martinez-Bazan, C., Montanes, J. L., & Lasheras, J. C. (1999). On the breakup of an air bubble injected into a fully developed turbulent flow. Part 2. Size PDF of the resulting daughter bubbles. *Journal of Fluid Mechanics, 401*, 183-207. doi:10.1017/s0022112099006692

Mei, Y., Li, G. X., Moldenaers, P., & Cardinaels, R. (2016). Dynamics of particle-covered droplets in shear flow: unusual breakup and deformation hysteresis. *Soft Matter, 12*(47), 9407-9412. doi:10.1039/c6sm02031c

Rueger, P. E., & Calabrese, R. V. (2013). Dispersion of water into oil in a rotor-stator mixer. Part 1: Drop breakup in dilute systems. *Chemical Engineering Research & Design, 91*(11), 2122-2133. doi:10.1016/j.cherd.2013.05.018

Sullivan, A. P., & Kilpatrick, P. K. (2002). The effects of inorganic solid particles on water and crude oil emulsion stability. *Industrial & Engineering Chemistry Research, 41*(14), 3389-3404. doi:10.1021/ie010927n

Tcholakova, S., Denkov, N. D., & Lips, A. (2008). Comparison of solid particles, globular proteins and surfactants as emulsifiers. *Physical Chemistry Chemical Physics, 10*(12), 1608-1627. doi:10.1039/b715933c

Tcholakova, S., Vankova, N., Denkov, N. D., & Danner, T. (2007). Emulsification in turbulent flow: 3. Daughter drop-size distribution. *J Colloid Interface Sci, 310*(2), 570-589. doi:10.1016/j.jcis.2007.01.097

Tsabet, E. (2014). *From Particle to Process: Modeling the production of Pickering emulsion.* (Doctorate), Polytechnique Montreal, Montreal.

Tsabet, E., & Fradette, L. (2015a). Effect of the properties of oil, particles, and water on the production of Pickering emulsions. *Chemical Engineering Research & Design, 97*, 9-17. doi:10.1016/j.cherd.2015.02.016

Tsabet, E., & Fradette, L. (2015b). Semiempirical Approach for Predicting the Mean Size of Solid-Stabilized Emulsions. *Industrial & Engineering Chemistry Research, 54*(46), 11661-11677. doi:10.1021/acs.iecr.5b02910

Tsouris, C., & Tavlarides, L. (1994). Breakage and coalescence models for drops in turbulent dispersions. *AIChE Journal, 40*(3), 395-406.

Valentas, K. J., Bilous, O., & Amundson, N. R. (1966). Analysis of breakage in dispersed phase systems. *Industrial & engineering chemistry fundamentals, 5*(2), 271-279.

Walstra, P. (1993). Principals of emulsion formation. *Chemical Engineering Science, 48*(2), 333.

Walstra, P. (1993). PRINCIPLES OF EMULSION FORMATION. *Chemical Engineering Science, 48*(2), 333-349. doi:10.1016/0009-2509(93)80021-h

Wan, B., & Fradette, L. (2017). PHASE INVERSION OF A SOLID-STABILIZED EMULSION: EFFECT OF PARTICLE CONCENTRATION. *Canadian Journal of Chemical Engineering, 95*(10), 1925-1933. doi:10.1002/cjce.22892

Whitesides, T. H., & Ross, D. S. (1995). EXPERIMENTAL AND THEORETICAL-ANALYSIS OF THE LIMITED COALESCENCE PROCESS - STEPWISE LIMITED COALESCENCE. *J Colloid Interface Sci, 169*(1), 48-59. doi:10.1006/jcis.1995.1005

Wright, H., & Ramkrishna, D. (1994). Factors affecting coalescence frequency of droplets in a stirred liquid-liquid dispersion. *AIChE Journal, 40*(5), 767-776.

Yan, N. X., & Masliyah, J. H. (1996). Effect of pH on adsorption and desorption of clay particles at oil-water interface. *J Colloid Interface Sci, 181*(1), 20-27. doi:10.1006/jcis.1996.0352

Zeitlin, M., & Tavlarides, L. (1972). Fluid-fluid interactions and hydrodynamics in agitated dispersions: A simulation model. *The Canadian Journal of Chemical Engineering, 50*(2), 207-215.

CHAPTER 5 ARTICLE 2: PHASE INVERSION OF A SOLID-STABILIZED EMULSION: EFFECT OF PARTICLE CONCENTRATION

Article history: Issue Online:18 September 2017, Manuscript accepted:18 April 2017, Manuscript received: 13 January 2017 on *Canadian Journal of Chemical Engineering*

Authors: Bing Wan, Louis Fradette

5.1 Summary

Tiny water droplets in oil emulsions are commonly encountered in the petroleum industry. The high viscosity of the oil hampers the physical separation of the water droplets from the oil. Phase inversion could be a potential workaround for this problem by making water, a much less viscous phase, the continuous medium. In the present work, we focused on triggering phase inversion of a solid-stabilized emulsion. We induced a catastrophic phase inversion by the continuous addition of a dispersed phase. The evolution of droplet morphology during the phase inversion process was observed and was measured in-line using a particle vision microscope, which proved to be a powerful tool for monitoring this rapid, unstable process. A linear relationship between the droplet size and the dispersed phase volume fraction before the phase inversion was observed, indicating that a higher dispersed phase volume fraction was needed for the phase inversion to occur with higher particle concentrations. The phase inversion conditions were applied in a regime where the particles were insufficient to fully cover the interface. Our findings indicated that the number of particles per surface area appears to be a crucial parameter in triggering phase inversion, regardless of the particle concentration. The phase inversion mechanism of our solid-stabilized emulsion can be explained by the relationship between the initial particle coverage of the interface and the coalescence rate of the system.

5.2 Introduction

Emulsions are used in the food, cosmetics, pharmaceutical, petroleum, and refining industries. In the crude oil industry, water-in-oil (W/O) emulsions formed by high shear stresses and naturally existing particles are extremely undesirable and pose daunting challenges for further refining. Salager et al. (2007) compared two approaches for reducing the viscosity of the oil: (1) by heating and (2) by diluting the heavy oil with light oil. Oil-in-water (O/W) emulsions

formed using a 30% aqueous phase resulted in the lowest viscosity at all temperatures, indicating that a phase inversion can, to some extent, facilitate separation.

Phase inversion is a process whereby the morphology of emulsions is altered from a W/O to an O/W emulsion or vice versa. Phase inversions are divided into two types that depend on two variables: transitional inversions triggered by varying the wettability of the particles (Binks et al., 2000) and catastrophic inversions triggered by altering the formulation or the mixing conditions, including the W/O ratio, phase viscosities, and stirring protocols (Rondon-Gonzalez et al., 2007). Binks et al. (2000) conducted a systematic study of the relationship between particle wettability and phase inversion. They reported that adding particles with a preference for the continuous phase or varying the particle ratio using particles with different wettabilities leads to phase inversion. An indirect approach for changing particle wettability has been described by Binks et al. (2005) whereby a transitional phase inversion can be triggered by increasing the nanoparticle concentration using equal volume fractions of water and silicone oil. The phase inversion is then triggered due to gel formation, resulting in a significant change in particle wettability. Stimuli-response particles have gained much attention recently as their wettabilities can be modified in response to changes in pH (Lan et al., 2007) and temperature (Tsuji et al., 2008), triggering phase inversion. A series of studies (Rondon-Gonzalez et al., 2005, 2006) have shown that phase inversions from abnormal to normal morphologies of conventional emulsions can be successfully triggered by stirring along. Inclusion kinetics and stirring duration before phase inversion are likely responsible for the close relationship between system parameters (W/O ratio, surfactant concentration, viscosity ratio) (Rondon-Gonzalez et al., 2005, 2006).

The mechanism of phase inversion of conventional emulsions evolves. Ostwald (1901) described the first mechanism of phase inversion, which was modeled based on the critical volume fraction where the minimum close packing of droplets was reached. However, both higher and lower volume fractions than the limit have also been found to trigger phase inversions. In addition, this limit fails to fully explain the case of phase inversions induced by continuous stirring without further addition of dispersed phase (Rondon-Gonzalez et al., 2005, 2006). Based on a kinetic modeling approach, Vaessen et al. (1996) suggested that phase inversion occurs when the coalescence event overwhelms the breakup event at a sufficiently highly dispersed phase volume and when there is a divergence in mean droplet size such that the enhanced coalescence can be caused either by increasing the dispersed phase volume or by providing continuous agitation. There is a close relationship between multiple emulsions and phase inversion when continuous agitation is applied. Multiple emulsions are emulsions of

emulsions: oil-in-water-in-oil (O/W/O) and water-in-oil-in-water (W/O/W) emulsions, for instance, It has been proposed that the multiple emulsion states is a precursor to and greatly facilitates phase inversion (Brooks et al., 1991; Sajjadi et al., 2000; Groeneweg et al., 1998; Jahanzad et al., 2009).

The general mechanism of phase inversion in conventional emulsions has been partially elucidated, although quantitative predictions of the phase inversion point remain limited to specific systems. However, to the best of our knowledge, all the factors that can trigger phase inversion in solid-stabilized emulsions have yet to be determined. Investigations of the mechanisms driving phase inversion are thus required. Due to the experimental difficulties involved in studying phase inversions, we first determined whether a probe-based particle vision microscope (PVM® V819; Mettler Toledo, USA) could be a valid tool for tracking droplet size during this unstable process. We characterized the effect of particle concentration on the catastrophic phase inversion point and identified the triggering factor for the phase inversion using different particle concentrations. We showed that particle concentration affects the phase inversion point and propose that the ratio of the number of particles to the size of the oil-water interface may explain this observation. Our results indicated that it is possible to control the occurrence of a catastrophic phase inversion by adjusting the relevant parameters.

5.3 Materials and methods

5.3.1 Materials

Pure silicone oil with a viscosity of 50cSt at 25°C (Clearco Products Co. Inc., USA) was used as the organic phase and distilled water was used as the aqueous phase. Soda lime glass microspheres with a primary diameter of $d_{50}= 4\times10^{-6}$ m (Cospheric, USA) were used for all the phase inversion experiments. The glass beads are hydrophilic and have a contact angle of 48°±4° (Emir Tsabet, 2014). Bromocresol dye was used to distinguish between the water and organic phases. The water phase is purple while the oil phase appears as clear droplets on the PVM® images.

5.3.2 Experimental methods

5.3.2.1 PVM® validation

A PVM® V819 (Mettler Toledo, USA) was used to view and save real-time microscope-quality images at full process concentration. High-resolution images of the mixing system were continuously acquired at rates ranging from 0.5 to 10 frames/s, without the need for sampling.

The dimensions of the observation area were $8\times10^{-4} \times 1.1\times10^{-3}$ m^2. Images were processed using an in-house program to automatically detect, measure, and record the sizes of the droplets and particles. This tool makes it possible to reliably track droplet morphology during the catastrophic phase inversion process and to analyze the size distribution statistics.

Measuring size distributions from images may lead to discrepancies with size distributions measured by light diffraction using a MasterSizer 3000 (Malvern Instruments, Canada). To validate the feasibility of using the PVM® V819 for our experiments, we compared size distributions obtained with the PVM® V819 to those obtained with an off-line MasterSizer 3000. To accomplish this, soda lime glass microspheres were passed through a vibratory sieve shaker AS200 (Retsch, Germany) for 24 h. The sieves separated particles ranging in size from 5.3×10^{-5} to 6.3×10^{-5} m. For comparison purposes, calibrated/reference particles from Malvern were also sized. The mean particle sizes and distributions from both instruments were compared. Three types of particles were used in the comparison: soda lime glass microspheres with a narrow size range (5.3×10^{-5} to 6.3×10^{-5} m) obtained by sieving, opaque particles (stainless steel microspheres ranging in size from 110 to 113 microns; Cospheric, USA), and a mixture of particles with a bi-modal distribution.

5.3.2.2 Phase inversion experiments

All the phase inversion experiments started by directly emulsifying the silicone oil in water. Initially, identical volumes of water were used and increasing volumes of oil were added over time until the phase inversion was detected. The mixing device (BDC-3030 stirrer; Caframo, Canada) was mounted with a 4-blade, 0.04-m-diameter, pitched blade impeller The tank was a 0.085-m diameter, non-baffled, 0.4 L beaker. A known mass of hydrophilic soda lime glass microspheres ($d_{50}= 4\times10^{-6}$ m) was dispersed in 0.05 L of distilled water using the BDC-3030 stirrer operating at 600 RPM for 10 min. The distilled water containing the hydrophilic particles and a known volume fraction of silicone oil were directly emulsified using the same setup operating at 1000 RPM for different times. Samples were periodically taken using a small pipette. The droplet size was measuring using a MasterSizer 3000 until a steady drop-size diameter was attained. The pipette was modified in such a way that its opening was many times wider than the expected droplet size in order to avoid extra shear that might generate additional drop rupture. The PVM® probe was then inserted in the emulsion, which was stirred at very low speed to avoid rupturing the droplets. Excellent-quality images were acquired for in-depth droplet size analyses. The conductivity of the emulsions was monitored using a CON11 handheld conductivity meter (Oakton, USA) to determine the type of emulsion. Samples from the steady-state emulsions were transferred to 0.02-L vials after the addition of each volume

fraction of oil. The locations of the droplets in the vials clearly indicated the phase inversion, with droplets creaming up at the top of the vials with O/W emulsions, and droplets settling to the bottom with W/O emulsions. PVM® images were also used to determine the type of emulsion. The aqueous phase contained the suspended hydrophilic particles. As can be seen in the PVM® images, when phase inversion occurs, the particles transfer from the suspending media to the inside of the droplets.

5.4 Results and discussion

5.4.1 Validation of the PVM® approach for measuring droplet size

A sufficient number of droplets in a size distribution is crucial for obtaining reliable statistics from image analyses such as PVM®. We determined the minimum number of droplets required to generate reliable distribution statistics by computing d_{32} and d_{43} for increasing numbers of droplets in the distributions. The average particle sizes (d_{32} and d_{43}) reached constant values when 600 or more droplets were included in the distributions.

The MasterSizer 3000 provided volume-based distributions whereas the PVM® images and analyses provided number-based distributions. To compare the PVM® and MasterSizer 3000 distributions, the volume-based distributions from the MasterSizer 3000 were converted to number-based distributions.

Figure 5.1 shows an example of a comparison indicating that the MasterSizer 3000 has a tendency to detect small particles whereas the PVM® detects larger particles in the same batch of soda lime glass microspheres, which ranged in size from 5.3×10^{-5} to 6.3×10^{-5} m. The PVM® probe detected approximately 13% of the 53-micron particles whereas the MasterSizer 3000 detected almost twice as many. On the other hand, the PVM® detected 26% of the 63-micron particles whereas the MasterSizer 3000 only detected 10%. The computed statistics are shown in Table 5.1. There was a ±5% difference between the two instruments, which is considered within a tolerable range. However, it was not possible to determine which of the two instruments was closer to reality.

In order to determine whether the PVM® probe had a tendency to detect more larger particles than smaller particles, we prepared a bi-modal particle sample by mixing equal numbers of particles of two known sizes. The mean size of the individual particles was measured using the MasterSizer 3000 and the PVM® (Table 5.2) in sequence. The bi-modal particle sample was initially stirred in a beaker. After capturing sufficient images with the PVM®, the content of the

beaker was transferred to the MasterSizer 3000 for analysis. The PVM® provided more accurate measurements than the MasterSizer 3000 for this bi-modal system of known properties.

Figure 5.2 (PVM®) shows two peaks centered around the average sizes of the known particles A and B (same frequency), which correspond to the same number of A and B particles, as expected. However, the pronounced difference between the two frequency peaks provided by the MasterSizer 3000 measurements did not correspond to the sample. Since the optical properties of particles may affect the light diffraction pattern, opaque stainless steel microspheres were tested using the PVM® and the MasterSizer 3000. The optical properties of the particles had no significant effect on the results (not shown). The PVM® was thus chosen for further experiments given that it provided the most accurate results, which were independent of the level of opacity of the particles. In addition, the PVM® did not introduce a bias toward small or large particles, unlike the Mastersizer 3000. The PVM® also tracked the evolution of the droplets in real-time, which was not possible with the MasterSizer 3000.

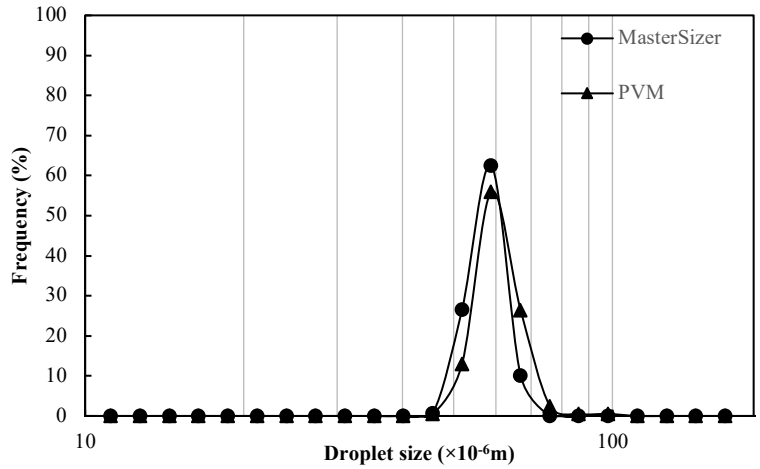

Figure 5.1 Number-based size distributions of particles in the 5.3×10-5~6.3×10-5 m range (from sieving).

Table 5.1 Statistics of sieved particles in the 5.3×10^{-5}~6.3×10^{-5} m

	MasterSizer 3000 (m)	PVM® (m)
d_{10}	5.42×10^{-5}	5.08×10^{-5}
d_{50}	6.17×10^{-5}	5.62×10^{-5}
d_{90}	6.71×10^{-5}	6.41×10^{-5}
$d_{4,3}$	6.15×10^{-5}	6.30×10^{-5}
$d_{3,2}$	6.12×10^{-5}	6.22×10^{-5}

Table 5.2 Individual size distribution statistics of particles A and B measured using the PVM® and the MasterSizer 3000.

	Particle A MasterSizer 3000 (m)	Particle A PVM® (m)	Particle B MasterSizer 3000 (m)	Particle B PVM® (m)
d_{10}	1.44×10^{-5}	1.63×10^{-5}	4.68×10^{-5}	5.01×10^{-5}
d_{50}	2.13×10^{-5}	2.48×10^{-5}	6.06×10^{-5}	6.43×10^{-5}
d_{90}	3.52×10^{-5}	3.54×10^{-5}	7.98×10^{-5}	8.01×10^{-5}
$d_{4,3}$	3.61×10^{-5}	3.45×10^{-5}	7.05×10^{-5}	7.47×10^{-5}
$d_{3,2}$	3.11×10^{-5}	3.21×10^{-5}	6.75×10^{-5}	7.29×10^{-5}

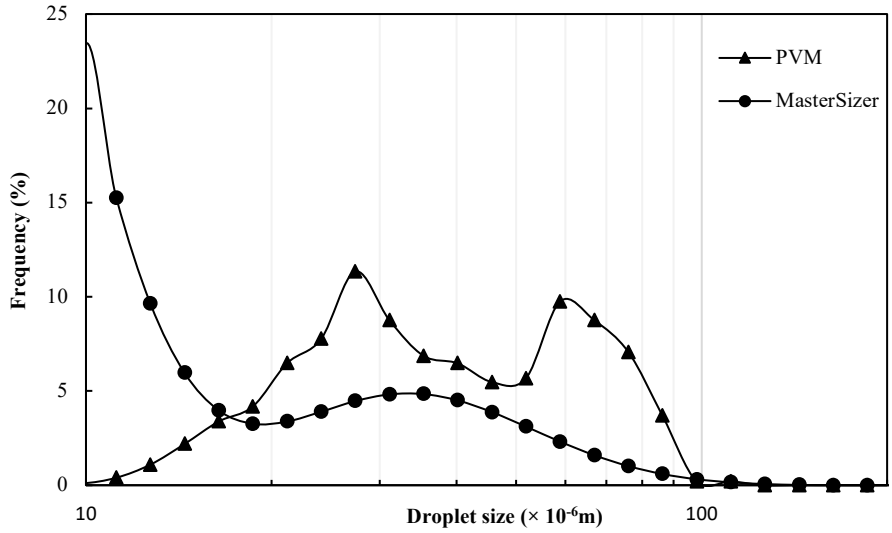

Figure 5.2 Comparison of the number-based size distributions resulting from mixing the same number of particles of two sizes, A and B. The statistics of the distributions are given in Table 5.2.

5.4.2 Evolution of droplet morphology during catastrophic phase inversion

Initially, the addition of oil to the mixing tank resulted in the formation of an O/W emulsion, as shown by the creaming of the droplets at the top of the vial. When the critical volume fraction of the oil phase was reached, the droplets suddenly moved toward the bottom of the vial,

indicating that a W/O emulsion had formed. The phase inversion point (indicated by the concentration of oil reached) was deduced by comparing two adjacent vials, one in which the droplets were at the top of the vial and one in which the droplets were at the bottom. As can be seen in the upper section of Figure 5.3, the O/W emulsion formed at a volume fraction of ≤50 vol%. However, at 55 vol% oil, the emulsion switched to a W/O emulsion, as shown by the accumulation of the droplets at the bottom of the vial. The vial marked (a) in the upper part of Figure 5.3 had a thin white bottom layer that consisted of tiny oil droplets stabilized by particles with a higher density than water, which led them to settle at the bottom of the vial together with some excess particles. The evolution of the morphology of the droplets, as observed by the PVM®, can be seen in the lower section of Figure 5.3. Images (a) through (e) show that the droplets increased in size with the increase in oil concentration until the phase inversion occurred (f). When the dispersed phase reached 50 vol%, just before the phase inversion, water entered the oil droplets (e), where a W/O/W emulsion could be observed. When the oil phase reached 55 vol%, the dispersed and continuous phases inverted. The emulsion type and phase inversion point determined from the PVM® images were in agreement with those of the samples in the vials. The emulsion type was also confirmed by the conductivity of the emulsion, which was zero when the oil phase exceeded 55 vol%.

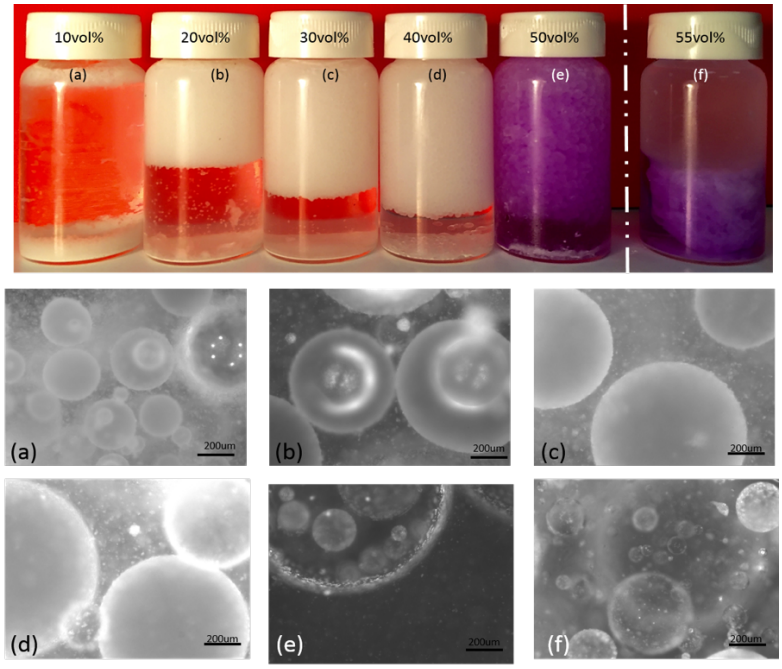

Figure 5.3 Vials with a particle concentration of 2 wt% (upper section). Emulsion samples were collected from vials containing different volume fractions (10 vol% (a), 20 vol% (b), 30 vol% (c), 4 0vol% (d), 50 vol% (e), and 55 vol% (f) (lower section)) corresponding to the PVM® images of volume fractions identical to those in the vials.

5.4.3 Effect of particle concentration on phase inversion

In order to investigate the effect of particle concentration on the phase inversion point, we induced phase inversion using particle concentrations ranging from 2 wt% to 20 wt%. The phase inversion point for each particle concentration was then determined. As can be seen in Figure 5.4, with a particle concentration of 8 wt%, the phase inversion point shifted to between 65 vol% and 70 vol%, a much higher value than with a particle concentration of 2 wt%. In addition, as can be seen in Figure 5.4(f), at a particle concentration of 8 wt%, the phase inversion occurred without a multiple emulsion precursor, as with lower particle concentrations.

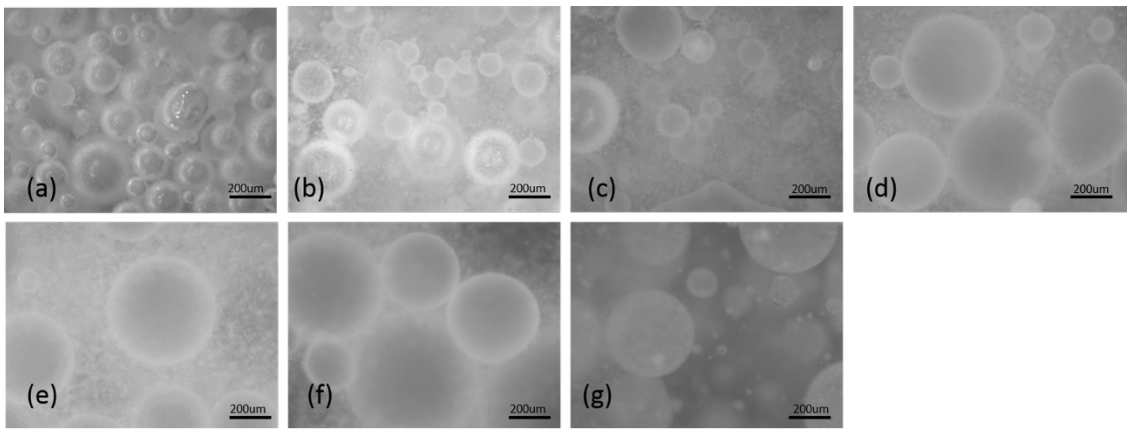

Figure 5.4 Images of emulsions obtained at a particle concentration of 8 wt% and oil volume fractions of (a) 20, (b) 30, (c) 40, (d) 50, (e) 60, (f) 65, and (g) 70 vol%.

The phase inversion points were plotted against the particle concentrations (Figure 5.5). Note that the phase inversion points were located within a range of volume fractions rather than at fixed values. We used the lower value of the range as the phase inversion point. The phase inversion points increased almost linearly with the particle concentrations. This trend suggested that a more internal phase volume was required to generated a phase inversion at a higher particle concentration. Based on these results, one way to create the a stable concentrated emulsion would be to increase the particle concentration. Similarly, based on a previous study on a surfactant-stabilized emulsion , the addition of a monoglyceride oil to a triglyceride oil significantly postpones the phase inversion to a higher water content. In this case, the W/O inversion occurred at 80 vol% water with 1 wt% of monoglyceride compared to 90 vol% water with 3 wt% of monoglyceride. Hence, the behavior we observed was similar to adding a surfactant to a conventional emulsion.

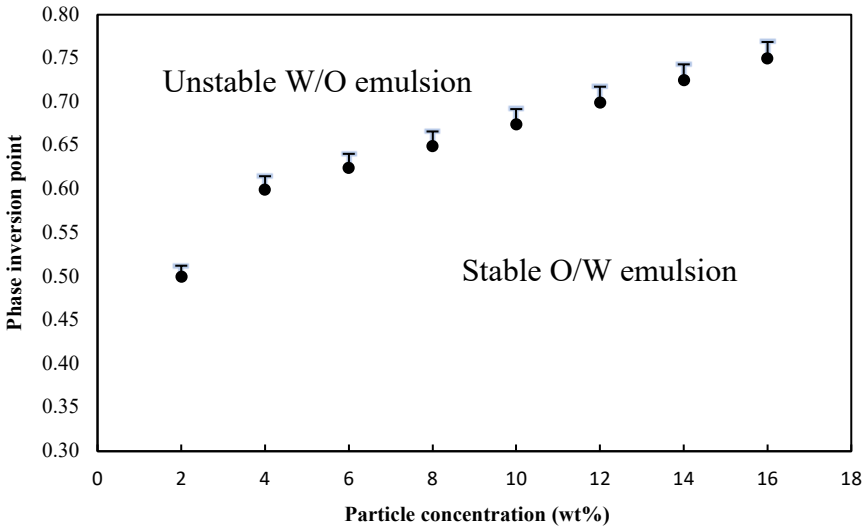

Figure 5.5 Volume fractions of oil required for phase inversion at particle concentrations ranging from 2 to 16 wt%.

5.4.4 Parameters of phase inversion

5.4.4.1 Droplet morphology at the phase inversion point

The droplet sizes measured just before the phase inversion can be seen in Figure 5.6. For each particle concentration, the droplet size exhibited a linear dependence on the dispersed phase volume fraction until the phase inversion occurred. Higher particle concentrations were associated with smaller droplet sizes at the phase inversion point while smaller particle concentrations were associated with larger droplet sizes. Multiple W/O/W emulsions were always observed at a particle concentration of 2 wt%. The effective volume fraction was thus greater than the actual oil volume fraction. For all other particle concentrations, the effective volume fraction equalled the actual oil volume fraction since no multiple emulsions were observed. This observation suggested that phase inversion does not occur at the critical effective volume fraction, which contradicts the results reported by Groeneweg *et al.* (1998). Our results also indicated that multiple emulsions could only be formed with a low particle concentration and a large oil volume fraction.

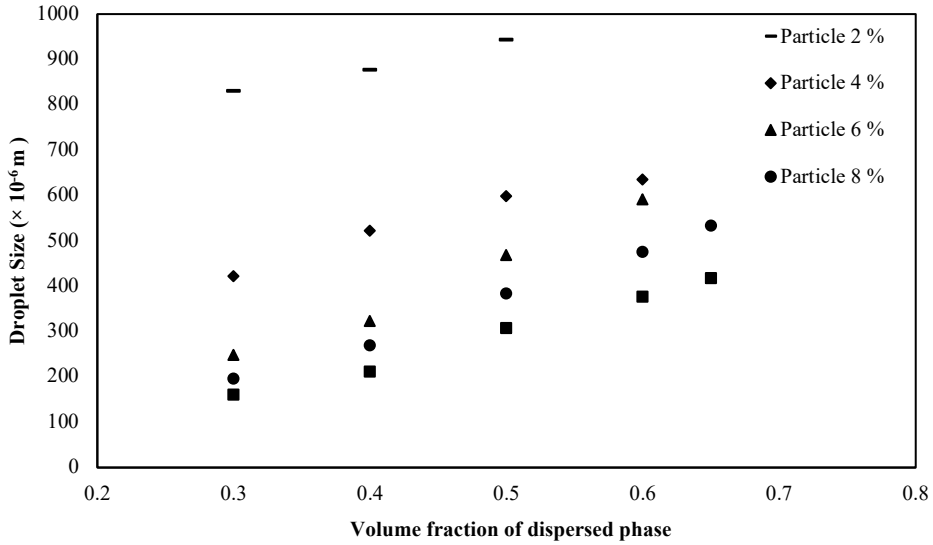

Figure 5.6 Evolution of droplet size before phase inversion at different particle concentrations (2, 4, 6 , 8, and 10 wt%).

5.4.4.2 Particle adsorption at the phase inversion point

The number of emulsified particles at the phase inversion point was deduced by plotting droplet size against particle concentration (Figure 5.7). With a 30 vol% of oil, adding particles beyond 8 wt% had no pronounced effect on further reducing the size of the droplets. Indeed, droplet size was initially controlled by the particle concentration until a limiting size was reached, beyond which some excess particles appeared at the bottom of the mixing vessel after emulsification. Aveyard et al. (2003) investigated the effect of particle concentration on droplet size by preparing PDMS in a water emulsion stabilized with hydrophobic silica particles. As can be seen in Figure 5.9, the ratio of the total number of available particles to the required number of particles was approximately 1 below a particle concentration of 3 wt%, suggesting that all the particles were used for emulsification, leading to a dramatic decline in droplet size. Beyond this value, excess particles always remained, and the droplet size remained constant. This allowed us to separate the generation of stabilized drops into two regimes: a first regime (left part of the figure) where insufficient particles are available to completely cover the interface, and a second regime (right part of figure) where there are more than enough particles available to fully cover the interface. The existence of excess particles was also confirmed by the bi-modal distribution curve based on the MasterSizer 3000 measurements. All the phase inversion points determined in our experiments stayed in the regime indicated on the left part of the figure, where droplet size depended on particle concentration. We thus assumed that all the particles had been emulsified at the phase inversion points.

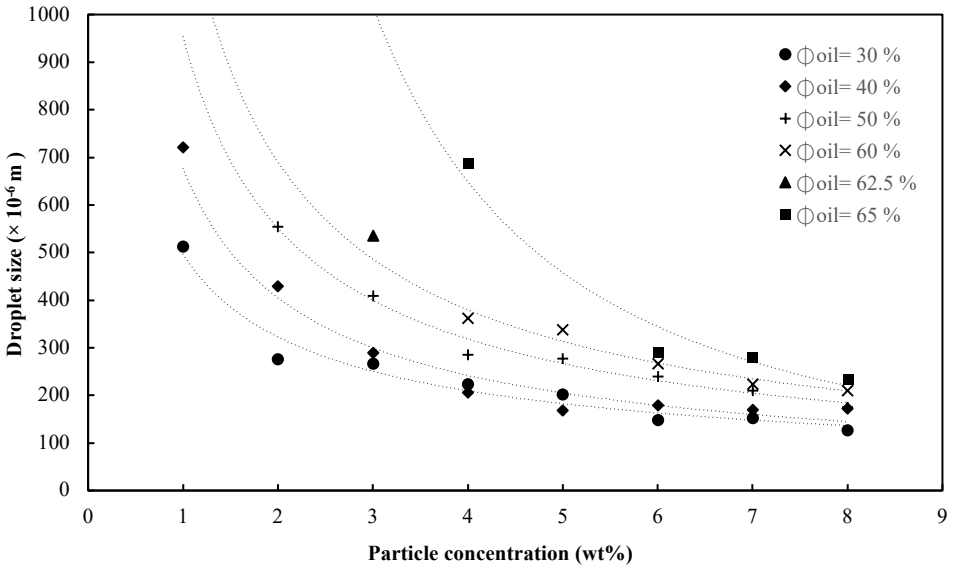

Figure 5.7 Droplets prepared with different volume fractions of 50cSt silicone oil ranging from 30 vol% to 65 vol% plotted as a function of the hydrophilic particle concentration.

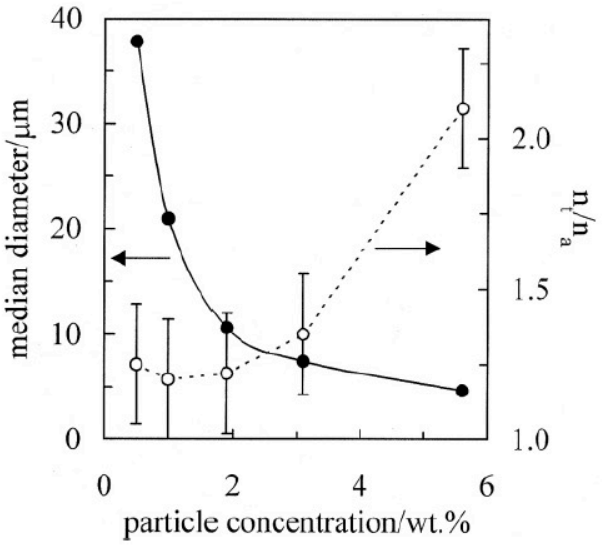

Figure 5.8 Median droplet diameter (left hand ordinate, filled points) as a function of the aqueous concentration of hydrophobic silica particles (25 nm in diameter) in a PDMS-in-water emulsion. Also shown is the ratio of the total number of particles available to the number required to produce a monolayer around all the droplets (right hand ordinate, open points) (adapted from Aveyard et al. (2003).

5.4.4.3 Interaction between the oil volume fraction and the particle concentration

If the particle concentration is kept constant, an increase in the oil volume fraction causes phase inversion from an O/W to an unstable W/O emulsion at some point. In order to display the

phase inversion points for different particle concentrations (Figure 5.5) in a straightforward way, we converted the volume fraction versus the particle concentration into the total surface area versus the particle mass, as shown in Figure 5.9. The surface area increased linearly as a function of the particle mass. The constant value at the phase inversion point was derived from the following trendline equation:

$$k_{PIP}= (S-S_0)/m_p \quad \ldots(5.1)$$

where S is the total surface area of the volume at the phase inversion point and m_p is the particle mass. Since the number of particles is proportional to the mass of the particles, the constant parameter K_{PIP} can be interpreted as the number of particles per surface area. The next issue was to explain the K_{PIP} ratio and to link it to the phase inversion point.

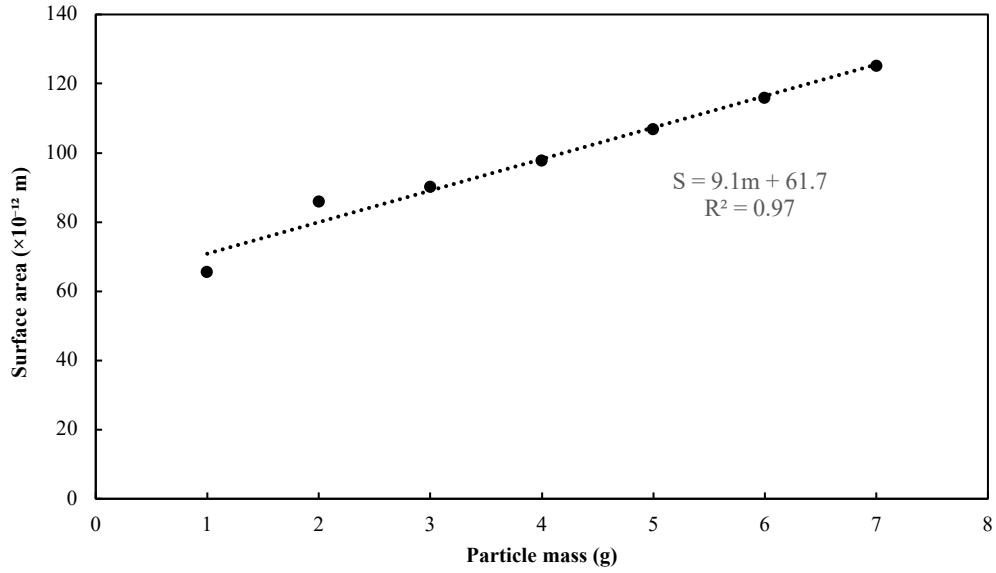

Figure 5.9 Equivalent surface area at the phase inversion points as a function of particle masses ranging from 1 g to 7 g.

5.4.5 Relationship between the determination factor and the coalescence rate

As reported by Tsabet et al. (2015), droplets are assumed to be initially produced by impeller shearing (Figure 5.10). Droplet size thus depends on the breakage potential of the mixing system, as described in step 1 of Figure 5.10. In the present study, the breakage potential was identical in each experiment since we used the same mixing conditions in all the experiments. Particle adsorption was then followed by the generation of an interface, as shown in step 2 of Figure 5.10. In this step, the initial particle coverage fraction was determined by the number of

particles and the available surface area. The droplets then coalesced until they reached the desired particle coverage fraction according to the coverage potential in step 3.

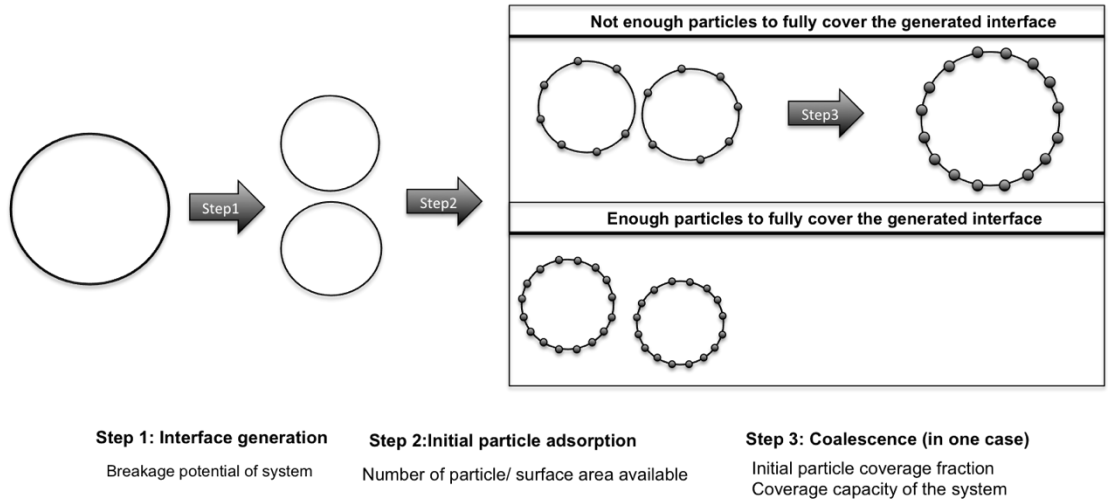

Figure 5.10 Schematic description of two different stabilization mechanisms in a solid-stabilized emulsion (adapted from reference (Tsabet et al., 2015a)).

Due to the limited coalescence phenomenon observed with solid-stabilized emulsions, droplets that are not initially covered will coalesce until they reach the saturated particle coverage fraction. Low n_p/S values lead to rapid coalescence to attain the maximum particle coverage on the droplets as shown in the first case of Figure 5.10. On the other hand, droplets that are initially fully covered (high n_p/S) require no or very little coalescence to reach the maximum particle coverage illustrated in the second case of Figure 5.10. This supports our assumption that the coalescence frequency with initially poor particle coverage is higher than with particle-saturated droplets.

To confirm the relationship between the initial particle coverage and the coalescence rate, we tracked the evolution of droplet size over time with the PVM® by adding a 4 vol% of dispersed oil to distilled water using three conditions: (a) no particles, (b) insufficient particles (6 wt% particle concentration), and (c) sufficient particles, with excess particles (12 wt% particle concentration). The instantaneous droplet size was determined by determining the equilibrium between the breakup and coalescence events. The equilibrium droplet size is determined by the competition between these two events. The dominant effect determines the equilibrium droplet size.

Figure 5.11 shows the results for all the cases. Without particles, the droplet size increased over a 5 to 20 min timeframe as the coalescence event overwhelmed the breakup event. Multiple emulsions were also observed (Figure 5.12), which were a result of the intense coalescence. With insufficient particles, the droplet size decreased slightly over a 5 to 20 min timeframe,

indicating that the coalescence event was slightly more dominant than the breakup event. With sufficient particles, the droplet size decreased significantly over a 5 to 20 min timeframe, suggesting that the breakup event had overwhelmed the coalescence event. The breakup rates in all three cases were identical due to the same mixing conditions and W/O ratio. The coalescence rates of the three cases were determined and tracked the particle concentrations, i.e., no particles > insufficient particles > sufficient particles. Coalescence is the driving mechanism of the phase inversion process (Groeneweg et al., 1998). In neat water-silicone oil systems, the interface between the silicone oil and the water allows for fast film drainage, leading to rapid coalescence with a relatively low volume fraction. On the other hand, a small number of particles provides a rigid steric film around the droplets, suppressing coalescence such that a more dispersed phase is required for phase inversion. This explains why the coalescence rate with no particles is higher than the rate with particles. The behaviors of the coalescence rates of the insufficient and sufficient particle cases were compared. The high coalescence rate observed with insufficient particles was deduced from the low initial particle coverage fraction. When the droplets were initially covered by a sufficient number of particles, each drop-drop collision did not result in film drainage, hence coalescence could not occur. Similar trends have been obtained with conventional emulsions (Henry et al. (2010) and, as can be seen in Figure 5.13, the increase in droplet size only occurs at lower emulsifier concentrations. The size increase corresponded to the coalescence observed with the lowest number of particles used in our experiments. Ata (2008) reported that there is a close relation between the particle coverage fraction and the coalescence rate, that the coalescence time of bubbles covered by particles varies with different surface coverage, and that the total coalescence time increases monotonically with surface coverage, which is consistent with what we observed. Moreover, Arditty et al. (2003) reported that the coalescence rate decreases as a function of surface coverage and that there is no further change in structure once the degree of surface coverage is sufficient to stabilize the droplets.

At the phase inversion points, a relatively low n_p/S ratio corresponding to a low coverage fraction leads to a higher coalescence rate. Once a critical n_p/S ratio is reached after adding more oil, the coalescence rate becomes so high that the breakup rate can no longer balance the events, and phase inversion occurs. This could explain why all the phase inversion points remained in the regime with insufficient particles.

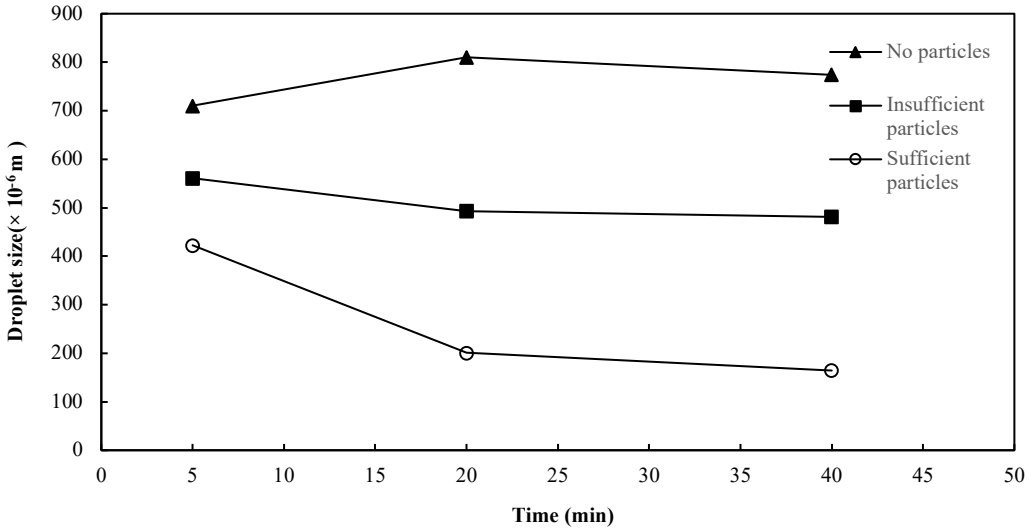

Figure 5.11 Evolution in mean droplet size following the addition of the 40 vol% dispersed oil phase. The droplet sizes were tracked as a function of time for three different conditions: (1) without particles, (2) with insufficient particles (6 wt% hydrophilic particles initially dispersed in the water phase), and (3) sufficient particles (12 wt% hydrophilic particles initially dispersed in the water phase).

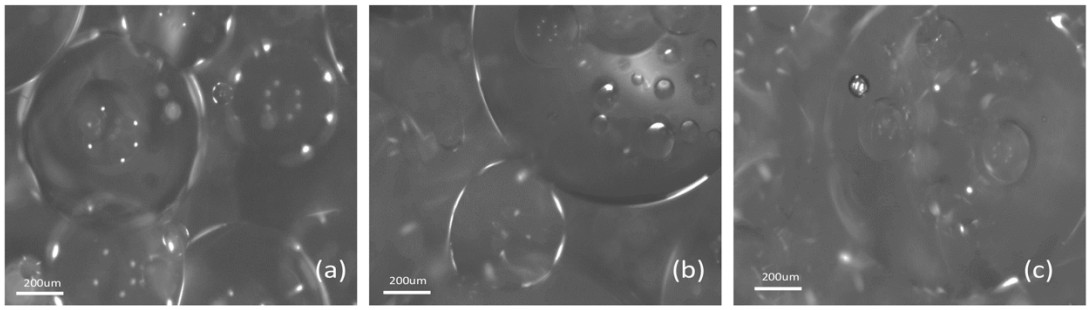

Figure 5.12 PVM® images of a 40 vol% oil dispersed phase with no particles. Morphologies of the droplets following the addition of the oil phase: (a) 5 min, (b) 20 min, (c) 40 min.

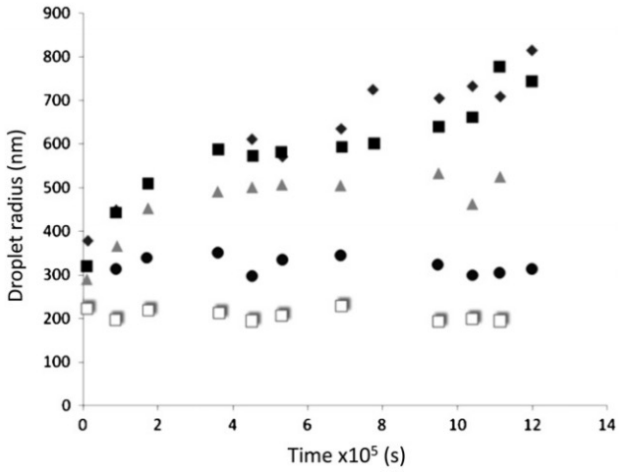

Figure 5.13 Droplet radius as a function of time for an emulsion stabilized with phosphatidylglycerol. From top to bottom, the emulsifier concentrations are 0.08, 0.2, 0.4, 0.8, and 1.6 wt% respectively (adapted from Henry et al. (2010)).

5.5 Conclusions

We used emulsions stabilized by hydrophilic particles initially dispersed in water to show that a catastrophic inversion from an O/W to a W/O emulsion can be triggered by the addition of a dispersed phase. Phase inversion points for a wide range of particle concentrations remained in a regime where there were not enough particles to fully cover the surface generated by the mixing system used. Additionally, a critical n_p/S ratio (number of particles available vs. the surface generated) was identified as a trigger of phase inversion under constant mixing conditions. The inversion of an O/W emulsion to an unstable W/O emulsion took place once the n_p/S ratio fell below a critical value. This was likely due to the fact that a low n_p/S ratio corresponds to a high coalescence rate that significantly exceeds the breakup rate, resulting in a phase inversion. However, the critical n_p/S ratio requires further investigation given that the quantitative relationship between this value and the corresponding coalescence rate remains unknown. Additional work on this aspect will be undertaken, with an emphasis on system parameters.

5.6 Ackowledgement

The authors gratefully acknowledge the financial support by the *Natural Sciences and Engineering Council of Canada* and *TOTAL S.A*.

5.7 Reference

Arditty, S., Whitby, C. P., Binks, B. P., Schmitt, V., & Leal-Calderon, F. (2003). Some general features of limited coalescence in solid-stabilized emulsions. *European Physical Journal E, 11*(3), 273-281. doi:10.1140/epje/i2003-10018-6

Ata, S. (2008). Coalescence of bubble covered by particles. In (Vol. 24, pp. 6085- 6091): Langmuir.

Aveyard, R., Binks, B. P., & Clint, J. H. (2003). Emulsions stabilised solely by colloidal particles. *Adv Colloid Interface Sci, 100*, 503-546. doi:10.1016/s0001-8686(02)00069-6

Binks, B. P., & Lumsdon, S. O. (2000). Transitional phase inversion of solid-stabilized emulsions using particle mixtures. *Langmuir, 16*(8), 3748-3756. doi:10.1021/la991427q

Binks, B. P., Philip, J., & Rodrigues, J. A. (2005). Inversion of silica-stabilized emulsions induced by particle concentration. *Langmuir, 21*(8), 3296-3302. doi:10.1021/la046915z

Brooks, B. W., & Richmond, H. N. (1991). DYNAMICS OF LIQUID LIQUID-PHASE INVERSION USING NONIONIC SURFACTANTS. *Colloids and Surfaces, 58*(1-2), 131-148. doi:10.1016/0166-6622(91)80203-z

Groeneweg, F., Agterof, W. G. M., Jaeger, P., Janssen, J. J. M., Wieringa, J. A., & Klahn, J. K. (1998). On the mechanism of the inversion of emulsions. *Chemical Engineering Research & Design, 76*(A1), 55-63. doi:10.1205/026387698524596

Henry, J. V. L., Fryer, P. J., Frith, W. J., & Norton, I. T. (2010). The influence of phospholipids and food proteins on the size and stability of model sub-micron emulsions. *Food Hydrocolloids, 24*(1), 66-71. doi:10.1016/j.foodhyd.2009.08.006

Jahanzad, F., Crombie, G., Innes, R., & Sajjadi, S. (2009). Catastrophic phase inversion via formation of multiple emulsions: A prerequisite for formation of fine emulsions. *Chemical Engineering Research & Design, 87*(4A), 492-498. doi:10.1016/j.cherd.2008.11.015

Lan, Q., Liu, C., Yang, F., Liu, S. Y., Xu, J., & Sun, D. J. (2007). Synthesis of bilayer oleic acid-coated Fe3O4 nanoparticles and their application in pH-responsive Pickering emulsions. *J Colloid Interface Sci, 310*(1), 260-269. doi:10.1016/j.jcis.2007.01.081

Rondon-Gonzalez, M., Madariaga, L. F., Sadtler, V., Choplin, L., Marquez, L., & Salager, J. L. (2007). Emulsion catastrophic inversion from abnormal to normal morphology. 6. Effect of the phase viscosity on the inversion produced by continuous stirring. *Industrial & Engineering Chemistry Research, 46*(11), 3595-3601. doi:10.1021/ie070145f

Rondon-Gonzalez, M., Sadtler, V., Choplin, L., & Salager, J. L. (2006). Emulsion catastrophic inversion from abnormal to normal morphology. 5. Effect of the water-to-oil ratio and surfactant concentration on the inversion produced by continuous stirring. *Industrial & Engineering Chemistry Research, 45*(9), 3074-3080. doi:10.1021/ie060036l

Sajjadi, S., Zerfa, M., & Brooks, B. W. (2000). Morphological change in drop structure with time for abnormal polymer/water/surfactant dispersions. *Langmuir, 16*(26), 10015-10019. doi:10.1021/la0004808

Tsabet, E. (2014). *From Particle to Process: Modeling the production of Pickering emulsion.* (Doctorate), Polytechnique Montreal, Montreal.

Tsabet, E., & Fradette, L. (2015). Effect of the properties of oil, particles, and water on the production of Pickering emulsions. *Chemical Engineering Research & Design, 97*, 9-17. doi:10.1016/j.cherd.2015.02.016

Tsuji, S., & Kawaguchi, H. (2008). Thermosensitive pickering emulsion stabilized by poly(N-isopropylacrylamide)-carrying particles. *Langmuir, 24*(7), 3300-3305. doi:10.1021/la701780g

Utada, A. S., Lorenceau, E., Link, D. R., Kaplan, P. D., Stone, H. A., & Weitz, D. A. (2005). Monodisperse double emulsions generated from a microcapillary device. *Science, 308*(5721), 537-541. doi:10.1126/science.1109164

Vaessen, G. E. J., Visschers, M., & Stein, H. N. (1996). Predicting catastrophic phase inversion on the basis of droplet coalescence kinetics. *Langmuir, 12*(4), 875-882. doi:10.1021/la950379g

W.Ostwald, K. Z. (1910). In (Vol. 6).

CHAPTER 6 ARTICLE 3: DESTABILIZING SOLID-STABILIZED EMULSIONS: PARTICLE ATTACHMENT DYNAMICS AT THE INTERFACE

Article history: Submitted to *Chemical Engineering Journal* on November 27, 2018.

Authors: Bing Wan, Emir Tsabet, Louis Fradette

6.1 Summary

The purpose of the present study was to provide new insights into the dynamics of particle behavior at oil-water interfaces during mixing. We used a novel approach to destabilize emulsions in the absence of chemicals by adding fresh particles to solid-stabilized emulsions. Glass microspheres with intermediate wettability were used to stabilize silicone oil-in-water emulsions (5 vol% oil fraction) in a standard mixing configuration. Colored and uncolored particles with the same properties were used to identify particle exchanges at the droplet interface and freshly added particles in the continuous phase during emulsification. The impact of the size and wettability of the freshly added particles on particle exchanges was investigated using real-time PVM® (Mettler Toledo, USA) images and by observing their behavior in vials. Emulsion destabilization occurred when larger and more hydrophobic particles were added to a stable emulsion during mixing. The destabilization may have been caused by the passage of droplets through the impeller zone in the tank and/or the contamination of the particles by oil. Freshly added particles, which are more competitive than oil-contaminated particle clusters, can attach to the droplet interface. These findings will have implications for applications where the destabilization of droplets covered by fine particles is the goal.

Keywords: particle attachment, attachment dynamics, interface, solid-stabilized emulsion (Pickering emulsion), destabilization

6.2 Introduction

It was first reported in the early 1990s that fine solid particles can stabilize emulsions (French et al., 2016; Pickering, 1907). The stability of solid-stabilized emulsions (SSEs, also known as Pickering emulsions) relies on the formation of particle networks around droplets, which hinders coalescence. The particles are physically attached to the oil/water interface, and it requires a significant amount of energy to detach them (Aveyard et al., 2003). The amount of energy required to detach the particles can be estimated using the following equation (Levine et al., 1989):

$$G = \pi R_p^2 \gamma_{ow}(1 \pm cos\theta_{ow})^2 \ldots (6.1)$$

where G is the detachment energy, R_p is the particle radius, γ_{ow} is the oil/water interfacial tension, and $\theta_{ow}$is the contact angle at the oil/water interface. The extraordinary stability of Pickering emulsions is a major challenge in applications requiring phase separation. One large-volume application that requires phase separation is the extraction of bitumen from the Canadian oil sands (Masliyah et al., 2004). In addition, the emulsified water droplets in crude oil create refining and corrosion problems (Sullivan et al., 2002).

A common strategy used to destabilize SSEs is to add surface-active molecules or surfactants to the emulsion. The impact of surfactants on SSE stability has been attributed to the modification of particle wettability (Alargova et al., 2004; Subramaniam et al., 2006), which affects the extent of the immersion of particles in the interface as well as the electrostatic dipole-dipole interaction forces of the particles (Reynaert et al., 2006). A number of researchers have reported that surfactant molecules can replace particles at the interface by reducing the interfacial energy below a certain level (Drelich et al., 2010; Katepalli et al., 2013; Vashisth et al., 2010), and that surfactant-stabilized emulsions can be destabilized by the addition of solid particles, which results in a higher coalescence rate (Katepalli et al., 2013). Binks et al. (2007) have argued that particle attachment energy results from competition between particle wettability and interfacial tension (Binks et al., 2007).

The stability of SSEs can be affected by mixtures of particles with different wettabilities. Whitby et al. (2010) reported that the capacity of partially hydrophobic titania particles to stabilize an emulsion is reduced when they are mixed with hydrophilic silica particles. The authors proposed that the silica particles hinder the formation of titania particle networks around the droplets, which destabilizes the emulsion at high silica particle concentrations (Whitby et al., 2010). Similarly, Briggs et al. (1921) suggested that silica particles should facilitate the generation of oil-in-water (O/W) emulsions while carbon black should facilitate the generation of water-in-oil (W/O) emulsions. However, they were unsuccessful in generating emulsions with a mixture of silica particles and carbon black (Briggs, 1921). In contrast, Tarimala et al. (2004) showed that emulsions can be stabilized with a mixture of 1 μm hydrophobic (~117°) and hydrophilic (~59°) solid particles. They reported that the particles simultaneously segregate to the same interface, which is likely due to the amphiphilic nature of the interface (Tarimala et al., 2004). Binks et al. (2017) observed colored hydrophilic and hydrophobic particles at the oil-water interface, indicating that a transitional phase inversion had occurred (Binks et al., 2017). Binks et al. (2000) also reported that a transitional phase inversion from an O/W to a

W/O emulsion occurs due to the alteration of the mass ratio of the particle mixture when there is an equal volume fraction of oil and water (Binks et al., 2000d).

Overall, the studies mentioned above indicate that emulsions can be destabilized or that their stabilization can be hindered when the particle networks around the droplets are disturbed by the addition of fresh solid particles or of surfactant molecules. The main approach for altering the stability of emulsions is based on controlling particle wettability since this property plays a crucial role in governing the type and stability of the resulting emulsion.

The aim of the present work was to investigate particle behavior during emulsification and to determine the optimal conditions for facilitating emulsion destabilization and phase separation.

6.3 Materials and Methods

6.3.1 Materials

Pure silicone oil (Clearco Products Co. Inc., USA) was used as the dispersed phase, distilled water was used as the continuous phase, and soda lime glass microspheres (particles) from different suppliers were used as stabilizers. The properties of the soda lime glass microspheres and the silicone oil are given in Table 6.1and Table 6.2 respectively. The anhydrous ethanol (95 vol%) and HCl (1 M) used to modify the surfaces of the particles were from Laboratoire Mat (Canada), and the (3-aminopropyl)trimethoxysilane (97%) was from Sigma-Aldrich (USA).

Table 6.1 Properties of the soda lime glass microspheres

Supplier	**d_{32} (µm)**	**Density (kg/m^3)**	**Type**	**Color**	**θ_{ow} (∘)**
Cospheric	3	2520	uncoated	white	90 ± 4
Cospheric	3	2520	silane coated	white	112 ± 8
Potters	35	2520	uncoated	white	85 ± 4
Potters	65	2520	uncoated	white	93 ± 3
Potters	35	2520	silane coated	white	90 ± 4
Ceroglass				green	
Ballotini	113	2520	modified	red	114 ± 3

Table 6.2 Properties of the silicone oil: viscosity and interfacial tension

Silicone Oil	Dynamic Viscosity (Pa·s)	Interfacial Tension (N/m)
S20	1.90E-02	(42 ± 2)E-03
S50	4.80E-02	
S8000	8.1E-01	
S1000	9.71E-01	

6.3.2 Experimental methods

6.3.2.1 Modification of particle surface wettability

The wettabilities of green (Ceroglass) and white (Potters) particles (D_{32}=35µm) were modified by grafting silane groups on their surfaces. The particles (10 g) were dispersed in 100 mL of ethanol under agitation. After reducing the pH to 1 using an appropriate volume of 1 M HCl, 1 mL of 97% (3-aminopropyl)trimethoxysilane was added to the dispersion under agitation. The mixtures were agitated in a fume hood for 12 h. The particles were subsequently allowed to settle for 2 h and were then dried in an oven at 60°C for 3 h.

6.3.2.2 Measurement of surface and interfacial tensions

Surface and interfacial tensions were measured with the pendant drop technique using an OCA 20 instrument from Data Physics (USA). The results are shown in the table 6.2.

6.3.2.3 Determination of particle wettability

Particle wettability was determined using the capillary rise technique (Fournier et al., 2009). Three capillaries were used in parallel to ensure reproducibility (Figure 6.1). Capillary rise was recorded using a video camera (DCR-PC101; Sony) to determine the rising height over time (h/t) and hence the contact angle. Contrast between wet and dry powders was enhanced using bromocresol dye, which turns purple when dissolved in water. Preliminary tests were conducted to ensure that the interfacial tension and capillary rise were not affected by the dye. After measuring the contact angle with the oil phase (θ_{oa}) and the water phase (θ_{wa}), the contact angle at the oil-water interface was estimated using the following Bartell-Osterhof equation, which was derived from Young's equation(Bartell et al., 1936):

$$\sigma_{wa}cos\theta_{wa} = \sigma_{oa}cos\theta_{oa} + \sigma_{ow}cos\theta_{ow} \ldots (6.2)$$

where σ_{wa} is the interfacial tension between water and air (surface tension of water), σ_{oa} is the surface tension of the oil, and σ_{ow} is the interfacial tension between the oil and the water. The results are given in Table 6.1.

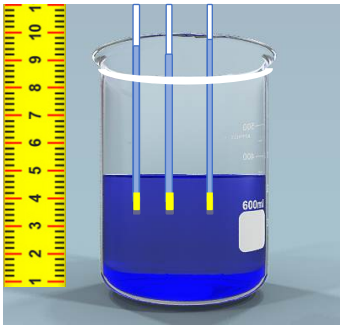

Figure 6.1 Schematic drawing of the capillary rise setup

6.3.2.4 Characterization of the emulsions

The stabilities and size distributions of the emulsions were characterized. Stability was evaluated by comparing the height of the released free oil layer to the overall height of the emulsion samples. The samples were collected using a large tip opening pipet during emulsification, were placed in 20 mL vials, and were kept at rest for 24 h.

Droplet size distributions were obtained with a particle vision microscope (PVM®; Mettler Toledo) using the procedure described by Wan et al. (2017) PVM® images were also used to observe the type of particles attached to the droplet interfaces during mixing.

6.3.2.5 Emulsification procedure

Emulsions were prepared using an off-centered pitched blade turbine in a 4 L flat bottom non-baffled tank. Table 6.3 gives the geometrical parameters of the emulsification setup.

Table 6.3 Geometrical parameters of the emulsification setup

Baffle	Non-baffled	
Agitator	Pitched blade turbine impeller	
Number of blades	3	
Tank diameter	T	0.1630 m
Impeller diameter	D=1/3T	0.0543 m
Clearance	C=1/2T	0.0815 m
Liquid height	H=T	0.1630 m

Two emulsification steps were used to investigate the dynamics of particle attachment and detachment at the interface following initial emulsification and following the addition of fresh particles.

O/W base emulsions (5 vol% oil fraction) were prepared using 323.5 g of silicone oil, 3064 g of water, and 10 g of a given type of particle. This amount of particles was insufficient to cover the entire interface and is referred to as RefEm (base emulsion) in Table 6.4.

The particles were first dispersed in water at an agitation rate of 700 RPM. The oil was then added at the same impeller speed. The agitation was maintained for 2 h in order for a stationary droplet size to be reached. Fresh particles were subsequently added periodically. New emulsions were characterized at each step after reaching the stationary droplet size and were compared to the base emulsion. The following particle properties were studied to compare the base and new emulsions:

(a) Particle color: After preparing RefEm_1 (see in the Table 6.4) 2h was stabilized with 10 g of 35 μm green particles of intermediate hydrophobicity (θ_{ow} =90 ± 4°), 10 g of 35 μm white particles with similar properties were added after 2 h of mixing. After an additional 2 h of mixing, 10 g of 35μm green particles were added.

For the following cases

(b) Particle size

(c) Particle wettability

(d) Particle wettability and size

10 g, 20 g, 20 g, 20 g, 20 g, or 20 g of fresh particles were added to the base emulsion at 2 h intervals. The properties of the particle types used for the different cases are given in Table 6.4.

Table 6.4 Particle types used in the corresponding cases, and names of the base emulsions

Cases	Particle type used in the base emulsion and the name of the base emulsion		Fresh particle type
Particle color	35 µm green particles	RefEm_1	35 m white particles
Particle size	3 µm uncoated particles	RefEm_2	35 m uncoated particles
Particle size	35 µm uncoated particles	RefEm_3	35 µm uncoated particles
Particle size (reverse)	35 µm uncoated particles	RefEm_3	3 µm uncoated particles
Particle wettability	3 µm uncoated particles	RefEm_2	3 µm hydrophobic particles
Particle wetability	3 µm uncoated particles	RefEm_2	3 µm uncoated particles
Particle wettability (reverse)	3 µm uncoated particles	RefEm_2	3 µm hydrophilic particles
Particle size and wettability	3 µm uncoated particles	RefEm_2	113 µm red coated particles

6.3.2.6 Colloidal probe technique (atomic force microscopy)

The colloidal probe technique was used to measure attachment time and detachment forces based on the procedure of Tsabet et al. (2016). A micromanipulator was used to attach a particle to the tip of the cantilever. The forces and time required to reach the equilibrium position were measured with a Dimension 3100 SFM microscope equipped with a Nanoscope V controller (VEECO) using the contact mode. Figure 6.2 shows a simplified representation of the measurement setup. Measurements were performed using 65 µm uncoated particles and silicone oil (8400 cSt).

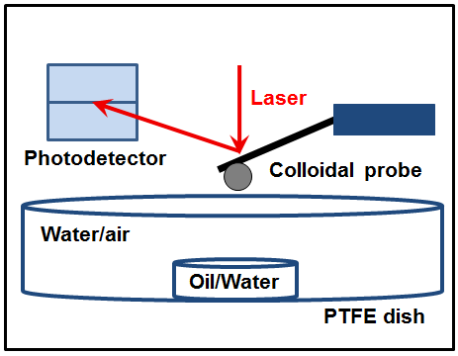

Figure 6.2 Colloidal probe setup (Tsabet et al., 2016)

6.4 Results and Discussion

6.4.1 Particle exchange at the interface during emulsification

Figure 6.3 shows optical microscopic images of droplets obtained following the procedure for case (a) where green and white particles with similar properties were added alternatively to RefEm_1. The interface of RefEm_1 was only filled with green particles (which appear dark) (Figure 6.3(a)). After the addition of white particles (Figure 6.3(b)), a mixture of white particles (which appear bright) and green particles could be seen at the interface, indicating that some initial green particles had been replaced by white particles. This finding was further confirmed by Figure 6.3(c), which shows a droplet that is mostly covered by newly added green particles.

These results suggest that some particles detach from the interface during mixing and are replaced by freshly added particles. However, additional studies are required to understand this behavior. It should also be noted that it is impossible to determine the attachment-detachment dynamics of the white particles in this particular experiment. It is, however, reasonable to assume that the white particles also keep attaching to and detaching from the oil-water interface.

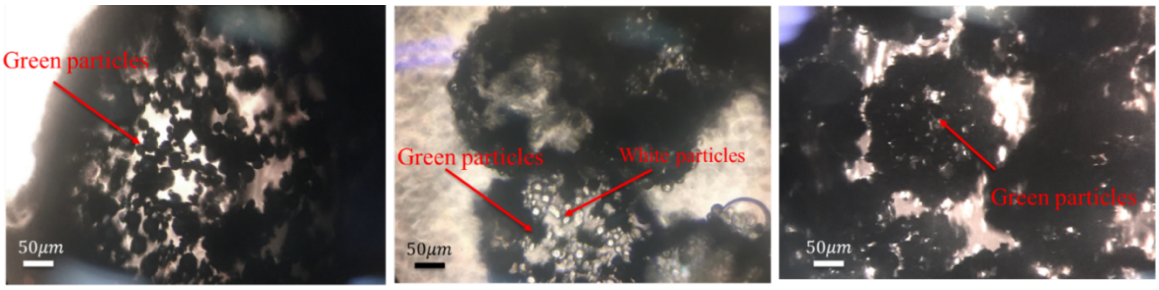

Figure 6.3 Microscope images of an O/W emulsion (10 vol% oil fraction) stabilized by different successively added particles. (a) RefEm_1; (b) addition of 35 μm white particles; (c) addition of 35 μm green particles.

6.4.2 The impact of particle size on the particle exchange process

Figure 6.4 presents the evolution of the Sauter mean diameter when 35 µm uncoated particles are sequentially added to RefEm_2 compared to the case when emulsions are stabilized with 35um uncoated particles alone. The Sauter mean diameter was plotted as a function of the mass ratio between the added particles and the initial particles.

Sequentially adding more particles to RefEm_2 resulted in a decrease in average droplet size due to the increase in the coverage potential of the system, which is expected for SSEs (Figure 6.4). In addition, larger droplets were initially obtained with 35 µm uncoated particles, which is also in agreement with the results reported in the literature (Binks et al., 2001).

The blue curve in Figure 6.4 shows that there was an increase in the droplet size for RefEm_2, which was initially stabilized with 3 µm particles. The size of the droplets began to increase immediately after the addition of the 35 µm uncoated particles to RefEm_2 and kept increasing with each addition of 35 µm uncoated particles until it reached the same size as the SSE obtained with 35 µm uncoated particles alone (red curve). This finding indicated that the initial 3 µm uncoated particles are gradually replaced by the 35 µm uncoated particles during emulsification. The gradual replacement of particles can be seen in the PVM® images in Figure 6.6(a).

The same behavior was seen with an emulsion stabilized with larger particles and to which smaller particles were added. This can be seen in Figure 6.5 (blue curve), where 3 µm uncoated particles are added to RefEm_3 and compared to the case when emulsion were produced with 3 µm uncoated particles alone. The droplet size decreased after the addition of 3 µm uncoated particles to RefEm_3. The decrease in size progressed until it reached the same evolution of droplet size observed when the emulsion was stabilized with 3 µm uncoated particles alone (red curve). The replacement of particles over time can be seen in the PVM® images in Figure 6.6(b).

The transition between stabilization controlled by 3 µm particles and stabilization controlled by 35 µm particles took place at a particle mass ratio of 9, while it occurred at a ratio of approximately 5 when smaller particles were added (Figure 6.5). This behavior can be attributed to the fact that 3 µm particles have a higher coverage capacity than 35 µm particles for the same mass. These findings also indicated that it is possible to control emulsion size and eventually emulsion stability by adding fresh particles of a given size.

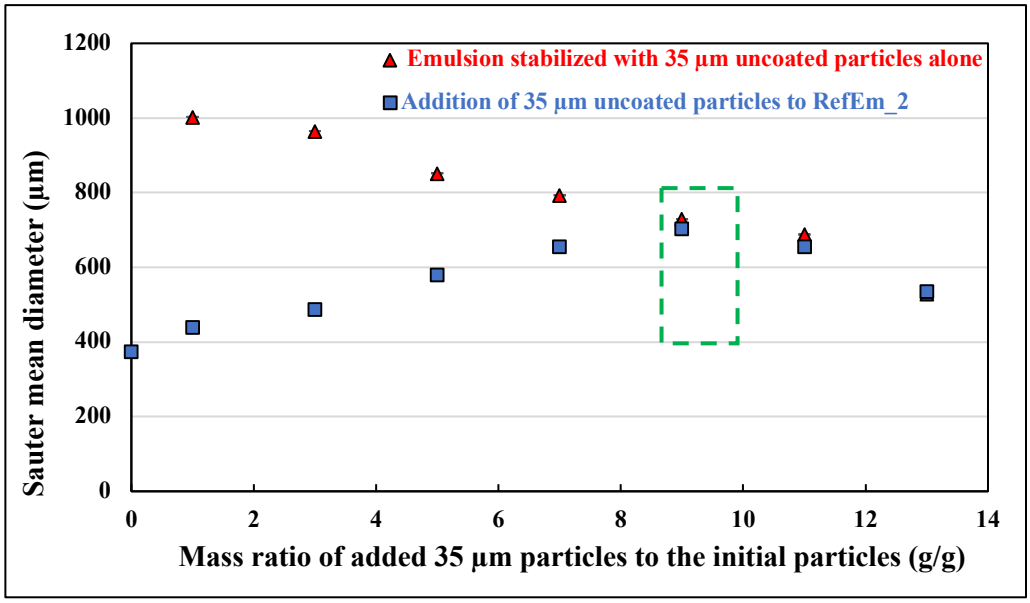

Figure 6.4 Evolution of the Sauter mean diameter when 35 µm uncoated particles are added to RefEm_2 compared to an emulsion stabilized with 35 µm uncoated particles alone.

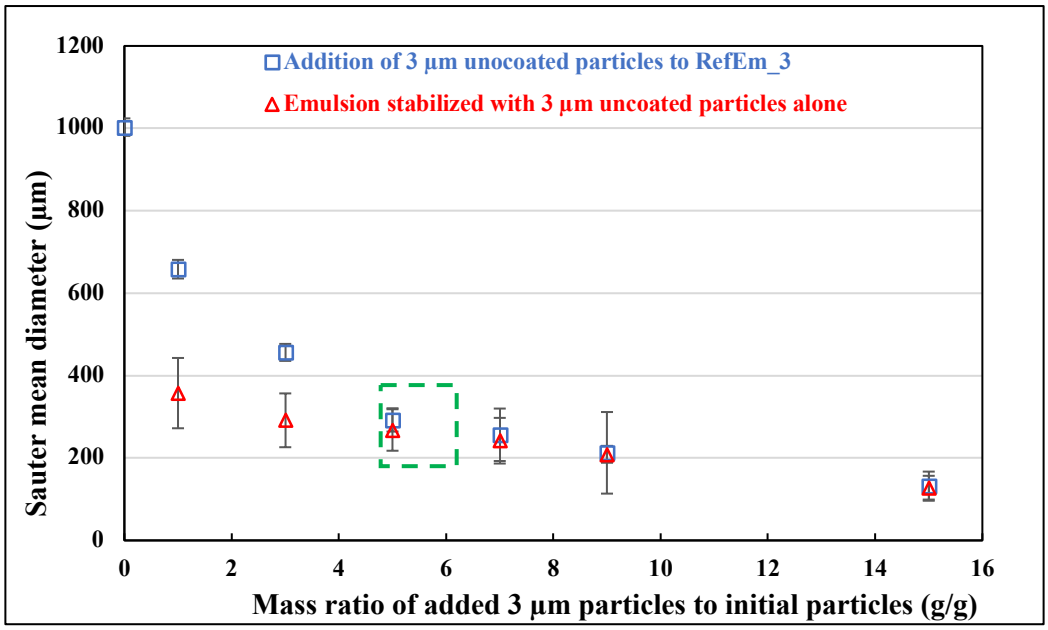

Figure 6.5 Evolution of the Sauter mean diameter when 3 µm uncoated particles are added to RefEm_3, which was stabilized with 35 µm uncoated particles, compared to an emulsion stabilized with 3 µm uncoated particles alone.

Fresh particle	**0 g**	**+10 g**	**+20 g**	**+20 g**
(a)	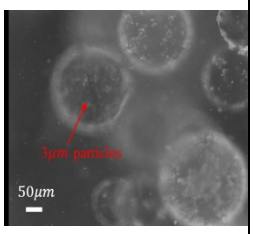	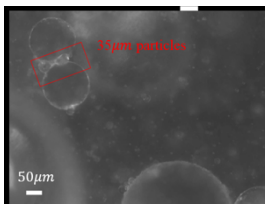	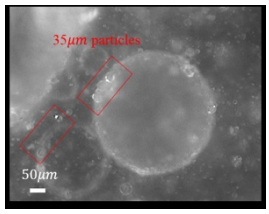	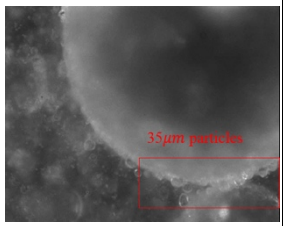
(b)	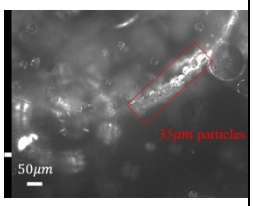	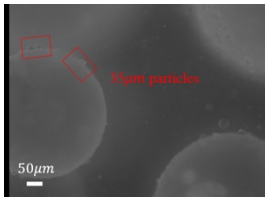	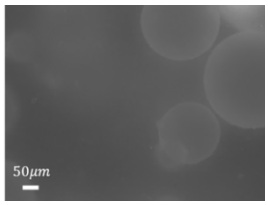	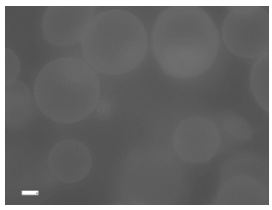

Figure 6.6 PVM® images showing particles attached at interface when fresh 35 μm particles are progressively added to RefEm_2 (a) and when fresh 3 μm uncoated particles are progressively added to RefEm_3 (b).

6.4.3 The impact of particle wettability on the particle exchange process

To study the impact of particle wettability, 3 μm uncoated particles ($\theta_{ow} = 90 \pm 4°$) and 3 μm modified hydrophobic particles ($\theta_{ow} = 112 \pm 8°$) are progressively added to RefEm_2, the starting emulsion. The evolution of Sauter mean diameter during this process is given in Figure 7. The addition of uncoated particles resulted in a continuous decrease in droplet size, indicating that stabilization was controlled by the coverage potential of the particles. The reduction in droplet size stopped beyond a mass ratio of 1 when modified hydrophobic particles were added to uncoated particles. After this, a plateau with a slight increase in droplet size beyond a mass ratio of 12 was reached.

The emulsion samples in Figure 6.8 show that oil droplets start to settle after sample (a), which corresponds to a mass ratio of 1, leaving a layer of oil on the top, which is more evident in samples (c), (d), and (e). Moreover, the amount of settled droplets increases with the mass of added particles as shown in Figure 6.8. After examining droplets from the last sample obtained with modified hydrophobic particles, it can be seen that particles are trapped inside the droplets of the last sample containing modified hydrophobic particles.

The impact of adding particles with different wettabilities on the emulsion destabilization is shown in Figure 6.9. It can be seen that adding modified hydrophobic particles to a base emulsion stabilized with uncoated particles results in increasing destabilization until a 50 vol%

free oil fraction is reached. Figure 6.9 also shows that this behavior is intermediate between the case where only modified particles are used and the case where only uncoated particles are used. Indeed, larger droplets with encapsulated particles are obtained, while uncoated particles produce smaller settled droplets, and modified hydrophobic particles produce bulk oil with trapped particles. It can be assumed that adding more modified particles to the base emulsion will lead to complete destabilization, with a sedimented structure containing oil and particles. This behavior suggests that the addition of particles with a given wettability can be used to destabilize an emulsion.

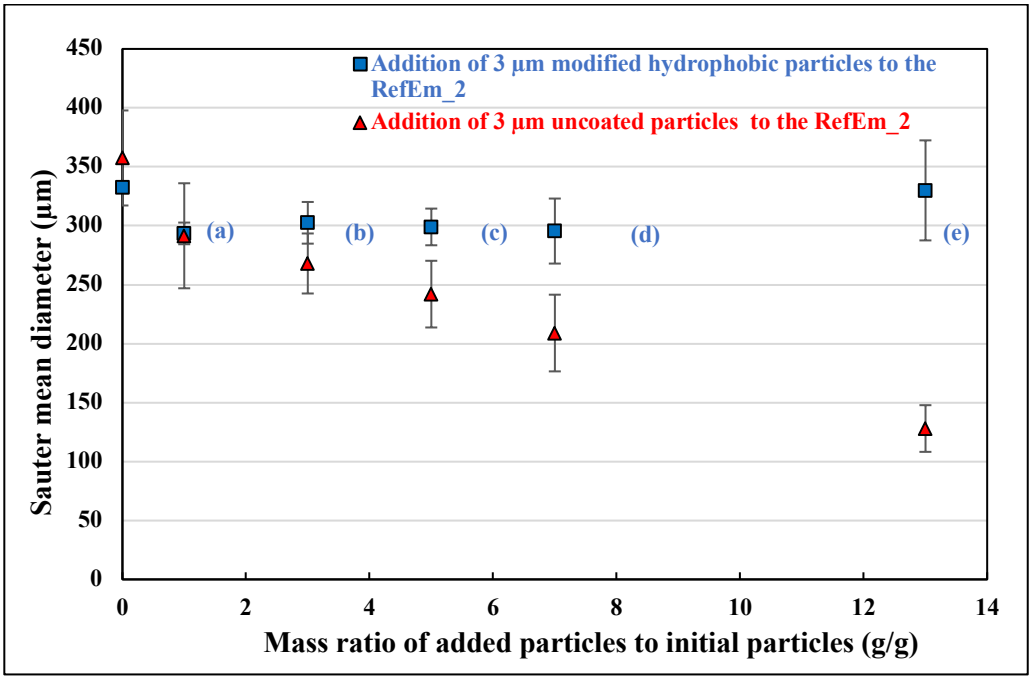

Figure 6.7 Evolution of the Sauter mean diameter when fresh 3 µm modified hydrophobic particles are added to RefEm_2 compared to an emulsion stabilized with 3 µm uncoated particles alone.

After investigating the effect of adding hydrophobic particles to an emulsion stabilized with particles of intermediate wettability, the reverse experiment was performed. Figure 6.10 reveals the behavior, size, and volume ratio of separated oil over initial oil following the addition of 3 µm modified hydrophilic particles to RefEm_2. The addition of modified hydrophilic particles had no impact on the properties of RefEm_2, indicating that an emulsion can only be destabilized if the fresh particles have an affinity for the oil phase.

	RefEm_2	+10 g	+20 g	+20 g	+20 g	+60 g
Adding uncoated 3 µm particles						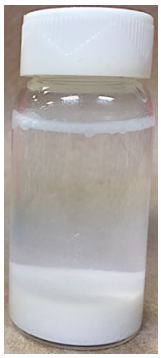
Adding modified hydrophobic 3 µm particles						

Figure 6.8 Photographs of emulsions stabilized with increasing amounts of 3 µm modified hydrophobic particles added to RefEm_2

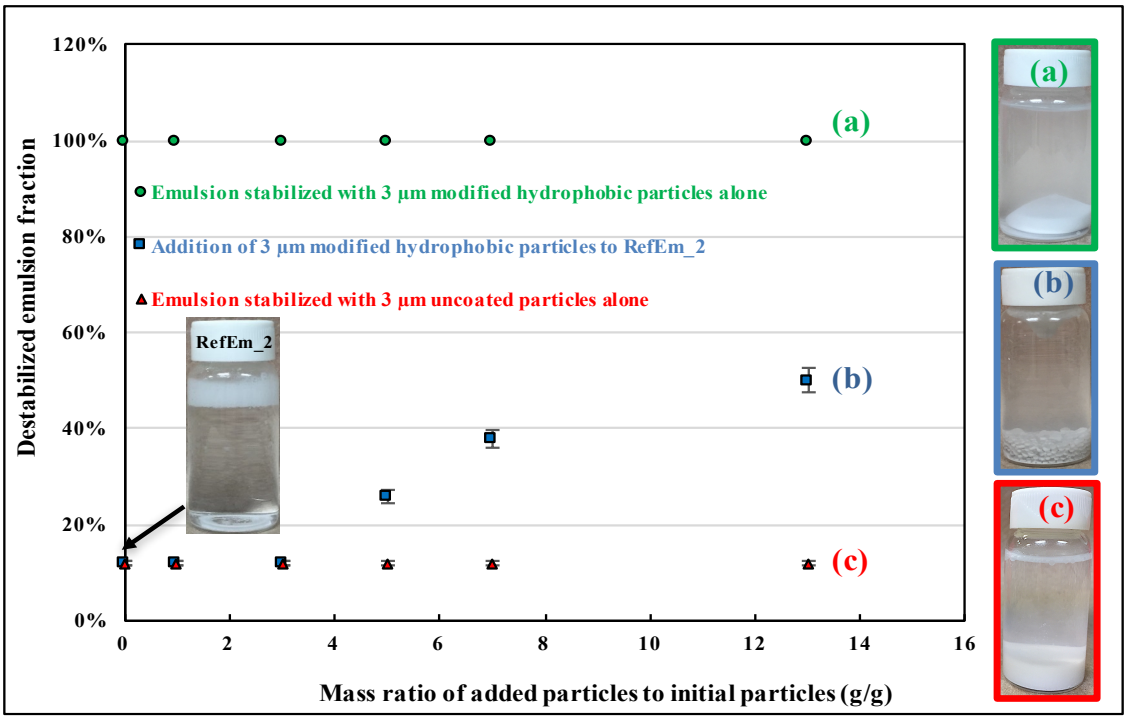

Figure 6.9 Evolution of a destabilized RefEm_2 as a function of the type of particle added

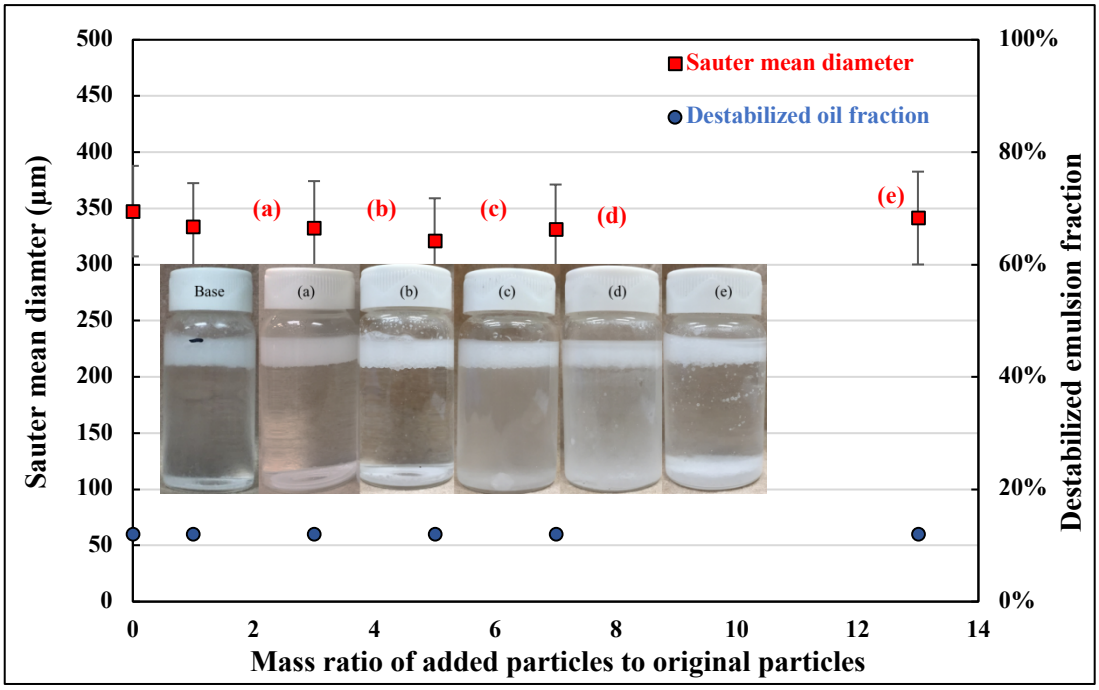

Figure 6.10 Evolution of emulsion behavior, Sauter mean diameter, and the destabilized oil fraction when very hydrophilic 3 µm particles are added to RefEm_2

6.4.4 Combined effect of particle wettability and size on emulsion behavior

Given that the addition of larger or hydrophobic particles resulted in an increase in droplet size and/or the partial or total destabilization of the O/W emulsion, we investigated the combined impact of these properties on a base emulsion.

Figure 6.11 presents the behavior of the emulsion and the proportion of destabilized emulsion when hydrophobic 113 µm red particles ($\theta_{ow} = 114 \pm 3°$) were added to RefEm_2 as per the methodology used for case (d). The droplet size began increasing as soon as the red particles were added (+10 g). This was followed by a destabilization process in which an increasing amount of coalesced droplets were formed when more particles were added. Complete destabilization was evident at the end of the process, with encapsulated particles in the oil phase at the top and the bottom of the sample. The destabilization process resulted from particle exchange at the interface during mixing. This can be seen in Figure 6.12, where the larger hydrophobic red particles progressively replaced the initial small white particles at the droplet surface. These findings indicated that freshly added particles control the properties of stable Pickering emulsions, including their size, behavior, and stability.

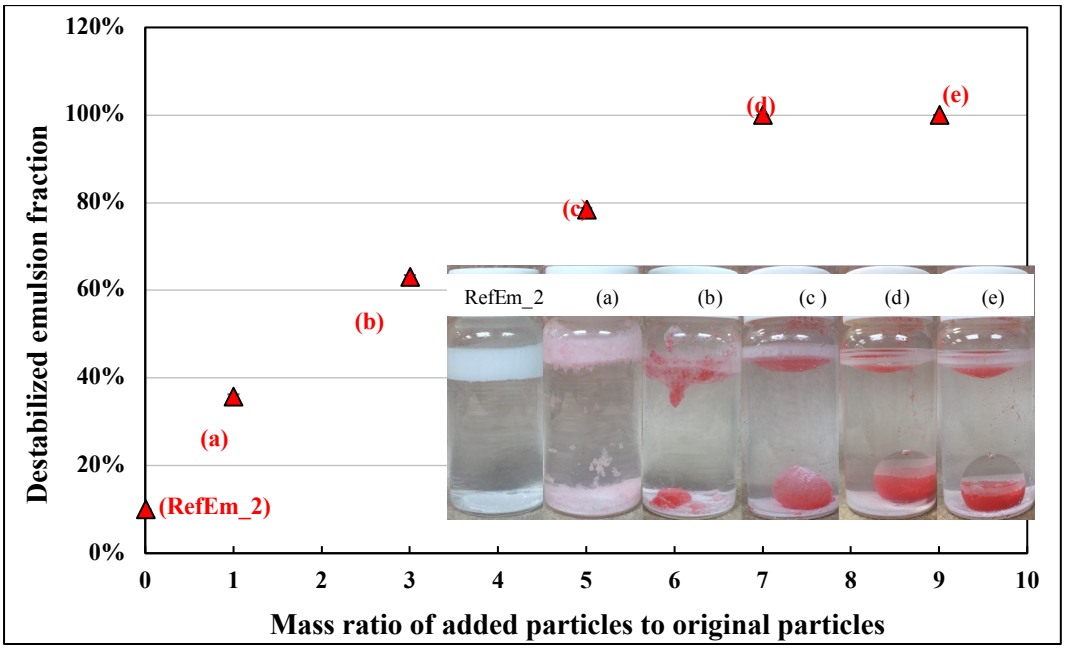

Figure 6.11 Emulsion behavior when hydrophobic 113 µm red particles ($\theta_{ow} = 114 \pm 3°$) are added to RefEm_2

(a)	(b)	(d)
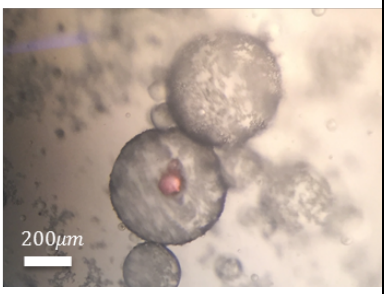	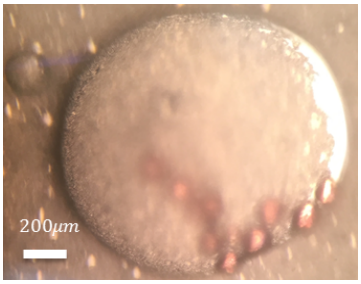	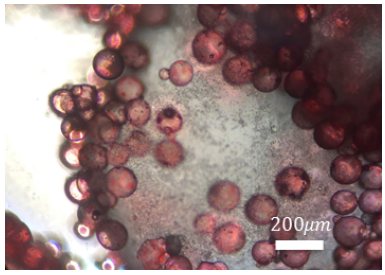

Figure 6.12 Microscopic images of the droplets obtained in cases (a), (b), and (d) in Figure 11 when hydrophobic 113 μm red particles ($\theta_{ow} = 114 \pm 3°$) are added to RefEm_2

Unlike the addition of 3 μm hydrophobic particles to RefEm_2 (Figure 6.9), where a large amount of particles must be added to cause destabilization, a significantly smaller amount of 113 μm hydrophobic particles is required to disrupt the particle coating of RefEm_2. This may be due to the relatively large particle coverage area of the 113 μm hydrophobic particles. Based on a simple calculation of the coverage area $\pi(sin\theta\ R_p)^2$(Tsabet et al., 2015b), a 113 μm red hydrophobic particle covers approximately 5115 μm^2 of a droplet, while a 3 μm modified particle only covers approximately 7 μm^2. The low coverage area would thus make it more difficult for 3 μm modified particles to destabilize the emulsion under similar mixing conditions.

6.4.5 Analysis of the particle exchange mechanism

Previous sections provided evidence of particle exchange at the interface during emulsification and during mixing after emulsification. We next focused on identifying the mechanisms involved in particle replacement. Since the stability of particles at the interface is ensured by the capillary force, the particles can be detached if a countervailing force that exceeds the capillary force is applied. The main forces acting on spherical particles, which are based on our previous investigation of process models (Tsabet et al., 2015b), are given in Table 6.5.

Figure 6.13 illustrates the amplitudes of the attachment and detachment forces for 3 μm and 35 μm uncoated particles (the particles used to stabilize RefEm_2 and RefEm_3, respectively) obtained from the equations given in Table 6.5. In both cases, the attachment forces were much higher than the detachment forces, suggesting that some other mechanism must be involved in detaching the particles from the interface.

Table 6.5 Forces acting on spherical particles during emulsification

Force	Nature	General Expression
Capillary	Attachment	$F_{att} = 2\pi\gamma_{ow}R_p(cos\left(\frac{\theta_{ow}}{2}\right))^2$
Particle weight	Attachment/Detachment	$F_g = \frac{4}{3}\pi R_p^3\rho_p g$
Hydrodynamic	Attachment/Detachment	$F_{hyd} = \frac{4}{3}\pi R_p^3\rho_p a_t, a_t = \frac{1.9\varepsilon^{\frac{2}{3}}}{(R_d + R_p)^{\frac{1}{3}}}$
Laplace pressure	Detachment	$F_{lap} = (\pi R_p^2 sin^2\theta_{ow})\frac{2\gamma_{ow}}{R_d}$

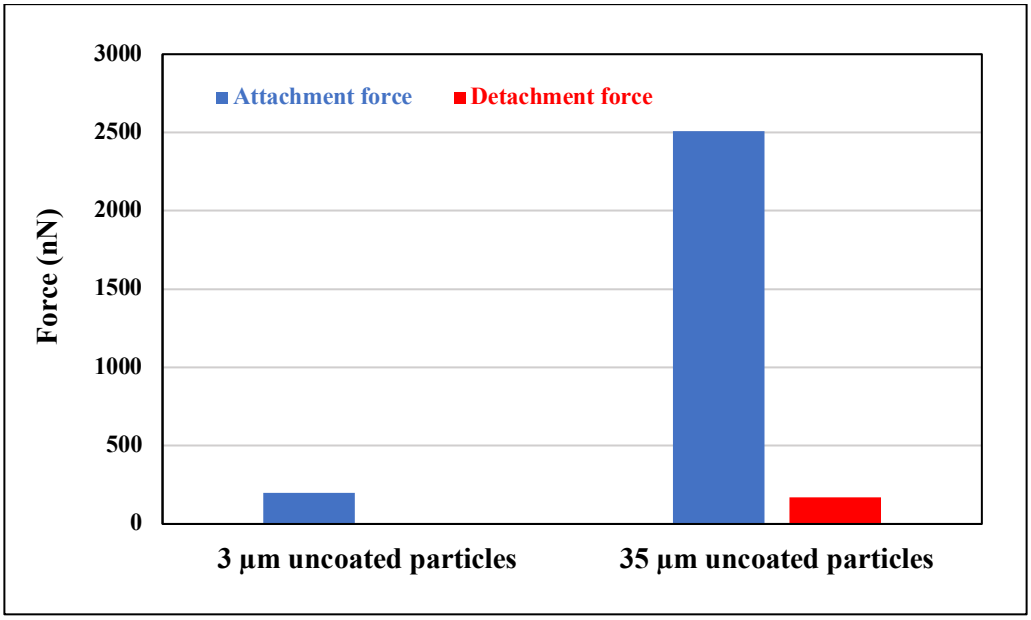

Figure 6.13 Estimated attachment and detachment forces

To better understand the detachment mechanism, we used the colloidal probe technique to measure the time required to reach the equilibrium position (Tsabet et al., 2016). We also measured the detachment force of a 65 µm uncoated particle at the W/O (oil viscosity: 8400 cSt) interface. Figure 6.14 shows the evolution of these parameters when the same particle is attached to and detached from the oil-water interface several times. When the particle reattached, the time required to reach the equilibrium position decreased, while the force required to detach the particle increased. This can be explained by the increased affinity of the particle for the oil phase after being attached and detached many times from the interface. It is reasonable to assume that a film of oil remains on the surface of the particle after detachment,

that the interaction of the particle with the interface occurs through the oil film on the particle surface, and that attachment relies on an oil-oil interaction rather than the expected capillary force.

This experiment provided an indication that, in our mixing tank, when the initial particles (particles used in the base emulsion) were detached from the interface in the high shear zone (around the impeller), the surfaces of the detached particles were contaminated with oil. It can be assumed that, after a certain emulsification time, the particles become so contaminated with oil that they are no longer able to reattach to the interface.

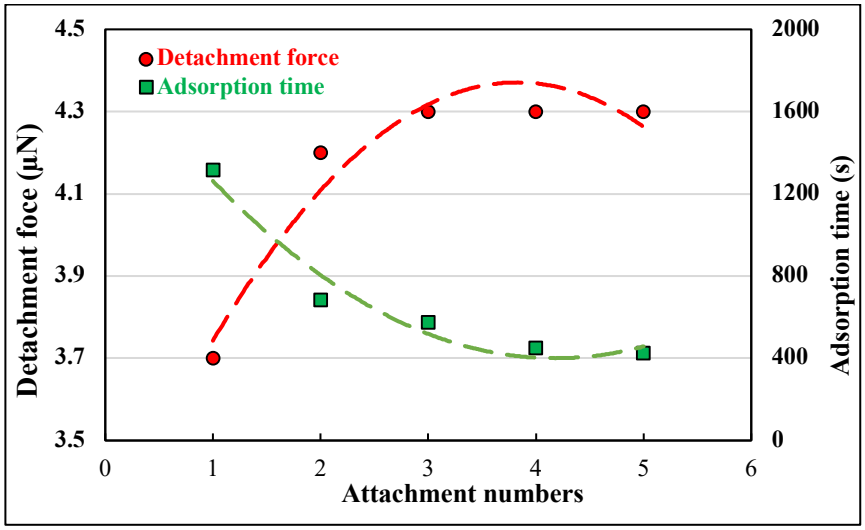

Figure 6.14 Impact of attaching and detaching the same particle at the oil-water interface

Our assumption was confirmed by the evolution of the droplet sizes observed in a 1000 cSt silicone O/W emulsion, which was tracked during 4 days of mixing. Characteristic diameters (d_{10}, d_{90}, and d_{32}) are shown in Figure 6.15. The droplet size increased considerably after mixing for 30 h, especially with d_{90}, which was more likely to generate larger droplets. This is in agreement with our observations and suggests that a destabilization process occurs after a given mixing time.

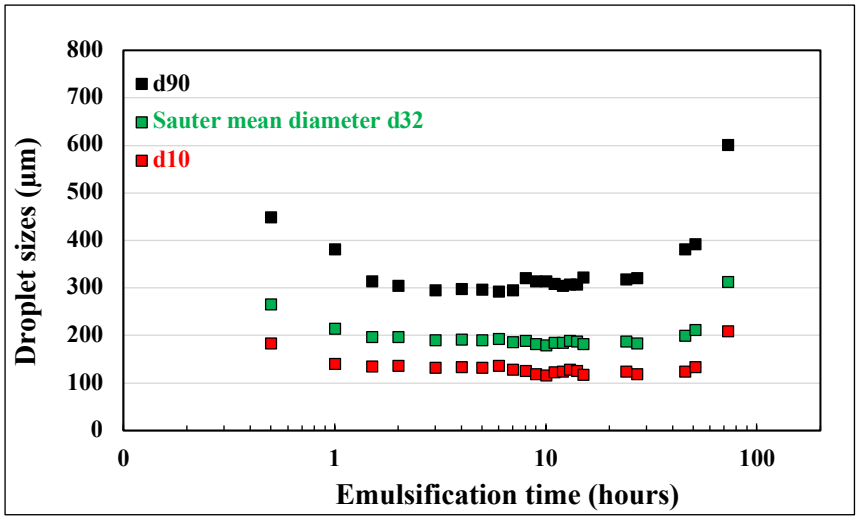

Figure 6.15 Impact of attaching and detaching the same particle at the oil-water interface of a 1000 cSt silicone oil-in-water emulsion stabilized with 600 g of 35 µm modified particles ($\theta_{ow} = 90 \pm 4°$) and mixed at an agitation rate of 560 RPM

Figure 6.16 compares the effect of emulsification time on the d_{90} of two oils with different viscosities (1000 cSt and 20 cSt) using 600 g of 3 µm uncoated particles ($\theta_{ow} = 90 \pm 4°$) mixed at an agitation rate of 560 RPM. The increase in droplet size was more marked with the highest viscosity oil while the droplet size remained almost constant with the lowest viscosity oil, indicating that the particles became more contaminated with the 1000 cSt oil than with the 20 cSt oil.

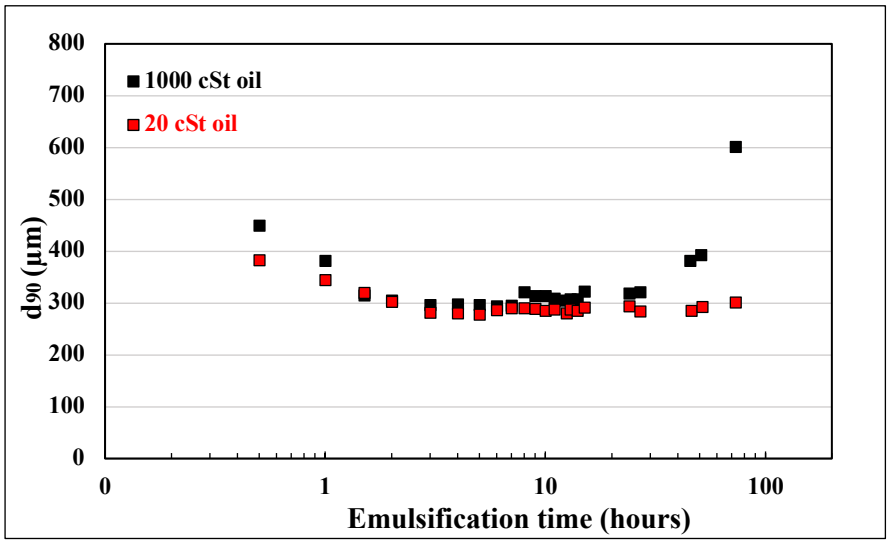

Figure 6.16 Impact of attaching and detaching the same particles at the oil-water interface

Tsabet et al. (2015) reported that droplets follow stream lines and regularly pass through the impeller zone(Tsabet et al., 2015a). During these passages, droplets are sheared off by hydrodynamic forces and particles are detached, with a thin film of oil coating the surfaces of

the particles. These oil-contaminated particles can form clusters when they collide. With low viscous oils, these clusters are more prone to breaking in the impeller zone, producing smaller clusters or free particles that can stabilize the droplets. However, with highly viscous oils, the clusters are stronger, are less prone to breaking in the impeller zone, and generate larger droplets that can only be destabilized after a long period of mixing.

As fresh particles were added during the emulsification process, they were more effective than oil-contaminated particles at forming clusters. The fresh particles were consequently more prone to attaching to the droplet surface at places freed up when the initial particles detached. It can, however, be assumed that if the mixing lasts long enough and if no fresh particles are added, the emulsion will be destabilized regardless of the viscosity of the oil.

6.5 Conclusion

We show for the first time that fresh particles added to an existing emulsion can replace the initial particles at the interface under the effect of fluid dynamics. The original droplet size and the stability of SEEs can be altered by adding particles of given sizes and wettability under constant agitation. The impact of particle size and particle wettability on the exchange process suggests that larger particles, which favor the dispersed phase, can destabilize the original emulsion. This was confirmed by the fact that an O/W emulsion covered with 3 µm uncoated particles with intermediate wettability was destabilized by adding 113 µm hydrophobic particles. Newly added particles are more effective than the initial particles at stabilizing an emulsion. Droplets pass continuously through the high-shear impeller zone in a mixing tank, resulting in the detachment of particles from their surface. The particles then re-attach to the droplets in the low-shear or stabilization zone. However, detached particles are contaminated with oil, as shown by the AFM (atomic force microscopy) measurements, and form clusters, which makes them less effective at re-attaching to exposed areas of the interface compared to the newly added, clean particles.

6.6 References

Alargova, R. G., Warhadpande, D. S., Paunov, V. N., & Velev, O. D. (2004). Foam superstabilization by polymer microrods. *Langmuir, 20*(24), 10371-10374. doi:10.1021/la048647a

Aveyard, R., Binks, B. P., & Clint, J. H. (2003). Emulsions stabilised solely by colloidal particles. *Adv Colloid Interface Sci, 100*, 503-546. doi:10.1016/s0001-8686(02)00069-6

Bartell, F., & Zuidema, H. (1936). Wetting characteristics of solids of low surface tension such as talc, waxes and resins. *Journal of the American Chemical Society, 58*(8), 1449-1454.

Binks, B. P., Desforges, A., & Duff, D. G. (2007). Synergistic stabilization of emulsions by a mixture of surface-active nanoparticles and surfactant. *Langmuir, 23*(3), 1098-1106. doi:10.1021/la062510y

Binks, B. P., & Lumsdon, S. O. (2000). Transitional phase inversion of solid-stabilized emulsions using particle mixtures. *Langmuir, 16*(8), 3748-3756. doi:10.1021/la991427q

Binks, B. P., & Olusanya, S. O. (2017). Pickering emulsions stabilized by coloured organic pigment particles. *Chemical Science, 8*(1), 708-723. doi:10.1039/c6sc03085h

Briggs, T. R. (1921). Emulsion with finely divided solids. *The journal of industrial and engineering chemistry, 13*(11).

Drelich, A., Gomez, F., Clausse, D., & Pezron, I. (2010). Evolution of water-in-oil emulsions stabilized with solid particles Influence of added emulsifier. *Colloids and Surfaces a-Physicochemical and Engineering Aspects, 365*(1-3), 171-177. doi:10.1016/j.colsurfa.2010.01.042

Fournier, C. O., Fradette, L., & Tanguy, P. A. (2009). Effect of dispersed phase viscosity on solid-stabilized emulsions. *Chemical Engineering Research & Design, 87*(4A), 499-506. doi:10.1016/j.cherd.2008.11.008

French, D. J., Brown, A. T., Schofield, A. B., Fowler, J., Taylor, P., & Clegg, P. S. (2016). The secret life of Pickering emulsions: particle exchange revealed using two colours of particle. *Scientific Reports, 6*. doi:10.1038/srep31401

Katepalli, H., John, V. T., & Bose, A. (2013). The Response of Carbon Black Stabilized Oil-in-Water Emulsions to the Addition of Surfactant Solutions. *Langmuir, 29*(23), 6790-6797. doi:10.1021/la400037c

Levine, S., Bowen, B. D., & Partridge, S. J. (1989). STABILIZATION OF EMULSIONS BY FINE PARTICLES .1. PARTITIONING OF PARTICLES BETWEEN CONTINUOUS PHASE AND OIL-WATER INTERFACE. *Colloids and Surfaces, 38*(4), 325-343. doi:10.1016/0166-6622(89)80271-9

Masliyah, J., Zhou, Z. J., Xu, Z. H., Czarnecki, J., & Hamza, H. (2004). Understanding water-based bitumen extraction from athabasca oil sands. *Canadian Journal of Chemical Engineering, 82*(4), 628-654. doi:10.1002/cjce.5450820403

Pickering, S. U. (1907). Emulsions. *Chem.Soc.*, 20.

Reynaert, S., Moldenaers, P., & Vermant, J. (2006). Control over colloidal aggregation in monolayers of latex particles at the oil-water interface. *Langmuir, 22*(11), 4936-4945. doi:10.1021/la060052n

Subramaniam, A. B., Mejean, C., Abkarian, M., & Stone, H. A. (2006). Microstructure, morphology, and lifetime of armored bubbles exposed to surfactants. *Langmuir, 22*(14), 5986-5990. doi:10.1021/la060388x

Sullivan, A. P., & Kilpatrick, P. K. (2002). The effects of inorganic solid particles on water and crude oil emulsion stability. *Industrial & Engineering Chemistry Research, 41*(14), 3389-3404. doi:10.1021/ie010927n

Tarimala, S., & Dai, L. L. (2004). Structure of microparticles in solid-stabilized emulsions. *Langmuir, 20*(9), 3492-3494. doi:10.1021/la036129e

Tsabet, E., & Fradette, L. (2015a). Effect of the properties of oil, particles, and water on the production of Pickering emulsions. *Chemical Engineering Research & Design, 97*, 9-17. doi:10.1016/j.cherd.2015.02.016

Tsabet, E., & Fradette, L. (2015b). Semiempirical Approach for Predicting the Mean Size of Solid-Stabilized Emulsions. *Industrial & Engineering Chemistry Research, 54*(46), 11661-11677. doi:10.1021/acs.iecr.5b02910

Tsabet, E., & Fradette, L. (2016). Study of the properties of oil, particles, and water on particle adsorption dynamics at an oil/water interface using the colloidal probe technique. *Chemical Engineering Research & Design, 109*, 307-316. doi:10.1016/j.cherd.2016.02.001

Vashisth, C., Whitby, C. P., Fornasiero, D., & Ralston, J. (2010). Interfacial displacement of nanoparticles by surfactant molecules in emulsions. *J Colloid Interface Sci, 349*(2), 537-543. doi:10.1016/j.jcis.2010.05.089

Wan, B., & Fradette, L. (2017). PHASE INVERSION OF A SOLID-STABILIZED EMULSION: EFFECT OF PARTICLE CONCENTRATION. *Canadian Journal of Chemical Engineering, 95*(10), 1925-1933. doi:10.1002/cjce.22892

Whitby, C. P., Fornasiero, D., & Ralston, J. (2010). Structure of oil-in-water emulsions stabilised by silica and hydrophobised titania particles. *J Colloid Interface Sci, 342*(1), 205-209. doi:10.1016/j.jcis.2009.10.068

CHAPTER 7 GENERAL DISCUSSION

Solid-stabilized emulsion brings about an increasing amount of attention over the last decades. In the field of the solid-stabilized emulsion, numerous efforts were made to investigating the influence of operating parameters on the properties of the end-product. Nevertheless, limited researches are related to the processing of SSEs. In this work, we focus on examining the role of particles in the dynamic processes, such as emulsion generation, coalescence and destabilization.

To validate PVM® (particle vision microscope), a real-time size measurement probe, a comparison of the volume-based particle size distribution (PSD) has been made with a widely used off-line size measurement device (Mastersizer 3000). Using a narrow-size-range particle sample (35 to 45 μm), we obtained the PSD results with almost no differences (around 5%) between these two instruments. Moreover, a similar size result is obtained when using opaque particles or transparent particles, which highlights that PVM® is not affected by the optical properties of the particles. Furthermore, a bimodal particles sample is prepared with a mixture of an equal number of larger ones and smaller ones. The PSD of the bimodal particle sample obtained from PVM® possesses two peaks of equal height as expected. Such behaviour confirms that the PVM® has no bias in detection frequency concerning different particles sizes. Therefore, PVM® is demonstrated to determine the dynamic size evolution during the emulsification and phase inversion process. Insertion of the PVM® into the mixing tank enables us to simultaneously capture the images up to a speed of 10 frames per second. Followed by that, the images are processed with a homemade software (sphere analysis) to obtain the average droplet size over time. Remarkably, this tool could provide precise size data during evolution regarding different locations, rapid phase change or time-dependent study.

Exploiting the PVM® probe, we demonstrated the variation of droplet size at different locations (impeller zone and coalescence zone) in the mixing tank before reaching the equilibrium state. The process of breakage and coalescence has thus been studied independently by subjecting to the following operating conditions respectively: 1) the droplet size evolution during the first 10 mins of emulsification in the impeller zone; 2) the droplet size evolution following a sudden reduction of the rotation speed from 700 RPM to 350 RPM in the coalescence zone. By analogy to the liquid-liquid system, the presence of particles yields relatively larger droplets during the droplets generation process. The same behaviour was observed when adding particles to the liquid-liquid dispersion during the early stage of emulsification. Thus, it is deduced that the particles lower the breakage efficiency by affecting the energy dissipation and getting involved in the particle adsorption process. This assumption is confirmed from the comparison of initial

droplet size among the systems containing attachable particles, unattachable particles (particles that are not able to adsorb to the interface) and without particles in the emulsification. After reaching equilibrium in a dilute O/W emulsion (0.5 vol%), a shift of DSD from bimodal to unimodal distribution are observed when increasing the number of particles. As no coalescence undergoes in such a low dispersed phase volume fraction, the breakage mechanism is responsible for the corresponding resulting droplet distribution. We then attributed the fragmentation mode to the stability of the initial droplets. For the stabilized droplets, they tend to break homogeneously with forming normal distribution as a result. In contrast, for the droplet covered with insufficient particles or no particles, they tend to form bi-modal distribution as a consequence of the collisions between the small eddies (Tcholakova S. et al. (2007)). Higher oil volume fraction, yet, weakens the breakage effect due to the increased notable coalescence effect. Followed by that, two types of equilibrium was reported based on the ratio between particle coverage potential (A_{cov}) and generated interface (A_{gen}): When the ratio is above 1, a stable equilibrium is established, as the balance cannot be interfered with impeller change or particle addition. On the other hand, the dynamic equilibrium is observed at the ratio smaller than 1. In other words, the balance between the breakage and the coalescence is broken under the variation of impeller speed. The coalescence frequency appears to be more significant under a lower ratio. Indeed, this ratio determines the emulsion stability and the possibility of further coalescence.

Therefore, the ratio ought to be lowered in order to induce the coalescence. It could be possibly achieved using two approaches 1) increasing the generated interface by adding dispersed phase volume or 2) decreasing the particle coverage potential by expelling particles at the interface.

The catastrophic phase inversion from 10 vol% O/W emulsion to W/O emulsion was achieved by a gradual addition of oil until reaching the phase inversion point, which is indicated from the conductivity meter. The PVM® images reveal the evolution of droplet morphology as the oil addition. It can be seen that the droplet size grows with the dispersed phase volume fraction, along with the formation of multiple emulsion before the phase inversion. To further investigate the impact of particles on the phase inversion, we used the particle concentration ranging from 2 wt% to 16 wt% respectively for such process. The linear increase of phase inversion points against the particle concentration suggests the instability of emulsion at a lower particle concentration. Based on the linear relationship, a constant slop defined as n_p/S was assumed to be the critical parameter of triggering the catastrophic phase inversion, below or beyond which could leads to an inverted emulsion or a stable O/W emulsion correspondingly. In addition, the phase inversion points are found to stay in the regime where the particles cannot

fully cover the system-generated interface, as the droplet size reduces dramatically over the particle concentration. The high coalescence rate associated with the low value of n_p/S is responsible for the occurrence of phase inversion.

Next, we considered the particle behaviour at the oil/water interface during the dynamic mixing. While the particles with different colours are introduced to the system alternatively, the corresponding change of the particles at the interface after each addition suggests the particle exchange phenomenon. Such behaviour changes our perspective that once particles are attached at the interface, the emulsion is well stabilized. Whether adding 35 μm particles to the base emulsion stabilized with 3 μm particles or the reverse experiment (adding 3 μm particles to the base emulsion stabilized with 35 μm particles) results in a stabilization process dominated by the freshly added particles. The wettability effect has been explored in a set of a reverse experiment by adding hydrophobic particles or the hydrophilic particles to the base emulsion stabilized with particles with intermediate wettability. The added particles are found to immigrant to the preferred phase instead of stabilizing the emulsion. In such manner, the attempt to destabilize the base emulsion by adding particles with different wettability and a larger size was successful. Subsequently, we raised a hypothesis regarding the detachment of the original particles and the attachment of newly added particles. The AFM test suggests the contamination of detached particles with an oil layer covered. Such particles are prone to form clusters with the collided particles and thus making it difficult to adsorb to the interface again. The significantly increased droplet size after mixing for a sufficiently long time (4 days) also provides evidence for the particle detachment and destabilization of the emulsion. Such that, if new particles are added to the fluid system, they will be adsorbed to the bare interface left by the detachment of the original particles.

Pure liquid-liquid dispersion rarely exists in industrial applications, as additional particles are always deliberately added or are naturally existing in the system (Paul et al., 2004). A better understanding of the impact of particles in breakage and coalescence process would permit to control the droplet behaviour in the agitated system. Equipped with this knowledge, a more rational approach will be available to proceed in the emulsification process. This will also establish a solid foundation for predicting phase inversion point which is governed by the competitive effect between coalescence and breakage. The ability to control the stability of SSEs by adjusting either the dispersed phase volume fraction or the particle amount at the interface paves the way for various industrial processes. For instance, it could contribute to the research of the micro-encapsulation system where only temporary stability is desired since the entrapped component is required to release under a specific trigger. Alternatively, the micro-

droplets serve as a micro-reactor in the microfluidic. In this case, the controlled stability and release will allow the research on time-dependent reactions inside. In the petroleum industry, stable water-in-crude oil is formed with clay particles present during the production. The ability to promote the coalescence among the stabilized water droplets inside promotes the crude oil recovery. In food processing, the coalescence process is desired in the application like whipping cream and ice-cream. In other cases, however, the food (milk) are required to remain stable for a long period and avoid separation.

CHAPTER 8 CONCLUSION AND RECOMMENDATIONS

8.1 Conclusion

The work aims at investigating the impact of particles in the processing of Solid-stabilized emulsion. To achieve this goal, we addressed three specific objectives, which involves determining the role of particles in the emulsification process, phase inversion process, and hydrodynamic environments accompanied.

PVM® has shown to be a powerful tool in determining the droplet size and morphology evolution during the rapid process. During the emulsion generation, the presence of particles weakens the breakage effect, due to a combined impact of the energy dissipation and particle adsorption process. On the other hand, the coalescence efficiency is related to the ratio between the particle coverage potential over system-generated interface. At a lower ratio <1 (A_{gen} dominated regime), the emulsion are shown to undergo notable coalescence in response to the step change reduction in impeller speed. In contrast, for a higher ratio >1, the amount particles are able to cover all the generated interface, and hence resulting in a stable equilibrium without being disrupted by the operating conditions.

The catastrophic phase inversion from O/W to W/O emulsion takes place at a low critical ratio between the number of particles over the system generated interface. That is to say, at a given dispersed phase volume fraction, emulsion containing a lower particles concentration is prone to trigger the phase inversion. It is further explained that when the particles cannot cover the generated interface and lead to a significant high coalescence rate, that overcomes the breakage frequency in the system, and thus resulting in the phase inversion. Therefore, if preparing a stable emulsion with high dispersed phase volume fraction is a goal, more particles ought to be used to avoid phase inversion.

The behavior of particle at the oil/water interface is affected by the fluid dynamics. The detachment of the particles at the interface in the high-shear zone is followed by the adsorption of the newly added particles in the stabilization zone. Taking advantage of this particle exchange phenomena, the introduction of larger particles with an affinity for the dispersed phase, which favours the destabilization process, into the original SSEs breaks the original emulsion.

This work provides a fundamental understanding of the role of particles are playing in the dynamic emulsification processes and a guideline to facilitate the coalescence process:

continuous addition of the dispersed phase in the emulsification system or trigger detachment of the particles at the interface.

8.2 Recommendations

This work identified approaches in promoting the destabilization of the SSEs, the following recommendations are proposed based on our findings.

We revealed a critical ratio (the number of particles over system generated interface), which could trigger the catastrophic phase inversion. As mentioned in the literature review, the oil viscosity plays a role in hindering the coalescence and breakage process. Therefore, an extensive exploration of the impact of oil viscosity on the phase inversion ought to be further carried out. Such investigation would be of significant interests to the crude oil industry, where the phase inversion of heavy oil poses a great challenge. Moreover, to predict the phase inversion points, a comprehensive study involving other system parameters (particle wettability, phase pH, mixing intensity) needs to be accomplished.

Limited by the detection scope, the PVM® probe is not able to track the evolution of a single target droplet. During the particle exchange process, the variation of the fraction of a given particle at the interface over time could hardly be identified. Therefore, it is vital to use an alternative technique (e.g. radioactive particle tracking) to track a single particle and its path in the mixing tank in real-time. Such technique will allow us to gain a better understanding of the dynamic particle detachment and attachment process. This will contribute to further demonstrating the particle exchange phenomenon and bringing new insights to this mechanism. In addition, the impact of oil viscosity needs to be further explored on the dynamic particle exchange process to validate our hypothesis in the 3rd paper.

The conclusions and results of this work are yield from a modeled SSEs system. Following this, further studies ought to be moved to the real-world system, such as extremely highly viscous oil, asphaltenes and clay particles. The scale-up and scale-down of the SSEs destabilization processes need to be further explored, which would provide valuable data to the industries and the micro-encapsulation studies.

BIBLIOGRAPHY

Abend, S., Bonnke, N., Gutschner, U., & Lagaly, G. (1998). Stabilization of emulsions by heterocoagulation of clay minerals and layered double hydroxides. *Colloid and Polymer Science, 276*(8), 730-737. doi:10.1007/s003960050303

Alargova, R. G., Warhadpande, D. S., Paunov, V. N., & Velev, O. D. (2004). Foam superstabilization by polymer microrods. *Langmuir, 20*(24), 10371-10374. doi:10.1021/la048647a

Arditty, S., Schmitt, V., Lequeux, F., & Leal-Calderon, F. (2005). Interfacial properties in solid-stabilized emulsions. *European Physical Journal B, 44*(3), 381-393. doi:10.1140/epjb/e2005-00137-0

Arditty, S., Whitby, C. P., Binks, B. P., Schmitt, V., & Leal-Calderon, F. (2003). Some general features of limited coalescence in solid-stabilized emulsions. *European Physical Journal E, 11*(3), 273-281. doi:10.1140/epje/i2003-10018-6

Ashby, N. P., & Binks, B. P. (2000). Pickering emulsions stabilised by Laponite clay particles. *Physical Chemistry Chemical Physics, 2*(24), 5640-5646. doi:10.1039/b007098j

Ata, S. (2008). Coalescence of bubble covered by particles. In (Vol. 24, pp. 6085- 6091): Langmuir.

Ata, S. (2008). Coalescence of bubbles covered by particles. *Langmuir, 24*(12), 6085-6091. doi:10.1021/la800466x

Aveyard, R., Binks, B. P., & Clint, J. H. (2003). Emulsions stabilised solely by colloidal particles. *Adv Colloid Interface Sci, 100*, 503-546. doi:10.1016/s0001-8686(02)00069-6

Bartell, F., & Zuidema, H. (1936). Wetting characteristics of solids of low surface tension such as talc, waxes and resins. *Journal of the American Chemical Society, 58*(8), 1449-1454.

Binks, B. P., Desforges, A., & Duff, D. G. (2007). Synergistic stabilization of emulsions by a mixture of surface-active nanoparticles and surfactant. *Langmuir, 23*(3), 1098-1106. doi:10.1021/la062510y

Binks, B. P., & Kirkland, M. (2002). Interfacial structure of solid-stabilised emulsions studied by scanning electron microscopy. *Physical Chemistry Chemical Physics, 4*(15), 3727-3733. doi:10.1039/b110031a

Binks, B. P., & lumsdon, S. O. (1999). Stability of oil-in-water emulsions stabilised by silica particles. *Physical Chemistry Chemical Physics, 1*(12).

Binks, B. P., & Lumsdon, S. O. (2000a). Catastrophic phase inversion of water-in-oil emulsions stabilized by hydrophobic silica. *Langmuir, 16*(6), 2539-2547. doi:10.1021/la991081j

Binks, B. P., & Lumsdon, S. O. (2000b). Effects of oil type and aqueous phase composition on oil-water mixtures containing particles of intermediate hydrophobicity. *Physical Chemistry Chemical Physics, 2*(13), 2959-2967. doi:10.1039/b002582h

Binks, B. P., & Lumsdon, S. O. (2000c). Influence of particle wettability on the type and stability of surfactant-free emulsions. *Langmuir, 16*(23), 8622-8631. doi:10.1021/la000189s

Binks, B. P., & Lumsdon, S. O. (2000d). Transitional phase inversion of solid-stabilized emulsions using particle mixtures. *Langmuir, 16*(8), 3748-3756. doi:10.1021/la991427q

Binks, B. P., & Olusanya, S. O. (2017). Pickering emulsions stabilized by coloured organic pigment particles. *Chemical Science, 8*(1), 708-723. doi:10.1039/c6sc03085h

Binks, B. P., Philip, J., & Rodrigues, J. A. (2005). Inversion of silica-stabilized emulsions induced by particle concentration. *Langmuir, 21*(8), 3296-3302. doi:10.1021/la046915z

Binks, B. P., & Rodrigues, J. A. (2003). Types of phase inversion of silica particle stabilized emulsions containing triglyceride oil. *Langmuir, 19*(12), 4905-4912. doi:10.1021/la020960u

Binks, B. P., & Whitby, C. P. (2004). Silica particle-stabilized emulsions of silicone oil and water: Aspects of emulsification. *Langmuir, 20*(4), 1130-1137. doi:10.1021/la0303557

Binks, B. P., & Whitby, C. P. (2005). Nanoparticle silica-stabilised oil-in-water emulsions: improving emulsion stability. *Colloids and Surfaces a-Physicochemical and Engineering Aspects, 253*(1-3), 105-115. doi:10.1016/j.colsurfa.2004.10.116

Blaker, J. J., Lee, K. Y., Li, X. X., Menner, A., & Bismarck, A. (2009). Renewable nanocomposite polymer foams synthesized from Pickering emulsion templates. *Green Chemistry, 11*(9), 1321-1326. doi:10.1039/b913740h

Bonakdar, L., Philip, J., Bardusco, P., Petkov, J., Potti, J. J., Meleard, P., & Leal-Calderon, F. (2001). Rupturing of bitumen-in-water emulsions: experimental evidence for viscous sintering phenomena. *Colloids and Surfaces a-Physicochemical and Engineering Aspects, 176*(2-3), 185-194. doi:10.1016/s0927-7757(00)00699-3

Briggs, T. R. (1921). Emulsion with finely divided solids. *The journal of industrial and engineering chemistry, 13*(11).

Brooks, B. W., & Richmond, H. N. (1991). DYNAMICS OF LIQUID LIQUID-PHASE INVERSION USING NONIONIC SURFACTANTS. *Colloids and Surfaces, 58*(1-2), 131-148. doi:10.1016/0166-6622(91)80203-z

Brugger, B., Rosen, B. A., & Richtering, W. (2008). Microgels as Stimuli-Responsive Stabilizers for Emulsions. *Langmuir, 24*(21), 12202-12208. doi:10.1021/la8015854

Calabrese, R. V., Wang, C. Y., & Bryner, N. P. (1986). Drop breakup in turbulent stirred-tank contactors. *American Institute of Chemical Engineers, 32*(4), 4.

Chen, G. L., & Tao, D. (2005). An experimental study of stability of oil-water emulsion. *Fuel Processing Technology, 86*(5), 499-508. doi:10.1016/j.fuproc.2004.03.010

Chen, H. T., & Middleman, S. (1967). Drop size distribution in agitated liquid-liquid systems. *AIChE Journal, 13*(5), 989-995.

Chen, T., Colver, P. J., & Bon, S. A. F. (2007). Organic-inorganic hybrid hollow spberes prepared from TiO2-stabilized pickering emulsion polymerization. *Advanced Materials, 19*(17), 2286-+. doi:10.1002/adma.200602447

Chesters, A. K. (1991). THE MODELING OF COALESCENCE PROCESSES IN FLUID LIQUID DISPERSIONS - A REVIEW OF CURRENT UNDERSTANDING. *Chemical Engineering Research & Design, 69*(4), 259-270.

Chevalier, Y., & Bolzinger, M. A. (2013). Emulsions stabilized with solid nanoparticles: Pickering emulsions. *Colloids and Surfaces a-Physicochemical and Engineering Aspects, 439*, 23-34. doi:10.1016/j.colsurfa.2013.02.054

Coulaloglou, L. L. T. (1977). Description of interaction processes in agitated liquid-liquid dispersions. *Chemical Engineering Science, 32*(11), 9.

Cristini, V., Guido, S., Alfani, A., Blawzdziewicz, J., & Loewenberg, M. (2003). Drop breakup and fragment size distribution in shear flow. *Journal of Rheology, 47*(5), 1283-1298. doi:10.1122/1.1603240

Danner, T., & Schubert, H. (2001). Coalescence processes in emulsions. *Food Colloids: Fundamentals of Formulation*(258), 116-124. doi:10.1039/9781847550842-00116

Danov, K. D., & Kralchevsky, P. A. (2010). Capillary forces between particles at a liquid interface: General theoretical approach and interactions between capillary multipoles. *Adv Colloid Interface Sci, 154*(1-2), 91-103. doi:10.1016/j.cis.2010.01.010

Daware, S. V., & Basavaraj, M. G. (2015). Emulsions Stabilized by Silica Rods via Arrested Demixing. *Langmuir, 31*(24), 6649-6654. doi:10.1021/acs.langmuir.5b00775

Derjaguin, B. V., & Dukhin, S. S. (1993). THEORY OF FLOTATION OF SMALL AND MEDIUM-SIZE PARTICLES. *Progress in Surface Science, 43*(1-4), 241-266. doi:10.1016/0079-6816(93)90034-s

Doulah, M. S. (1975). An effect of hold-up on droplet sizes on liquid-liquid disperseion. *Industrial chemical engineering fundamentals, 14*(2), 2.

Drelich, A., Gomez, F., Clausse, D., & Pezron, I. (2010). Evolution of water-in-oil emulsions stabilized with solid particles Influence of added emulsifier. *Colloids and Surfaces a-*

Physicochemical and Engineering Aspects, 365(1-3), 171-177. doi:10.1016/j.colsurfa.2010.01.042

Ettelaie, R., & Murray, B. (2014). Effect of particle adsorption rates on the disproportionation process in pickering stabilised bubbles. *Journal of Chemical Physics, 140*(20). doi:10.1063/1.4878501

Feng, X. H., & Behles, J. A. (2015). Understanding the Demulsification of Water-in-Diluted Bitumen Froth Emulsions. *Energy & Fuels, 29*(7), 4616-4623. doi:10.1021/acs.energyfuels.5b00798

Fournier, C. O., Fradette, L., & Tanguy, P. A. (2009). Effect of dispersed phase viscosity on solid-stabilized emulsions. *Chemical Engineering Research & Design, 87*(4A), 499-506. doi:10.1016/j.cherd.2008.11.008

Frelichowska, J., Bolzinger, M. A., & Chevalier, Y. (2010). Effects of solid particle content on properties of o/w Pickering emulsions. *J Colloid Interface Sci, 351*(2), 348-356. doi:10.1016/j.jcis.2010.08.019

Frelichowska, J., Bolzinger, M. A., Pelletier, J., Valour, J. P., & Chevalier, Y. (2009). Topical delivery of lipophilic drugs from o/w Pickering emulsions. *International Journal of Pharmaceutics, 371*(1-2), 56-63. doi:10.1016/j.ijpharm.2008.12.017

French, D. J., Brown, A. T., Schofield, A. B., Fowler, J., Taylor, P., & Clegg, P. S. (2016). The secret life of Pickering emulsions: particle exchange revealed using two colours of particle. *Scientific Reports, 6*. doi:10.1038/srep31401

French, D. J., Taylor, P., Fowler, J., & Clegg, P. S. (2015). Making and breaking bridges in a Pickering emulsion. *J Colloid Interface Sci, 441*, 30-38. doi:10.1016/j.jcis.2014.11.032

Fujii, S., Armes, S. P., Binks, B. P., & Murakami, R. (2006). Stimulus-responsive particulate emulsifiers based on lightly cross-linked poly(4-vinylpyridine)-silica nanocomposite microgels. *Langmuir, 22*(16), 6818-6825. doi:10.1021/la060349l

Gautier, F., Destribats, M., Perrier-Cornet, R., Dechezelles, J. F., Giermanska, J., Heroguez, V., . . . Schmitt, V. (2007). Pickering emulsions with stimulable particles: from highly- to weakly-covered interfaces. *Physical Chemistry Chemical Physics, 9*(48), 6455-6462. doi:10.1039/b710226g

Gelot, A., Friesen, W., & Hamza, H. A. (1984). EMULSIFICATION OF OIL AND WATER IN THE PRESENCE OF FINELY DIVIDED SOLIDS AND SURFACE-ACTIVE AGENTS. *Colloids and Surfaces, 12*(3-4), 271-303. doi:10.1016/0166-6622(84)80105-5

Graillat, C., Lepaismasmejean, M., & Pichot, C. (1990). STABILIZATION OPTIMIZATION OF AQUEOUS MONOMER SOLUTIONS IN OIL-EMULSIONS USING THE

COHESIVE ENERGY RATIO CONCEPT. *Journal of Dispersion Science and Technology, 11*(5), 455-477.

Groeneweg, F., Agterof, W. G. M., Jaeger, P., Janssen, J. J. M., Wieringa, J. A., & Klahn, J. K. (1998). On the mechanism of the inversion of emulsions. *Chemical Engineering Research & Design, 76*(A1), 55-63. doi:10.1205/026387698524596

Haase, M. F., Grigoriev, D., Moehwald, H., Tiersch, B., & Shehukin, D. G. (2010). Encapsulation of Amphoteric Substances in a pH-Sensitive Pickering Emulsion. *Journal of Physical Chemistry C, 114*(41), 17304-17310. doi:10.1021/jp104052s

Henry, J. V. L., Fryer, P. J., Frith, W. J., & Norton, I. T. (2010). The influence of phospholipids and food proteins on the size and stability of model sub-micron emulsions. *Food Hydrocolloids, 24*(1), 66-71. doi:10.1016/j.foodhyd.2009.08.006

Horozov, T. S., Aveyard, R., Binks, B. P., & Clint, J. H. (2005). Structure and stability of silica particle monolayers at horizontal and vertical octane-water interfaces. *Langmuir, 21*(16), 7405-7412. doi:10.1021/la050923d

Horozov, T. S., & Binks, B. P. (2006). Particle-stabilized emulsions: A bilayer or a bridging monolayer? *Angewandte Chemie-International Edition, 45*(5), 773-776. doi:10.1002/anie.200503131

Horozov, T. S., Binks, B. P., & Gottschalk-Gaudig, T. (2007). Effect of electrolyte in silicone oil-in-water emulsions stabilised by fumed silica particles. *Physical Chemistry Chemical Physics, 9*(48), 6398-6404. doi:10.1039/b709807n

Hsia, M. A., & Tavlarides, L. L. (1983). Simulation analysis of drop breakage, coalescence and micromixing in liquid-liquid stirred tanks. *The Chemical Engineering Journal, 26*(3), 189-199.

Ikem, V. O., Menner, A., Horozov, T. S., & Bismarck, A. (2010). Highly Permeable Macroporous Polymers Synthesized from Pickering Medium and High Internal Phase Emulsion Templates. *Advanced Materials, 22*(32), 3588-+. doi:10.1002/adma.201000729

Jahanzad, F., Crombie, G., Innes, R., & Sajjadi, S. (2009). Catastrophic phase inversion via formation of multiple emulsions: A prerequisite for formation of fine emulsions. *Chemical Engineering Research & Design, 87*(4A), 492-498. doi:10.1016/j.cherd.2008.11.015

JEAN-LOUIS SALAGER, M. I. B., CARLOS LUIS BRACHO. (2001). *Heavy Hydrocarbon Emulsions. Making use of the state of art in formulation engineering*. New York: Encyclopedic Handbook of Emulsion Technology.

Jeelani, S. A. K., & Hartland, S. (1994). EFFECT OF INTERFACIAL MOBILITY ON THIN-FILM DRAINAGE. *J Colloid Interface Sci, 164*(2), 296-308. doi:10.1006/jcis.1994.1171

Juarez, J. A., & Whitby, C. P. (2012). Oil-in-water Pickering emulsion destabilisation at low particle concentrations. *J Colloid Interface Sci, 368*, 319-325. doi:10.1016/j.jcis.2011.11.029

Kamp, J., Villwock, J., & Kraume, M. (2017). Drop coalescence in technical liquid/liquid applications: a review on experimental techniques and modeling approaches. *Reviews in Chemical Engineering, 33*(1), 1-47. doi:10.1515/revce-2015-0071

Kaptay, G. (2006). On the equation of the maximum capillary pressure induced by solid particles to stabilize emulsions and foams and on the emulsion stability diagrams. *Colloids and Surfaces a-Physicochemical and Engineering Aspects, 282*, 387-401. doi:10.1016/j.colsurfa.2005.12.021

Katepalli, H., John, V. T., & Bose, A. (2013). The Response of Carbon Black Stabilized Oil-in-Water Emulsions to the Addition of Surfactant Solutions. *Langmuir, 29*(23), 6790-6797. doi:10.1021/la400037c

Klahn, J. K., Janssen, J. M. M., Vaessen, G. E. J., de Swart, R., & Agterof, W. G. M. (2002). On the escape process during phase inversion of an emulsion. *Colloids and Surfaces a-Physicochemical and Engineering Aspects, 210*(2-3), 167-181. doi:10.1016/s0927-7757(02)00376-x

Larsen, K. R. (2013). Managing Corrosion of Pipelines that Transport Crude Oils. *Materials Performance, 52*(5), 28-35.

Lee, C.-H., Erickson, L., & Glasgow, L. (1987). Bubble breakup and coalescence in turbulent gas-liquid dispersions. *Chemical Engineering Communications, 59*(1-6), 65-84.

Legrand, J., Chamerois, M., Placin, F., Poirier, J. E., Bibette, J., & Leal-Calderon, F. (2005). Solid colloidal particles inducing coalescence in bitumen-in-water emulsions. *Langmuir, 21*(1), 64-70. doi:10.1021/la047649s

Lehr, F., Millies, M., & Mewes, D. (2002). Bubble-size distributions and flow fields in bubble columns. *AIChE Journal, 48*(11), 2426-2443. doi:10.1002/aic.690481103

Levine, S., Bowen, B. D., & Partridge, S. J. (1989). STABILIZATION OF EMULSIONS BY FINE PARTICLES .1. PARTITIONING OF PARTICLES BETWEEN CONTINUOUS PHASE AND OIL-WATER INTERFACE. *Colloids and Surfaces, 38*(4), 325-343. doi:10.1016/0166-6622(89)80271-9

Li, X. D., Sun, G. Q., Li, Y. C., Yu, J. C., Wu, J., Ma, G. H., & Ngai, T. (2014). Porous TiO2 Materials through Pickering High-Internal Phase Emulsion Templating. *Langmuir, 30*(10), 2676-2683. doi:10.1021/la404930h

Liang, C., Liu, Q. X., & Xu, Z. H. (2014). Surfactant-Free Switchable Emulsions Using CO2-Responsive Particles. *Acs Applied Materials & Interfaces, 6*(9), 6898-6904. doi:10.1021/am5007113

Liao, Y. X., & Lucas, D. (2009). A literature review of theoretical models for drop and bubble breakup in turbulent dispersions. *Chemical Engineering Science, 64*(15), 3389-3406. doi:10.1016/j.ces.2009.04.026

Lucassen-Reynder, E. H., & Van Den Tempel, M. (1963). Stabilization of water in oil emulsion by solid particles. *Journal of physical chemistry, 67*(4).

Lucassen-Reynders, E. H., & VAN DEN Tempel, M. (1963). Stabilization of water in oil emulsions by solid particles. *The journal of physical chemicstry, 67*(4), 4.

Martinez-Bazan, C., Montanes, J. L., & Lasheras, J. C. (1999). On the breakup of an air bubble injected into a fully developed turbulent flow. Part 2. Size PDF of the resulting daughter bubbles. *Journal of Fluid Mechanics, 401*, 183-207. doi:10.1017/s0022112099006692

Martinez-Palou, R., Ceron-Camacho, R., Chavez, B., Vallejo, A. A., Villanueva-Negrete, D., Castellanos, J., . . . Aburto, J. (2013). Demulsification of heavy crude oil-in-water emulsions: A comparative study between microwave and thermal heating. *Fuel, 113*, 407-414. doi:10.1016/j.fuel.2013.05.094

Masliyah, J., Zhou, Z. J., Xu, Z. H., Czarnecki, J., & Hamza, H. (2004). Understanding water-based bitumen extraction from athabasca oil sands. *Canadian Journal of Chemical Engineering, 82*(4), 628-654. doi:10.1002/cjce.5450820403

Mei, Y., Li, G. X., Moldenaers, P., & Cardinaels, R. (2016). Dynamics of particle-covered droplets in shear flow: unusual breakup and deformation hysteresis. *Soft Matter, 12*(47), 9407-9412. doi:10.1039/c6sm02031c

Menner, A., Verdejo, R., Shaffer, M., & Bismarck, A. (2007). Particle-stabilized surfactant-free medium internal phase emulsions as templates for porous nanocomposite materials: Poly-pickering-foams. *Langmuir, 23*(5), 2398-2403. doi:10.1021/la062712u

Mercado, R. A., Sadtler, V., Marchal, P., Choplin, L., & Salager, J. L. (2012). Heteroflocculation of a Cationic Oil-in-Water Emulsion Resulting from Fontainebleau's Sandstone Powder Addition as a Model for Asphalt Emulsion Breakup. *Industrial & Engineering Chemistry Research, 51*(36), 11688-11694. doi:10.1021/ie300835q

Mercado, R. A., Salager, J. L., Sadtler, V., Marchal, P., & Choplin, L. (2014). Breaking of a cationic amine oil-in-water emulsion by pH increasing: Rheological monitoring to

modelize asphalt emulsion rupture. *Colloids and Surfaces a-Physicochemical and Engineering Aspects, 458*, 63-68. doi:10.1016/j.colsurfa.2014.03.109

Mira, I., Zambrano, N., Tyrode, E., Marquez, L., Pena, A. A., Pizzino, A., & Salager, J. L. (2003). Emulsion catastrophic inversion from abnormal to normal morphology. 2. Effect of the stirring intensity on the dynamic inversion frontier. *Industrial & Engineering Chemistry Research, 42*(1), 57-61. doi:10.1021/ie020535w

Moghimi, E., Goharpey, F., & Foudazi, R. (2014). Role of droplet bridging on the stability of particle-containing immiscible polymer blends. *Rheologica Acta, 53*(2), 165-180. doi:10.1007/s00397-013-0752-0

Morse, A. J., Armes, S. P., Thompson, K. L., Dupin, D., Fielding, L. A., Mills, P., & Swart, R. (2013). Novel Pickering Emulsifiers Based on pH-Responsive Poly(2-(diethylamino)ethyl methacrylate) Latexes. *Langmuir, 29*(18), 5466-5475. doi:10.1021/la400786a

Nagarkar, S. P., & Velankar, S. S. (2012). Morphology and rheology of ternary fluid-fluid-solid systems. *Soft Matter, 8*(32), 8464-8477. doi:10.1039/c2sm25758k

Nesterenko, A., Drelich, A., Lu, H. L., Clausse, D., & Pezron, I. (2014). Influence of a mixed particle/surfactant emulsifier system on water-in-oil emulsion stability. *Colloids and Surfaces a-Physicochemical and Engineering Aspects, 457*, 49-57. doi:10.1016/j.colsurfa.2014.05.044

Ngai, T., Auweter, H., & Behrens, S. H. (2006). Environmental responsiveness of microgel particles and particle-stabilized emulsions. *Macromolecules, 39*(23), 8171-8177. doi:10.1021/ma061366k

Nienow, A. W. (1994). *Fundamental studies of phase inversion*. Paper presented at the Proc. 8th Europ Mixing Conf. Cambridge.

Norton, I. T., Spyropoulos, F., & Cox, P. W. (2009). Effect of emulsifiers and fat crystals on shear induced droplet break-up, coalescence and phase inversion. *Food Hydrocolloids, 23*(6), 1521-1526. doi:10.1016/j.foodhyd.2008.09.014

Ohtake, T., Hano, T., Takagi, K., & Makashio, f. (1988). Analysis of water entrainment into dispersed W/O emulsion drops. *Chem. Eng. Jpn, 21*, 272.

Pauchard, V., & Roy, T. (2014). Blockage of coalescence of water droplets in asphaltenes solutions: A jamming perspective. *Colloids and Surfaces a-Physicochemical and Engineering Aspects, 443*, 410-417. doi:10.1016/j.colsurfa.2013.12.001

Paul, E. L., Atiemo-Obeng, V. A., & Kresta, S. M. (2004). *Handbook of industrial mixing: science and practice*: John Wiley & Sons.

Pickering, S. U. (1907). Emulsions. *Chem.Soc.*, 20.

Preuss, M., & Butt, H. J. (1998). Measuring the contact angle of individual colloidal particles. *J Colloid Interface Sci, 208*(2), 468-477. doi:10.1006/jcis.1998.5833

Qian, Y., Zhang, Q., Qiu, X. Q., & Zhu, S. P. (2014). CO2-responsive diethylaminoethyl-modified lignin nanoparticles and their application as surfactants for CO2/N-2-switchable Pickering emulsions. *Green Chemistry, 16*(12), 4963-4968. doi:10.1039/c4gc01242a

Reynaert, S., Moldenaers, P., & Vermant, J. (2006). Control over colloidal aggregation in monolayers of latex particles at the oil-water interface. *Langmuir, 22*(11), 4936-4945. doi:10.1021/la060052n

Rondon-Gonzalez, M., Madariaga, L. F., Sadtler, V., Choplin, L., Marquez, L., & Salager, J. L. (2007). Emulsion catastrophic inversion from abnormal to normal morphology. 6. Effect of the phase viscosity on the inversion produced by continuous stirring. *Industrial & Engineering Chemistry Research, 46*(11), 3595-3601. doi:10.1021/ie070145f

Rondon-Gonzalez, M., Madariaga, L. F., Sadtler, V., Choplin, L., & Salager, J. L. (2009). Emulsion Catastrophic Inversion from Abnormal to Normal Morphology. 8. Effect of Formulation on the Inversion Produced by Continuous Stirring. *Industrial & Engineering Chemistry Research, 48*(6), 2913-2919. doi:10.1021/ie801225h

Rondon-Gonzalez, M., Sadtler, V., Choplin, L., & Salager, J. L. (2006). Emulsion catastrophic inversion from abnormal to normal morphology. 5. Effect of the water-to-oil ratio and surfactant concentration on the inversion produced by continuous stirring. *Industrial & Engineering Chemistry Research, 45*(9), 3074-3080. doi:10.1021/ie060036l

Rondon-Gonzalez, M., Sadtler, V., Marchal, P., Choplin, L., & Salager, J. L. (2008). Emulsion catastrophic inversion from abnormal to normal morphology. 7. Emulsion evolution produced by continuous stirring to generate a very high internal phase ratio emulsion. *Industrial & Engineering Chemistry Research, 47*(7), 2314-2319. doi:10.1021/ie071482r

Rueger, P. E., & Calabrese, R. V. (2013). Dispersion of water into oil in a rotor-stator mixer. Part 1: Drop breakup in dilute systems. *Chemical Engineering Research & Design, 91*(11), 2122-2133. doi:10.1016/j.cherd.2013.05.018

Saigal, T., Dong, H. C., Matyjaszewski, K., & Tilton, R. D. (2010). Pickering Emulsions Stabilized by Nanoparticles with Thermally Responsive Grafted Polymer Brushes. *Langmuir, 26*(19), 15200-15209. doi:10.1021/la1027898

Sajjadi, S., Zerfa, M., & Brooks, B. W. (2000). Morphological change in drop structure with time for abnormal polymer/water/surfactant dispersions. *Langmuir, 16*(26), 10015-10019. doi:10.1021/la0004808

Scheludko, A., Toshev, B. V., & Bojadjiev, D. T. (1976). Attachement of particles to a liquid surface (capillary theory of flotation). *Journal of the Chemical Society, 72*(0), 14.

Scheulze, H. J., & Stockelhuber, W. (1993). Flotation as a heterocoagulation process: possibilities of calculating the probability of the flotation. *Coagulation and flotation*, 32.

Shah, R. K., Kim, J. W., & Weitz, D. A. (2010). Monodisperse Stimuli-Responsive Colloidosomes by Self-Assembly of Microgels in Droplets. *Langmuir, 26*(3), 1561-1565. doi:10.1021/la9041327

Subramaniam, A. B., Mejean, C., Abkarian, M., & Stone, H. A. (2006). Microstructure, morphology, and lifetime of armored bubbles exposed to surfactants. *Langmuir, 22*(14), 5986-5990. doi:10.1021/la060388x

Sullivan, A. P., & Kilpatrick, P. K. (2002). The effects of inorganic solid particles on water and crude oil emulsion stability. *Industrial & Engineering Chemistry Research, 41*(14), 3389-3404. doi:10.1021/ie010927n

Tambe, D. E., & Sharma, M. M. (1994). THE EFFECT OF COLLOIDAL PARTICLES ON FLUID-FLUID INTERFACIAL PROPERTIES AND EMULSION STABILITY. *Adv Colloid Interface Sci, 52*, 1-63. doi:10.1016/0001-8686(94)80039-1

Tang, J. T., Quinlan, P. J., & Tam, K. C. (2015). Stimuli-responsive Pickering emulsions: recent advances and potential applications. *Soft Matter, 11*(18), 3512-3529. doi:10.1039/c5sm00247h

Tarimala, S., & Dai, L. L. (2004). Structure of microparticles in solid-stabilized emulsions. *Langmuir, 20*(9), 3492-3494. doi:10.1021/la036129e

Tcholakova, S., Denkov, N. D., & Lips, A. (2008). Comparison of solid particles, globular proteins and surfactants as emulsifiers. *Physical Chemistry Chemical Physics, 10*(12), 1608-1627. doi:10.1039/b715933c

Tcholakova, S., Vankova, N., Denkov, N. D., & Danner, T. (2007). Emulsification in turbulent flow: 3. Daughter drop-size distribution. *J Colloid Interface Sci, 310*(2), 570-589. doi:10.1016/j.jcis.2007.01.097

Tobin, T., Muralidhar, R., & Wright, H. (1990). Determination of coalescence frequencies in liquid-liquid dispersions effect of drop size dependence. *Chemical Engineering Science, 45*(12).

Tsabet, E. (2014). *From Particle to Process: Modeling the production of Pickering emulsion.* (Doctorate), Polytechnique Montreal, Montreal.

Tsabet, E., & Fradette, L. (2015a). Effect of the properties of oil, particles, and water on the production of Pickering emulsions. *Chemical Engineering Research & Design, 97*, 9-17. doi:10.1016/j.cherd.2015.02.016

Tsabet, E., & Fradette, L. (2015b). Semiempirical Approach for Predicting the Mean Size of Solid-Stabilized Emulsions. *Industrial & Engineering Chemistry Research, 54*(46), 11661-11677. doi:10.1021/acs.iecr.5b02910

Tsabet, E., & Fradette, L. (2016). Study of the properties of oil, particles, and water on particle adsorption dynamics at an oil/water interface using the colloidal probe technique. *Chemical Engineering Research & Design, 109*, 307-316. doi:10.1016/j.cherd.2016.02.001

Tsouris, C., & Tavlarides, L. (1994). Breakage and coalescence models for drops in turbulent dispersions. *AIChE Journal, 40*(3), 395-406.

Utada, A. S., Lorenceau, E., Link, D. R., Kaplan, P. D., Stone, H. A., & Weitz, D. A. (2005). Monodisperse double emulsions generated from a microcapillary device. *Science, 308*(5721), 537-541. doi:10.1126/science.1109164

Vachova, T., Brabcova, Z., & Basarova, P. (2013, Nov 19-22). *Description of the three-phase contact line expansion.* Paper presented at the 8th International Conference on Experimental Fluid Mechanics, TU Liberec, Kutna Hora, CZECH REPUBLIC.

Vaessen, G. E. J., Visschers, M., & Stein, H. N. (1996). Predicting catastrophic phase inversion on the basis of droplet coalescence kinetics. *Langmuir, 12*(4), 875-882. doi:10.1021/la950379g

Valentas, K. J., Bilous, O., & Amundson, N. R. (1966). Analysis of breakage in dispersed phase systems. *Industrial & engineering chemistry fundamentals, 5*(2), 271-279.

Vashisth, C., Whitby, C. P., Fornasiero, D., & Ralston, J. (2010). Interfacial displacement of nanoparticles by surfactant molecules in emulsions. *J Colloid Interface Sci, 349*(2), 537-543. doi:10.1016/j.jcis.2010.05.089

Verbich, S. V., Dukhin, S. S., Tarovski, A., Holt, O., Saether, O., & Sjoblom, J. (1997). Evaluation of stability ratio in oil-in-water emulsions. *Colloids and Surfaces a-Physicochemical and Engineering Aspects, 123*, 209-223. doi:10.1016/s0927-7757(96)03939-8

W.J.Howarth. (1967). Measurement of coalescence frequency in an agitated tank. *AlChE, 13*(5), 7.

Walker, E. M., Frost, D. S., & Dai, L. L. (2011). Particle self-assembly in oil-in-ionic liquid Pickering emulsions. *J Colloid Interface Sci, 363*(1), 307-313. doi:10.1016/j.jcis.2011.07.056

Walstra, P. (1993). Principals of emulsion formation. *Chemical Engineering Science, 48*(2), 333.

Walstra, P. (1993). PRINCIPLES OF EMULSION FORMATION. *Chemical Engineering Science, 48*(2), 333-349. doi:10.1016/0009-2509(93)80021-h

Wan, B., & Fradette, L. (2017). PHASE INVERSION OF A SOLID-STABILIZED EMULSION: EFFECT OF PARTICLE CONCENTRATION. *Canadian Journal of Chemical Engineering, 95*(10), 1925-1933. doi:10.1002/cjce.22892

Whitby, C. P., Anwar, H. K., & Hughes, J. (2016). Destabilising Pickering emulsions by drop flocculation and adhesion. *J Colloid Interface Sci, 465*, 158-164. doi:10.1016/j.jcis.2015.11.063

Whitby, C. P., Fornasiero, D., & Ralston, J. (2009). Effect of adding anionic surfactant on the stability of Pickering emulsions. *J Colloid Interface Sci, 329*(1), 173-181. doi:10.1016/j.jcis.2008.09.056

Whitby, C. P., Fornasiero, D., & Ralston, J. (2010). Structure of oil-in-water emulsions stabilised by silica and hydrophobised titania particles. *J Colloid Interface Sci, 342*(1), 205-209. doi:10.1016/j.jcis.2009.10.068

Whitesides, T. H., & Ross, D. S. (1995). EXPERIMENTAL AND THEORETICAL-ANALYSIS OF THE LIMITED COALESCENCE PROCESS - STEPWISE LIMITED COALESCENCE. *J Colloid Interface Sci, 169*(1), 48-59. doi:10.1006/jcis.1995.1005

Wright, H., & Ramkrishna, D. (1994). Factors affecting coalescence frequency of droplets in a stirred liquid‐liquid dispersion. *AIChE Journal, 40*(5), 767-776.

Xu, B. (2017). Fast and Energy-efficient Demulsification for Crude Oil Emulsions Using Pulsed Electric Field. *International Journal of Electrochemical Science, 12*(10), 9242-9249. doi:10.20964/2017.10.84

Xu, Q. Y., Nakajima, M., & Binks, B. P. (2005). Preparation of particle-stabilized oil-in-water emulsions with the microchannel emulsification method. *Colloids and Surfaces a-Physicochemical and Engineering Aspects, 262*(1-3), 94-100. doi:10.1016/j.colsurfa.2005.04.019

Yan, N. X., Kurbis, C., & Masliyah, J. H. (1997). Continuous demulsification of solids-stabilized oil-in-water emulsions by the addition of fresh oil. *Industrial & Engineering Chemistry Research, 36*(7), 2634-2640. doi:10.1021/ie960807t

Yan, N. X., & Masliyah, J. H. (1996). Effect of pH on adsorption and desorption of clay particles at oil-water interface. *J Colloid Interface Sci, 181*(1), 20-27. doi:10.1006/jcis.1996.0352

Yang, D. H., Xu, M. H., He, L. M., Luo, X. M., Lu, Y. L., Yan, H. P., & Tian, C. K. (2015). The influence and optimisation of electrical parameters for enhanced coalescence under pulsed DC electric field in a cylindrical electrostatic coalescer. *Chemical Engineering Science, 138*, 71-85. doi:10.1016/j.ces.2015.07.049

Yang, F., Liu, S. Y., Xu, J., Lan, Q., Wei, F., & Sun, D. J. (2006). Pickering emulsions stabilized solely by layered double hydroxides particles: The effect of salt on emulsion formation and stability. *J Colloid Interface Sci, 302*(1), 159-169. doi:10.1016/j.jcis.2006.06.015

Zeitlin, M., & Tavlarides, L. (1972). Fluid‐fluid interactions and hydrodynamics in agitated dispersions: A simulation model. *The Canadian Journal of Chemical Engineering, 50*(2), 207-215.

Zhang, K., Wu, W., Meng, H., Guo, K., & Chen, J. F. (2009). Pickering emulsion polymerization: Preparation of polystyrene/nano-SiO2 composite microspheres with core-shell structure. *Powder Technology, 190*(3), 393-400. doi:10.1016/j.powtec.2008.08.022

Zheng, Z., Zheng, X. H., Wang, H. T., & Du, Q. G. (2013). Macroporous Graphene Oxide-Polymer Composite Prepared through Pickering High Internal Phase Emulsions. *Acs Applied Materials & Interfaces, 5*(16), 7974-7982. doi:10.1021/am4020549

Zoppe, J. O., Venditti, R. A., & Rojas, O. J. (2012). Pickering emulsions stabilized by cellulose nanocrystals grafted with thermo-responsive polymer brushes. *J Colloid Interface Sci, 369*, 202-209. doi:10.1016/j.jcis.2011.12.011